Investigations on use of Satellite Data and Back Trajectory Analysis for Prediction and Retrieval of $PM_{2.5}$ and Identification of Regional Contributions by Long Range Transport

A thesis

Submitted in partial fulfilment of the requirements
for the award of the degree of

DOCTOR OF PHILOSOPHY

by

SELVETIKAR ASHOK

(Roll No: 716109)

DEPARTMENT OF CIVIL ENGINEERING
NATIONAL INSTITUTE OF TECHNOLOGY
WARANGAL, TELANGANA – 506004, INDIA

JULY – 2023

Investigations on use of Satellite Data and Back Trajectory Analysis for Prediction and Retrieval of $PM_{2.5}$ and Identification of Regional Contributions by Long Range Transport

Submitted in partial fulfilment of the requirements
for the award of the degree of

DOCTOR OF PHILOSOPHY
in
CIVIL ENGINEERING
by

SELVETIKAR ASHOK
(Roll No: 716109)

Supervisor
Prof. M. Chandra Sekhar

DEPARTMENT OF CIVIL ENGINEERING
NATIONAL INSTITUTE OF TECHNOLOGY
WARANGAL, TELANGANA – 506004, INDIA

JULY – 2023

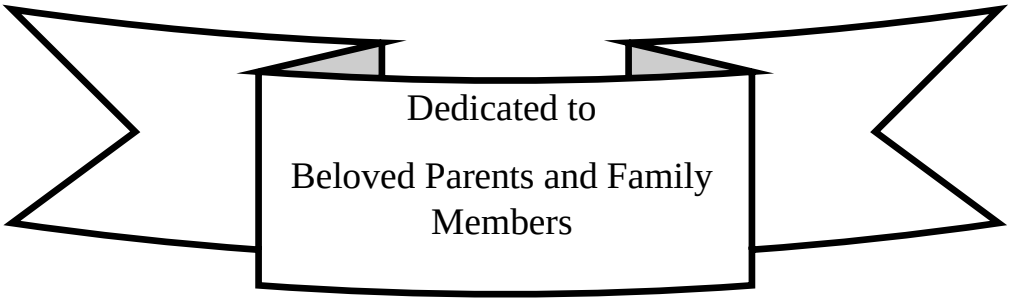
Dedicated to
Beloved Parents and Family Members

NATIONAL INSTITUTE OF TECHNOLOGY WARANGAL

CERTIFICATE

This is to certify that the thesis entitled **"INVESTIGATIONS ON USE OF SATELLITE DATA AND BACK TRAJECTORY ANALYSIS FOR PREDICTION AND RETRIEVAL OF $PM_{2.5}$ AND IDENTIFICATION OF REGIONAL CONTRIBUTIONS BY LONG RANGE TRANSPORT"** being submitted by **Mr. SELVETIKAR ASHOK** for the award of the degree of **DOCTOR OF PHILOSOPHY** in the Department of Civil Engineering, National Institute of Technology, Warangal, is a record of bonafide research work carried out by him under my supervision and it has not been submitted elsewhere for the award of any degree.

Prof. M. Chandra Sekhar
Thesis Supervisor
Professor-HAG
Department of Civil Engineering
National Institute of Technology
Warangal (T.S) – India

Dissertation Approval

This dissertation entitled **"INVESTIGATIONS ON USE OF SATELLITE DATA AND BACK TRAJECTORY ANALYSIS FOR PREDICTION AND RETRIEVAL OF $PM_{2.5}$ AND IDENTIFICATION OF REGIONAL CONTRIBUTIONS BY LONG RANGE TRANSPORT"** by **Mr. Selvetikar Ashok** is approved for the degree of **Doctor of Philosophy**.

Examiners

_____

_____

_____

Supervisor(s)

_____

_____

_____

Chairman

_____

Date:_____

Place:_____

DECLARATION

This is to certify that the work presented in the thesis entitled **"INVESTIGATIONS ON USE OF SATELLITE DATA AND BACK TRAJECTORY ANALYSIS FOR PREDICTION AND RETRIEVAL OF $PM_{2.5}$ AND IDENTIFICATION OF REGIONAL CONTRIBUTIONS BY LONG RANGE TRANSPORT"** is a bonafide work done by me under the supervision of **Dr. M. Chandra Sekhar** and was not submitted elsewhere for the award of any degree. I declare that this written submission represents my ideas in my own words and where others' ideas or words have been included, I have adequately cited and referenced the original sources. I also declare that I have adhered to all principles of academic honesty and integrity and have not misrepresented or fabricated or falsified any idea /data/fact/source in my submission. I understand that any violation of the above will be a cause for disciplinary action by the Institute and can also evoke penal action from the sources which have thus not been properly cited or from whom proper permission has not been taken when needed.

_____

(SELVETIKAR ASHOK)
(Roll No: 716109)

Date:_____

Acknowledgements

Since research requires ample resources, support, and motivation, I would like to thank and extend my gratitude to the ***National Institute of Technology, Warangal (NITW),*** for allowing me to work with such wonderful people and their support to complete this thesis work.

First and foremost, I would like to express my deep sense of gratitude to my thesis supervisor ***Dr. M. Chandra Sekhar***, Professor, Department of Civil Engineering for his continuous monitoring, invaluable guidance, moral support, patience, encouragement, and timely inputs throughout my doctoral study and research work. The present research would not have been possible without his continuous support. His dedication to research work will always be a source of inspiration for the rest of my life.

I am thankful to my Doctoral Scrutiny Committee: Chairman ***Dr. T.D Gunneswara Rao,***
Professor, and Head, Department of Civil Engineering and members ***Dr. N. V Umamahesh***, Professor, Department of Civil Engineering, ***Dr. P. Hari Prasad Reddy***, Associate Professor, Department of Civil Engineering, and ***Dr K. Laxma Reddy***, Professor, Department of Chemistry Engineering for their continuous monitoring, keen interest, insightful comments and encouragement during the active research period.

I am also thankful to ***Prof. K. Venkata Reddy***, and ***Dr. Sumanth Chinthala***, Assistant Professor, Department of Civil Engineering NITW for the moral support given during the period of research work.

I am also thankful to ***Dr. K. Rakesh***, Principal Scientist, CTM Division, NEERI, Nagpur, and ***Dr. Praveen Kumar Sappidi,*** Assistant Professor, Department of Chemical Engineering, IIT Jodhpur and ***Dr. Dudam Bharath Kumar***, Assistant Professor, Department of Civil Engineering, CBIT Hyderabad, Although they presence is remote, he is always willing to help at any time whenever

I thank my fellow research scholars and friends ***Mr. Sai krishna, Dr. Shashank Srivastava (PDF-fellow), Mr. Nithin Kumar, Mr. Sandeep, Mr. Aravind, Mr. Sudheekar, Mr. Prasanta Majee, Mrs. M Sagarika, Mr. Uppala Lava Kumar, Mr. Manikanta, Mr. K Satish Kumar, Mrs. K Sreelatha, Mr. A Ashok, Dr. P Shruthi Mr. J. Narendra (M.Tech), Mr. Rama Bhupal Reddy (Internship) and Mr. Naveen Kumar (Lab asst)*** for their direct or indirect help throughout research work and creating an enjoyable and fun work environment.

Last but not least, I extend my biggest and whole hearted thanks to my parents

Mr. Selvetikar Bapu and ***Mrs. Selvetikar Narsubai,*** family members ***Mr. S.Umamaheshwar, Mr. S. Anand Kumra, Mrs. S. Sumalatha*** and ***Mrs. D. Kavitha,*** my friend deepest gratitude to Late ***Mr. G. Venkatesh (B.Tech Civil engineering)*** for standing with me in testing times and offering good moral support all these years.

Selvetikar Ashok
Roll No: 716109

Abstract

Air pollution is a major cause of illness and death in the world, but inadequate ground-based monitoring (both spatial and temporal) hampers effective air quality management. To address this challenge, satellite data can play a crucial role. Over the past two decades, various sensors worldwide have routinely measured Aerosol Optical Depth (AOD), to provide qualitative information about air quality. Recent advancements in satellite retrieval and modelling techniques now allow us to estimate $PM_{2.5}$ levels from AOD, enabling quantitative applications. Additionally, the current network of 308 monitoring stations in India is inadequate and unevenly distributed, which limits accurate measurement of air quality and in particular $PM_{2.5}$, which has detrimental effect on human health. The lack of air quality monitoring network in many parts of the country further emphasizes the necessity for more monitoring sites. By utilizing satellite-based AOD data, this study aims to estimate ground-level $PM_{2.5}$ concentrations and hence, the associated health risks. If these estimations are validated, monitoring becomes inexpensive and investments on monitoring networks can be limited.

$PM_{2.5}$ in the atmosphere is widely reported, but few studies have focussed on the metal-bound particle concentration of $PM_{2.5}$ in urban areas. The present study on Warangal, aims to quantify Heavy Metals (HM) concentration associated with $PM_{2.5.}$ The average daily $PM_{2.5}$ values were found to be above the annual average (40 $\mu g/m^3$) set by the National Ambient Air Quality Standard (NAAQS) of India. Slightly higher concentrations of Zn and Fe were observed as compared to Cu, Ni and Cd. The order of heavy metal based on the concentration levels was as follows: Zn>Fe>Cu>Ni>Cd (higher to lower concentration). Analysis of enrichment factor showed that the Zn, Cu and Cd fall in the highly enriched element category. Based on health risk assessment for three intake pathways, the risk of exposure was found to be in the following order: Ingestion>Dermal>Inhalation. Non-carcinogenic and carcinogenic risks for children and adults were found to be negligible. Source identification of all the elements and $PM_{2.5}$ study based on Concentration Weighted Trajectory (CWT), Potential Source Contribution Function (PSCF) and cluster analysis results indicated dominant contributions from West and North-West regions of India. Furthermore, cluster IV was reported to have high significance (with 27.11%) and dominant contributions of trajectories were observed from the regions of Maharashtra, Chhattisgarh, Rajasthan, and Madhya Pradesh over the Warangal region.

The results of the source identification study observed that the gap in the spatial pattern was due to limited primary data collected during the study period. Backward trajectory methodologies require huge data to arrive at accurate source regions. To address this challenge, $PM_{2.5}$ retrievals were attempted for the Hyderabad region using satellite AOD and meteorological data. Satellite measurements are important for quantifying the ground observations and atmosphere columnar properties like AOD, especially in developing countries like India. In this study Moderate Resolution Imaging Spectroradiometer (MODIS) retrieval's AOD product has been used having 3 km and 10 km spatial resolution from Terra and Aqua satellites. The MODIS AOD data and meteorological parameters from May 2017 to May 2019 were used. The Multiple linear regression method is implemented in this study. The study concluded that there is good agreement in the prediction of $PM_{2.5}$ at the Zoopark location. The PM concentrations are influenced by the local source regions and the long-range transport of pollutants through the wind, whereas the potential source regions identified based on the PSCF, CWT, and Cluster analysis. The cluster analysis indicated that the Winter season surface layer trajectories with a ratio of 38.1% (cluster III) have a high intensity from Central India (Madhya Pradesh and Chhattisgarh). In the pre-monsoon season cluster IV dominated with a ratio of 31.3% from the Bay of Bengal region. As well as the elevated layer analysis showed that the Winter season cluster IV (57%) was predominantly from Central India. Results indicate that the Central India and East India regions are the more dominating source regions at the Hyderabad location in the winter season. It was found that the lower altitude layer showed the major source of the local region's nearby receptors.

The cluster analysis concluded that Central India was the major dominating region in the surface and elevated layers at Hyderabad regions. The long-range transport of the sources may be due to open-cast coal mining and open biomass burning. The study also briefs on the intensity of surface and elevated layer transport of $PM_{2.5}$ at receptor locations. The surface layer pollutants are more dominating at the receptor location compared to the elevated layer pollutants. The results of the study can help policymakers to implement mitigation measures and formulate suitable regulations to reduce the health risk associated with $PM_{2.5}$ and heavy metals in the atmosphere. Methodological improvements in back trajectory receptor models (like 3D trajectories, wind speed analysis, import of data from dispersion models, the height of mixing layer, etc,.) can improve the findings of the study and help in regional air quality management.

Keywords: $PM_{2.5}$, Heavy Metal, Health Impact, Backward trajectory, and Cluster analysis.

Table of Contents

List of Figures

List of Tables

List of Acronyms

μg	Microgram
%	Percentage
^{o}C	centigrade
α	Alpha
ABL	Atmospheric Boundary Layer
ADD	Average Daily Doses
AE	Angstrom exponent
AERONET	Aerosol Robotic Network
AN	Afternoon
AOD	Aerosol Optical Depth
AOPs	Aerosol optical properties
AQI	Air Quality Index
AQMs	Air quality Monitoring Stations
ARL	Air Resources Laboratory
ARL	Air Resources Laboratory, United States
BC	Black Carbon
CALIPSO	Cloud-Aerosol Lidar and Infrared Pathfinder Satellite Observations
CMB	Chemical Mass Balance
CNG	Compressed Natural Gas
CO	Carbon Monoxide
CR	Cancer Risk
CWT	Concentration Weighted Trajectory
Cd	Cadmium
Conc	Concentration
Cr	Chromium
Cu	Copper
DB	Deep Blue
DT	Dark Target

ECMWF	European Centre for Medium-Range Weather Forecasts,
EF	Enrichment factor
EU	European Union
fAOD	fine-mode AOD
FB	Fractional Bias
GDP	Gross Domestic Product
GIS	Geographical Information Systems
GUI	Graphical User Interface
GW	Gigawatt
HI	Hazard Index
HM	Heavy Metal
HPBL	Height of the Planetary Boundary Layer
HQ	Hazard Quotient
HYSPLIT	HYbrid Single Particle Lagrangian Integrated Trajectory Model
IGP	Indo-Gangetic Plain
KM	Kilometres
LPM	Liters Per Minute
MLR	Multiple linear Regression
MoEF	Ministry of Environment and Forestry, Turkey
NAAQS	National Ambient Air Quality Standards
NCAP	National Clean Air Programme
NCAR	National Center for Atmospheric Research, United States
NCEP	National Centers for Environmental Protection, United States
NCR	Delhi National Capital Region
NMSE	Normalized Mean Square Error
NOAA	National Oceanic and Atmospheric Administration, United States
NOx	Nitrogen oxide
NWP	Numerical Weather Prediction
Ni	Nickel
O_3	Ozone

Pb	Lead
PCA	Principal components analysis
PM	Particulate matter
PM2.5	particulate matter with particles of aerodynamic diameter<2.5 μm
PM10	particulate matter with particles of aerodynamic diameter<10 μm
PMF	Positive Matrix Factorization
PPB	Parts Per Million
PSCF	Potential Source Contribution Function
R	Correlation
READY	Real-time Environmental Applications and Display sYstem
RH	Relative Humidity
RMSE	root-mean-square error
RPM	Respirable Particulate Matter
SPM	Suspended Particulate Matter
SA	Source Apportionment
SO_2	Sulfur Dioxide
SO_x	Sulfur Oxides
STILT	Stochastic Time-Inverted Lagrangian Transport
T	Temperature
TOMS	Total Ozone Mapping Spectrometer
TPD	Tons per Day
UK	United Kingdom
UN	United Nations
US EPA	United States Environmental Protection Agency
WHO	World Health Organization
WS	wind speed
w.r.t	With respect to
Zn	Zinc

Chapter 1 Introduction

1.1 Background

The World Health Organization (WHO) has been monitoring and studying the effects of air pollution on human health for several decades. Air pollution is a major environmental risk to health, causing an estimated 7 million premature deaths annually worldwide (WHO, 2009). WHO's research shows that air pollution is linked to a range of health problems, including respiratory and cardiovascular diseases, cancer, and adverse birth outcomes. According to the World Health Organization, air pollution is the contamination of the environment both indoor and outdoor by any type of chemical, physical or biological agents that may lead to modification in the natural characteristics of the atmosphere (Hoffmann et al., 2021).

The sources of air pollution are diverse, including industrial emissions, transportation, open-cast coal mines, biomass burning, and forest fires. Particulate matter (PM), Nitrogen oxide (NO_x), Sulfur Dioxide (SO_2), Ozone (O_3), and Carbon Monoxide (CO) are among the most harmful air pollutants. The burden of incident childhood asthma may be attributable to outdoor Nitrogen Dioxide (NO_2), PM, and Black Carbon (BC) in Europe (Khreis et al., 2019). WHO provides guidance and technical support to countries and works to raise awareness about the health impacts of air pollution. The organization has set air quality guidelines to protect public health and recommends measures such as promoting clean energy sources, improving transportation systems, and reducing emissions from industrial and household sources. WHO also works with governments and other stakeholders to strengthen the monitoring and reporting of air pollution levels and to develop policies to reduce exposure to air pollution.

Source reduction of pollutants is the best and most efficient method for controlling pollution. However, for source reduction, it is essential to identify the sources of pollution in the ambient air. As there are several sources for a particular pollutant under consideration, source apportionment (SA) methods are used for the identification of the source and categorization. However, these methodologies like Chemical mass balance (CMB), Positive matrix factorization (PMF), and Principal components analysis (PCA) are time-consuming processes. Hence that the backward trajectory analysis, introduced by the NOAA’s Air Resources Laboratory (ARL)-Hybrid Single-Particle Lagrangian Integrated Trajectory (HYSPLIT) model run interactively on

the Real-time Environmental Applications and Display system (READY) web site is used by researchers.

Reducing ambient $PM_{2.5}$ levels requires a concerted effort from governments, industry, and individuals. Strategies to reduce ambient $PM_{2.5}$ levels include improving energy efficiency, increasing the use of renewable energy sources, promoting cleaner transportation, and implementing regulations to reduce emissions from industry. Implementing these strategies will not only reduce the health impacts of ambient $PM_{2.5}$ but also contribute to a healthier and more sustainable environment

1.2 Atmospheric aerosol science

Pollution levels become colossal problems in Indian cities not only in urban regions but in the rural regions as well. The reasons include an increase in industries, vehicle population, and lifestyle changes. The Indian population is exposed to the highest level of particulate pollution (Ravishankara et al., 2020; Sharma and Kulshrestha, 2014) because of the increase in fine particulate matter that affects the environment and health (Balakrishnan et al., 2018; Niu et al., 2022). The outdoor biomass burning releases enormous concentrations of particulate matter which are dispersed to faraway locations also depending on meteorological conditions. The sources contributing to $PM_{2.5}$ in ambient air are shown in Figure 1.1 The emitted pollutants undergo dispersions in the atmosphere contributing to pollution through long-range transport.

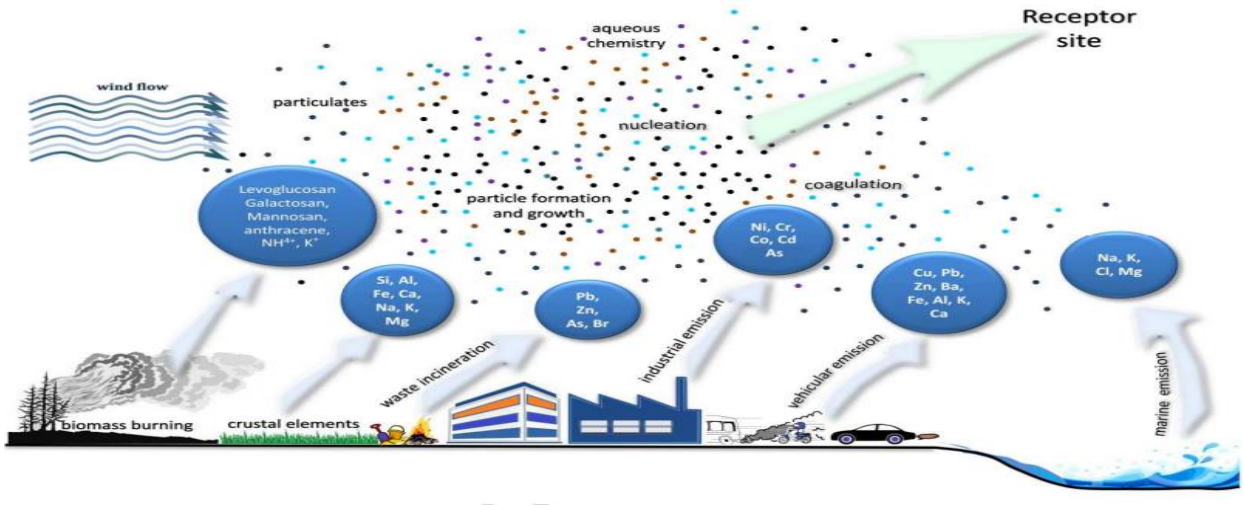

Figure 1.1 $PM_{2.5}$ sources and dispersion of air mass to the receptor location. **Source**:(Banerjee et al., 2015a)

In addition to ambient air quality, indoor air quality also affects human health and results in different health problems (Datta et al., 2017). Indoor air quality is reported to influence development as well (Rohra and Taneja, 2016). Exposure and risk assessment of concentrations of fine and coarser particles indicate that finer particles cause higher carcinogenic risk than particles in coarse fractions (Shikha et al., 2023). Many studies reported that the $PM_{2.5}$ and PM_{10} concentrations in Indian cities are higher than the prescribed standards (Ambade, 2014a; Das et al., 2015). However, the accumulation of toxic heavy metals with particulates associated with air pollution by various sources is a challenge. The fine particles from coal combustion and non–ferrous metal smelting units are associated with heavy metals. Particulates from the above sources are reported to contribute toxic metals (Cr, Ni, Zn, Mo, Sn, Sb, V, Co, Cu, Cd, and Pb) in the $PM_{2.5}$ fraction (Das et al., 2015). Enrichment factor analysis reveals that metallic pollutants are emitted from anthropogenic sources or associated with natural sources (Ambade, 2014a).

1.3 Ambient $PM_{2.5}$ bound heavy metals

Ambient $PM_{2.5}$ refers to particulate matter in the air with a diameter of 2.5 µm or less. These particles can be emitted directly into the atmosphere by sources such as transportation, power generation, and industrial processes, or they can be formed through chemical reactions between other pollutants in the atmosphere. The $PM_{2.5}$ particles penetrate deeply into the lungs when inhaled or find entry through different pathways which can cause a range of health problems, including respiratory and cardiovascular diseases. These particles can also travel long distances through the air as a media to influence the other regions, which means that air pollution can be transported from one region to another, affecting air quality in areas far from the origin source of pollution (Liao et al., 2017; Shanavas et al., 2020).

However, the ambient $PM_{2.5}$ levels are monitored by regulatory agencies to ensure that they meet established air quality standards. In many parts of the world, ambient $PM_{2.5}$ levels exceed these standards. Ambient $PM_{2.5}$ has a significant impact on the world's population, making it one of the leading environmental risk factors for death and disease. Exposure to high levels of ambient $PM_{2.5}$ can also worsen pre-existing health conditions, such as asthma and chronic obstructive pulmonary disease. Ambient $PM_{2.5}$ also has environmental impacts, such as contributing to climate change and reducing visibility. Additionally, $PM_{2.5}$ can harm ecosystems and agricultural productivity, as

well as damage buildings and monuments. Air pollution is a leading risk factor for stroke, heart disease, and lung cancer.

The State of Global Air Report (Health Effects Institute and the Institute for Air Pollution and Brain Outcomes in Children) reveals that air pollution affects the development of the brain. A strong correlation was noted between many pollutants and prenatal and childhood exposure (Mònica et al., 2022). The Air Quality Life Index, developed by researchers at the Energy Policy Institute at the University of Chicago, estimates that air pollution, including ambient $PM_{2.5}$, reduces global life expectancy by an average of 1.8 years, and by more than 4 years in some countries (Lee and Greenstone, 2021). The study also highlights the significant impact of ambient $PM_{2.5}$ on human health and the urgent need for action to reduce air pollution levels worldwide.

Heavy metals released into the atmosphere can remain suspended in the air for extended periods and can be transported over long distances. Common heavy metals found in ambient air include Lead, Cadmium, Mercury, Arsenic, Chromium, and Nickel (Ambade, 2014a; Khan et al., 2020; Tian et al., 2015). Exposure to high levels of these metals in ambient air can pose a significant health risk to humans and wildlife. Once in the body, heavy metals can accumulate in tissues and organs, leading to a range of health problems, including respiratory and cardiovascular diseases, neurological disorders, and cancer. To reduce the health risks associated with exposure to ambient heavy metals, it is important to monitor and reduce emissions from sources such as transportation and industry and to take steps to improve air quality in affected areas. This includes implementing regulations to limit emissions of heavy metals from industrial processes, promoting the use of cleaner transportation options, and encouraging the use of cleaner sources of energy.

1.4 Health impact of ambient Heavy metals

The impact of heavy metals in ambient air is significant even while the concentrations are low. Zn is an essential trace element that plays a crucial role in numerous biological processes in the human body. It is necessary for proper immune function, growth and development, wound healing, and enzyme activity. While zinc is essential for health, excessive exposure to zinc, particularly in ambient environments, can have adverse effects on human health. The impact of Zn on human health can vary depending on specific circumstances, concentrations, and individual susceptibility. Therefore, considering local environmental conditions, regulatory measures and individual factors is crucial when assessing the potential health risks associated with zinc exposure. High levels of

zinc ingestion can cause gastrointestinal disturbances such as nausea, vomiting, abdominal cramps, and diarrhea. Acute ingestion of large amounts of zinc can lead to stomach and intestinal irritation. Copper (Cu) deficiency shows that excessive zinc intake can interfere with the absorption and utilization of copper in the body. Prolonged high levels of zinc can lead to copper deficiency, which may result in anemia, neurological symptoms, and impaired immune function. Respiratory effects include irritation in the respiratory system and respiratory distress, coughing, and difficulty in breathing. Occupational exposure to high levels of zinc fumes, particularly in industries like galvanizing or welding, can lead to a condition called metal fume fever. To minimize the potential impact of ambient zinc on human health, the following measures can be taken occupational safety, consuming a balanced diet that includes foods rich in zinc, and adequate but not excessive zinc intake is important to maintain proper health. However, it is important to note that zinc toxicity from ambient exposure is relatively rare and Zn primarily occurs through ingestion of large amounts of zinc supplements or occupational exposure to high levels of zinc. For most individuals, maintaining a balanced diet and following recommended zinc intake guidelines are sufficient to meet nutritional needs without posing a significant health risk.

Iron (Fe) is an essential nutrient for the human body and plays a vital role in various physiological processes. However, excessive exposure to iron, particularly in ambient environments, can have adverse effects on human health. The health effects of iron exposure depend on the dose, duration, and route of exposure. Gastrointestinal effects, iron overload disorders, and iron overload can lead to organ damage, including liver cirrhosis, heart problems, and diabetes. Excessive iron levels can contribute to oxidative stress, which may damage cells, tissues, and DNA, potentially increasing the risk of various diseases, including cardiovascular disease, neurodegenerative disorders, and cancer. As with any heavy metal, the impact of ambient iron on human health can vary depending on specific circumstances, concentrations, and individual susceptibility. Therefore, considering local environmental conditions, regulatory measures and individual factors is crucial when assessing the potential health risks associated with iron exposure.

One of the most dangerous substances to which a person may be exposed at work or in the environment is cadmium (Cd), a by-product of the manufacturing of zinc. Cd is efficiently preserved in the human body, where it builds up throughout a lifetime and is toxic to the kidney, especially to the proximal tubular cells, either through direct bone damage. The overall impact of

the kidneys and bones may be negatively impacted by the current levels of Cd in industrialized zones (Bernard, 2008). According to Nawrot et al., (2006), lung cancer development is associated with an increased Cd.

Nickel (Ni) is a heavy metal that can have an impact on human health when present in ambient environments. Exposure to nickel can occur through inhalation, ingestion, or dermal contact with nickel-containing particles or compounds. Which influences the allergic reactions contact dermatitis, which is characterized by skin redness, itching, and rashes. People with a nickel allergy may experience these symptoms when they meet nickel-containing objects like jewellery, coins, or metal alloys. Fumes with Ni lead to respiratory effects like irritation of the respiratory system, coughing, wheezing, and shortness of breath. High-level exposure to nickel compounds, particularly nickel sub sulfide is linked to an increased risk of lung cancer. Asthmatic reactions such as difficulty in breathing and chest tightness are also associated with Ni ingestion. Nickel refining by-products are carcinogenic to humans. Industries like mining, smelting, and nickel refining, are associated with an increased risk of lung and nasal cancers. The regulation includes implementing engineering controls, providing personal protective equipment, and conducting regular monitoring of workplace air quality. Environmental regulations by government agencies establish and enforce regulations within acceptable environmental standards. This helps to reduce the overall ambient nickel levels in the environment.

Cadmium (Cd) is a toxic heavy metal that has adverse effects on human health when present in the ambient environment. Exposure to cadmium can occur through inhalation of contaminated air, ingestion of contaminated food or water, or direct dermal contact with cadmium-containing materials. The health effects of cadmium include kidney damage, and kidney dysfunction, leading to conditions such as tubular proteinuria, renal tubular dysfunction, and ultimately, kidney failure. Cadmium can interfere with calcium metabolism, leading to reduced bone density and increased risk of osteoporosis, including joint pain and fractures. Occupational exposure to cadmium has been linked to an increased risk of lung cancer. Reproductive and developmental effects are high levels associated with adverse reproductive effects, including reduced fertility and potential harm to fetal development. Some studies suggest that chronic cadmium exposure may contribute to cardiovascular diseases. Cadmium contamination like certain shellfish, cereals, and vegetables, can help reduce dietary exposure. Public awareness about cadmium exposure can help individuals

make informed choices and take appropriate precautions to minimize their exposure. It is important to note that the impact of ambient cadmium on human health varies depending on the specific circumstances and concentrations involved.

Copper is an essential trace element required for various physiological processes in the human body. It is necessary for optimal health in small amounts, and gastrointestinal distress, including nausea. This is often associated with acute exposure or accidental ingestion of copper-contaminated substances. Prolonged exposure to elevated levels of copper can lead to disrupt liver function. Neurological symptoms such as tremors and cognitive impairments are associated with high Cu levels. Allergic reactions are possible on skin contact with copper-containing materials. Genetic disorders, such as Wilson's disease, are characterized by impaired copper metabolism and excessive copper accumulation in various organs, including the liver, brain, and kidneys. The focus should be on minimizing excessive exposure to copper, particularly from non-dietary sources or in cases of specific health conditions that require careful copper management, such as Wilson's disease. As with any heavy metal, the impact of ambient copper on human health can vary depending on specific circumstances, concentrations, and individual susceptibility. Therefore, considering local environmental conditions, regulatory measures and individual factors is crucial when assessing the potential health risks associated with copper exposure.

The assessment of heavy metal contents in the ambient air of Coimbatore City, Tamil Nadu, India, revealed elevated levels of lead. The study emphasizes the importance of addressing the sources of HM pollution and implementing appropriate measures (Vijayanand et al., 2008). The health risks associated with heavy metals in coarse and quasi-accumulative particulate matter in Mumbai City, located on the Western Coast of India. The study identified the presence of six (Zn, Fe, Cu, Pb, Ni, and Cr) heavy metals at detectable and one (Cd) heavy metal at below-detectable levels (Botle et al., 2020).

1.5 Columnar properties of aerosols based on Satellite observations

Satellite observations refer to the use of satellite instruments and sensors to gather data and information about the Earth and its environment from space. These observations provide valuable insights into a wide range of natural and human-induced phenomena occurring on our planet. Satellites are different types of sensors and instruments, including cameras, spectrometers, radar systems, and thermal sensors. Each sensor captures specific wavelengths of electromagnetic

radiation or other signals, allowing to study different aspects of the Earth's atmosphere, land surface, oceans, and other environmental variables. Satellite observations have proven to be crucial for remote areas such as difficult to take manual readings. Satellite monitoring is useful for some extent of research areas like weather Forecasting satellites provide continuous monitoring of the Earth's atmosphere, collecting data on cloud cover, temperature, humidity, wind patterns, and other meteorological parameters. This information is crucial for weather forecasting, storm tracking, and understanding climate patterns. Climate monitoring satellites play a vital role in monitoring climate-related variables, such as sea surface temperatures, ice cover, vegetation health, and atmospheric greenhouse gas concentrations. Long-term satellite observations contribute to understanding climate change and its impacts on the earth's climate. Environmental monitoring satellites helps in monitoring environmental changes and provide data on deforestation, land use changes, urbanization, pollution, and natural disasters like wildfires, floods, and hurricanes. This information aids in land management, conservation efforts, and disaster response planning. Air Quality Monitoring satellite observations contribute to monitoring air pollution by measuring the atmospheric composition and identifying sources of pollutants. This data assists in assessing the quality of the air we breathe and supporting efforts to mitigate pollution. Geology and Geophysics satellites with radar systems can map and monitor changes in Earth's topography, measure surface deformations caused by tectonic activity or volcanic eruptions, and detect the groundwater. These observations aid in geological and geophysical studies.

Oceanography satellites provide valuable data on ocean currents, such as the sea surface temperatures, and other marine ecosystems. These observations are crucial for studying ocean circulation patterns, monitoring marine life, and understanding the impacts of climate change on oceans. Satellite observations provide a global perspective and enable scientists to gather data over vast areas, they complement ground-based observations and models, filling gaps in spatial and temporal coverage. These observations are vital for scientific research, policy-making, resource management, and understanding our planet's dynamic processes.

Furthermore, satellite observations support various applications in sectors like agriculture, transportation, communication, and navigation systems. They contribute to disaster management, early warning systems, and humanitarian efforts during natural disasters. As satellite technology continues to advance, satellite observations are becoming increasingly sophisticated, providing

higher-resolution data, improved accuracy, and real-time monitoring capabilities. These advancements further enhance our understanding of the Earth's systems and contribute to addressing global challenges related to climate change, natural resource management, and sustainable development. Satellite observations clearly show the regional-scale changes in aerosol content as well as composition and absorption. The analysis of the aerosol loading in the last 2-decades shows a positive (increasing) trend over Kanpur and other locations in South Asia (Ramachandran and Rupakheti, 2022).

1.6 Source –receptor modeling

The source of airborne particulate matter using receptor models has been widely practiced. In recent years factor analysis-based models such as Positive Matrix Factorization (PMF) and UNMIX have gained popularity in this field of source analysis. However, accurate interpretation of the results relies on understanding the various influencing variables involved in the modelling process. The main chemical species reported as markers in the source studies. These species as a valuable resource for interpreting source profiles and enhancing the accuracy of source apportionment studies. The significance of considering multiple variables, employing appropriate sources, and understanding the complexities involved in source apportionment modelling to ensure reliable and meaningful results in the field of airborne particulate matter analysis.

Air quality models simulate the impact of emission scenarios on pollutant concentrations. In certain cases, source-receptor relationships can replace these models to quickly represent the link between emissions and concentrations. Integrated Assessment Models also employ source-receptor relationships for rapid scenario responses. This study introduces a new approach to designing a source-receptor relationship in air quality modelling. The approach reduces the number of simulations needed for training and offers flexibility in defining emission sources. A regional domain application demonstrates the effectiveness of the proposed approach. The following researchers demonstrated and included such type of study in the analysis of the source-receptor relationship.

Soni et al., (2020) investigated PM_{10} and $PM_{2.5}$ concentrations in Dehradun, Himalayas. The study indicated seasonal variations with higher concentrations in the winter season (PM_{10}: 90 ± 32 μg/m³, $PM_{2.5}$: 63 ± 27 μg/m³). The major sources identified in the study include soil/road dust, vehicular and industrial activities, mixed aerosols, and anthropogenic burning. Polluted aerosols at higher

altitudes indicated the movement of neighbouring region pollutants toward the receptor location. Health risks from PM inhalation were identified. The CALIPSO data assessed aerosol vertical profiles to study neighbouring pollution transport.

Tasic et al., (2010), demonstrated the use of back trajectory analysis for source identification with the help of a 5-year PM_{10} dataset (2004-2008). PSCF values obtained in the study represent the conditional probability of higher PM concentrations being related to the passage of air parcels through specific cells during transport to the receptor site. Cells with high PSCF values indicated areas with potential high contributions of PM. HYSPLIT model was employed to compute backward trajectories at different heights above ground levels (300, 500, 1000, 1500, 2000, 3000 m). Daily trajectories were evaluated for 2 days using a grid with 0.50 X 0.50 latitude and longitude cells. The study identified three $PM_{2.5}$ sources - fossil fuel combustion (40%), metallurgical industry (13%), and resuspended road dust (47%). PSCF indicated frequent PM_{10} transport from the west, northwest, and southwest, suggesting multiple source regions. CWT analysis revealed local and regional sources as major contributors to PM_{10} concentrations.

The significance of implementing new emission inventories in Seoul, Korea reported a notable decrease in NO concentrations from 33.1 to 21.3 ppb (Vellingiri et al., 2016). Both trajectory analysis and potential source contribution function indicated that the primary source pathways responsible for the recent rise in NO_2 concentration at the study site are the northern China region and local emission sources, emphasizing their significant influence (Li et al., 2022).

The advanced 3D-PSCF-CONC method yielded important findings in the Metropolitan Area of São Paulo (Dos and Hoinaski, 2021). Local vehicular sources significantly contributed to pollution levels at the receptor, while long-range transport from industries and biomass burning impacted the region. Incorporating concentration fields improved source estimation accuracy, benefiting air quality management efforts.

The majority of Source Apportionment studies (94% of 51 studies) are attempted during the period between 2007 and 2016 (Singh et al., 2017). Approximately 55% of these studies focused on a few specific urban stations, namely Delhi, Dhaka, Mumbai, Agra, and Lahore. Due to the lack of local particulate source profiles and emission inventories, positive matrix factorization and principal component analysis were the primary choices (62% of studies), followed by chemical

mass balance (CMB) (18%). Metallic species were commonly used as source tracers, while back trajectory analysis methods were used less frequently.

To update the emission inventories of primary $PM_{2.5}$ from major sectors, a combination of source-oriented and receptor models was utilized (Zhang et al., 2023). The Bayesian Inference method was employed to enhance the accuracy of these updates. To efficiently construct the source-receptor sensitivity matrix, an adjoint model was developed. This matrix provided crucial information regarding the relationship between measurements and changes in emissions from different sources in various regions.

1.7 NOAA HYSPLIT Back trajectory analysis

NOAA's Air Resources Laboratory (ARL) conducts innovative research on the boundary layer, a critical part of our atmosphere. The studies in boundary layer chemistry and physics enhance regional weather, air quality, and climate predictions. ARL provides essential information and forecasts for emergencies like industrial accidents, wildfires, volcanoes, and severe air pollution events. By utilizing ARL's data, local managers can make informed decisions regarding evacuations. To establish all decisions HYSPLIT model is a versatile tool used for over 30 years in atmospheric sciences. It analyses air pollutant transport, identifies sources, and calculates concentrations using a hybrid approach. HYSPLIT tracks release, forecasts smoke, analyses dust, studies emissions, and assesses allergen and ash transport. With a user-friendly interface, it computes trajectories, supports various motion options, and integrates ensemble dispersion. The model also evaluates air concentrations, including particles, deposition, and multiple pollutants. HYSPLIT aids in understanding pollution dynamics, developing mitigation strategies, and is essential in air pollution research. HYSPLIT model enhances air pollution research with trajectory analysis, and air concentration capabilities, and automates source-receptor assessment. It supports ensemble trajectories, high-resolution simulations, and diverse meteorological datasets. Utility programs aid data manipulation. HYSPLIT enables comprehensive and accurate air pollution studies.

The HYSPLIT model is a basic GUI interface model. Outputs can be displayed as postscript files and converted to GIF, GrADS, ArcView, and Vis5D formats for easy sharing. With continuous development, HYSPLIT remains valuable for air pollution research (Stein et al., 2015). Its robust capabilities and support for diverse meteorological data sources make it versatile. HYSPLIT aids

in investigating pollutant transport, dispersion, and deposition, understanding their impacts, and informing air quality management decisions.

The incorporation of features from the Stochastic Time-Inverted Lagrangian Transport (STILT) model into the Hybrid Single-Particle Lagrangian Integrated Trajectory (HYSPLIT) model has resulted in a unified dispersion model that offers a wide range of applications and improved capabilities (Loughner et al., 2021). The ability to perform both time-forward and time-reversed simulations enhances the versatility and flexibility of the model. The inclusion of STILT's stochastic elements adds realism and uncertainty analysis to the model, providing a more accurate representation of pollutant dispersion in complex meteorological conditions. Overall, this integration represents a significant advancement in dispersion modelling, benefiting researchers and practitioners in the field of atmospheric sciences and air pollution studies.

Lagrangian trajectory models require meteorological data, emission inventories, and information about the initial location or release point (Bowman et al., 2013). These inputs determine the movement of air parcels or particles, enabling accurate simulations of atmospheric transport and dispersion. Comprehensive data ensures reliable model outputs for studying air quality and environmental impacts. Lagrangian kinematic models and suggests changes in model output practices to enhance accuracy.

Yassin et al., (2018) investigated the dust storms in Kuwait through backward trajectory simulations and source identification. By utilizing the NOAA HYSPLIT model and MODIS satellite observations, the origins of dust storms are identified, with the Sahara Desert and Arabian Desert being the primary sources. The study highlighted the impact of atmospheric conditions, particularly visibility and wind direction, on dust storm occurrences. The findings contribute to a better understanding of dust storm patterns and provide valuable insights for developing measures to mitigate the effects of dust storms on various aspects of life in Kuwait.

1.8 Lifetime and long-range transport of atmospheric aerosol

The lifetime and long-range transport of atmospheric aerosols play crucial roles in the Earth's climate system and air quality. Aerosols are tiny suspended particles in the atmosphere, ranging in size from a few nanometre’s to several micrometre’s. They can originate from natural sources such as dust storms, volcanic eruptions, sea spray, human activities like industrial emissions, and the

burning of fossil fuels. Local sources and long-range transport of pollutants significantly affect $PM_{2.5}$ at receptor locations (Mahapatra et al., 2018).

The lifetime of atmospheric aerosols refers to the time they spend suspended in the air before being removed through various processes. This lifetime can vary greatly depending on the aerosol type, size, and atmospheric conditions. The residence time of atmospheric aerosol particles is presented in Table 1.1. Some aerosols have short lifetimes, remaining in the atmosphere for hours to days, while others can persist for weeks to months. The removal mechanisms for aerosols include wet deposition (precipitation), dry deposition (settling onto surfaces), and gravitational settling.

Table 1.1 Residence Time of Atmospheric Aerosol Particles

Level in the Atmosphere	**Residence Time**
Below about 1.5 km	0 to 2 days
Lower troposphere	2 days to 1 week
Middle and upper troposphere	1 to 2 weeks
Tropopause level	3 weeks to 1 month
Lower stratosphere	1 to 2 months
Upper stratosphere	1 to 2 years
Lower mesosphere	4 to 20 years

However, the long-range transport of aerosols allows them to travel vast distances, often crossing continents and even oceans. This transport occurs primarily in the free troposphere, the layer of the atmosphere above the planetary boundary layer where most of the weather phenomena and surface emissions are concentrated. Aerosols can be transported over thousands of kilometres, leading to their redistribution on a global scale. Several factors influence the long-range transport of aerosols. First, meteorological conditions such as wind patterns, atmospheric stability, and air masses play a significant role. Prevailing winds and weather systems can carry aerosols over long distances, especially in the mid-latitudes where the jet streams are prominent. Strong vertical mixing and convective processes can also lift aerosols high into the atmosphere, enhancing their potential for long-range transport. Second, the size and properties of aerosols affect their transport

behaviour. Larger particles tend to settle more quickly due to gravitational forces, while smaller particles can remain suspended for longer periods and travel farther distances. Additionally, aerosols can undergo physical and chemical transformations during transport, such as collision and merging of particles and chemical reactions, which can alter their size, composition, and hygroscopic properties, further influencing their transport characteristics.

Long-range transport of aerosols has important implications for climate and air quality. Aerosols can scatter and absorb sunlight, affecting the Earth's energy balance and influencing regional and global climate patterns. They can also act as cloud condensation nuclei, altering cloud properties and precipitation patterns. In terms of air quality, long-range transport can transport pollutants over significant distances, impacting remote areas far from their sources and leading to transboundary pollution. Understanding the lifetime and long-range transport of atmospheric aerosols is crucial for accurate climate modelling, air quality assessments, and the development of effective mitigation strategies. Scientists employ satellite observations, ground-based measurements, and atmospheric models to study and predict aerosol transport patterns, unravel their sources and transformations, and assess their impacts on climate, air quality, and human health.

The diurnal variation of black carbon concentration is influenced by boundary layer mixing and anthropogenic activities (Tripathi, 2005). Kanpur's black carbon levels are comparable to other Indian megacities but much higher than similar locations in Europe, the USA, and Asia. These high black carbon concentrations in Kanpur contribute to large surface cooling and lower atmospheric heating, which can have regional climate impacts.

Jethva et al., (2005) presented a comparison of AOD retrieved from MODIS with the Aerosol Robotic Network (AERONET) data for the year 2004 over Kanpur, an industrial city lying in the Ganga Basin in the northern part of India. The entire Indo-Gangetic basin was dominated by the fine-mode particles during the winter (November to January) with AOD in the range of 0.4–0.6. The study seasonal variability of aerosols over the Indo-Gangetic basin. Results reported indicate that the Indo-Gangetic basin has the largest aerosol optical depth in India during both seasons.

Sarkar et al., (2006) discuss the analysis of the spatial variations of aerosol and aerosol forcing for major populated cities in India. A sensitivity study reported that longwave atmospheric cooling becomes more prominent with the increase in the amount of absorbing aerosols and a decrease in

water vapor, while longwave forcings are found to vary only by 1% for differing ozone concentrations (Ramachandran et al., 2006).

The Trajectory-based Potential Source Apportionment tool kit was utilized to identify sources of respirable particulates in Kochi, India (Shanavas et al., 2020). Data from five regulatory monitoring stations collected over five years (January 2011 to October 2016) were analysed at both local and regional scales. Concentration field analysis utilized back trajectories generated by the HYSPLIT model with atmospheric reanalysis data.. Findings revealed contributions from local traffic activities during low wind conditions and from a nearby industrial area during high-speed winds at most stations. Back trajectory analysis identified potential source areas in Kerala and the neighbouring state of Tamil Nadu, as well as the Arabian Sea to the west. The study showcased the effectiveness of TraPSA as a tool for understanding the potential source areas impacting particulate matter concentrations in Kochi.

(Jia et al., 2021) The results of the study revealed two distinct periods with different Odor sources. In Period 1 (January 1st, 2019 to October 31st, 2020), the landfill emerged as the major source of the Odor, the complaints received, 65% reported wind-carrying Odors from the landfill, and 88% of these complaints originated from residences located within a 500-meter radius of the landfill site. And the wind predominantly transported the Odor from the landfill. In Period 2 (November 1st, 2020 to December 15th, 2020), the sewage plant became the major source, Among the total complaints, 33% indicated wind direction from the sewage plant, and a significant 85% of these complaints were registered by residents living within a 1000-meter distance from the sewage plant. Using the trajectory and proximity analyses.

The influence of continental outflow on long-range transport was attempted by Hsiao et al., (2017). The variations were associated with different long-range transport patterns of air pollutants, including biomass-burning aerosols in spring and potential anthropogenic emissions in autumn. Comparisons with measurements from Doi Ang Kang Meteorology Station in Thailand and backward trajectories provided insights into the origin of aerosol types transported to the Atmospheric Background Station during different seasons.

Concentrations of water-soluble ions, organic carbon, and elemental carbon of size-resolved atmospheric aerosols were measured in Shanghai, China in July and August 2015. Backward trajectory and PSCF models were used to identify the potential source distributions of size-

resolved particles and $PM_{1.8}$-associated atmospheric inorganic and carbonaceous aerosols (Ding et al., 2017). The results showed the air masses originated from heavily industrialized areas, including the Pearl River Delta region, the Yangtze River Delta region, and the Beijing-Tianjin region. Long-range transport influenced the pollution in July, while local and intra-regional transport played a significant role in August. These findings highlight the significant contributions of particulate pollutants from long-range transport and shipping to air pollution in Shanghai. The significant contribution of particulate pollutants from long-range transported air masses to PM levels of Shanghai in summer.

(Kumari et al., 2020) Ground-based measurements and satellite observations were used in Indo-Gangetic Plain to study the impact of long-range transport from dust storms (event 1) and crop residue burning (event 2). The spatial distribution and temporal variation of ambient PM were assessed at 15 air quality monitoring stations in Rajasthan, the north-western IGP, and the downwind region. During the dust event, $PM_{2.5}$ and PM_{10} mass concentrations were 1.2-3.3 and 2.2-4.6 times higher than the National Ambient Air Quality Standards (NAAQS) near the Thar Desert. Stations in the north-western IGP showed increased $PM_{2.5}$ and PM_{10} levels during the crop residue burning period. Satellite observations and backward air-mass trajectories indicated that aerosols transported from the Thar Desert resulted in reduced O_3 levels during the dust event, whereas transport of O_3 precursors enhanced the photochemical production of O_3 during the crop residue burning period at Agra.

One of the significant findings of this research is the identification and quantification of marine-derived aerosols in the Arabian Sea region (Bikkina et al., 2020). The study highlights the importance of sea-surface emissions in contributing to aerosol composition, particularly the presence of sea salts and organic compounds originating from marine biota. This understanding of marine sources is crucial for accurately assessing regional air quality and its impact on climate.

1.9 Importance of the study

The study on the use of satellite data and back trajectory analysis for prediction and retrieval of $PM_{2.5}$ and identification of regional contributions by long-range transport is of significant importance for several reasons.

- Improved Air Quality Prediction of $PM_{2.5}$, the $PM_{2.5}$ major air pollutant that poses serious health risks to humans and the environment. By utilizing satellite data, researchers can

enhance their ability to predict and forecast $PM_{2.5}$ concentrations more accurately at ground-level concentrations. This information is crucial for issuing timely air quality alerts, implementing pollution control measures, and protecting public health.

- Satellite Remote Sensing Advancements, the study highlights the advancements in satellite remote sensing technology, which enables the measurement of ground-level $PM_{2.5}$ concentrations over large geographical areas with less resolution. Satellite data provide a comprehensive view of aerosol particulates distribution, overcoming the limitations of ground-based monitoring networks that may have sparse coverage, especially in remote locations or less-developed regions.
- Long-Range Transport of pollutants from their sources, impacting air quality in faraway distant regions. By employing backward trajectory analysis, researchers can trace the origins of $PM_{2.5}$ and identify the regions responsible for its long-range transport. This understanding is crucial for developing effective air quality management strategies that involve cooperation between different regions and countries' boundaries.
- The study's focus on the source-identifying regional contributions to $PM_{2.5}$ levels helps in source-origin impact. By distinguishing between local emissions and transported pollutants, policymakers can prioritize control measures and allocate resources more effectively to mitigate the impacts of specific pollution sources.
- Long-range transport of $PM_{2.5}$ is not only an air quality issue but also has implications for climate change. Black carbon, a component of $PM_{2.5}$, can accelerate the melting of snow and ice when deposited on these surfaces. Understanding the sources of $PM_{2.5}$ through satellite data and trajectory analysis can help assess its contributions to regional climate impacts.
- Policy Formulation and Implementation will consider the accurate information about the sources and transport of $PM_{2.5}$ is essential for designing evidence-based air quality policies. Governments and regulatory bodies can use the findings from this study to develop measures that target specific emission sources and address regional disparities in air pollution levels.
- Studies that utilize satellite data and trajectory analysis to assess $PM_{2.5}$ levels can raise public awareness about air quality issues. When citizens are informed about the sources

and long-range transport of pollutants, they are more likely to engage in sustainable practices, demand cleaner technologies, and support air quality improvement initiatives.

- This study bridges the gap between atmospheric science, remote sensing, and public health. It demonstrates the importance of collaboration between these disciplines to tackle complex environmental challenges like air pollution effectively.

In summary, the study focusing on the utilization of satellite data and back trajectory analysis to predict $PM_{2.5}$ levels, identify pollution sources, and assess regional contributions plays a crucial role in advancing air quality research, informing policy-making, safeguarding public health, and promoting global collaboration to combat the far-reaching consequences of air pollution

1.10 Need and Scope of thesis

This research study aims to explore and harness the potential of satellite data and back trajectory analysis as valuable tools for the identification of the source origins. Identification of Regional Contributions by Long Range Transport to employ back trajectory analysis to trace the origins of $PM_{2.5}$ pollutants over long distances. By identifying the source regions and understanding the pathways of these pollutants, we aim to assess the extent of regional contributions to local $PM_{2.5}$ levels.

The scope of this investigation encompasses various aspects related to the use of satellite data and back trajectory analysis for $PM_{2.5}$ source identification and the health impact of ambient heavy metals.

- The study will involve the collection of satellite-derived data, including aerosol optical thickness, and meteorological data. Appropriate data processing techniques will be explored to convert raw data into usable $PM_{2.5}$ concentration information.
- MLR model development will be employed to create accurate predictions for $PM_{2.5}$ concentrations. The aim is to achieve high accuracy in predictions of $PM_{2.5}$ levels across different spatial regions.
- By integrating the findings from satellite data and back trajectory analysis, the study will attempt to identify specific sources that contribute to $PM_{2.5}$ pollution in target areas. The research will assess the impact of long-range transport on regional air quality, particularly the introduction of external $PM_{2.5}$ pollutants from distant sources.

- The insights from this investigation will help the policy implications for air quality management, emphasizing the importance of regional cooperation to mitigate $PM_{2.5}$ pollution and its adverse effects on both local environments and public health. The study may require collaboration between atmospheric scientists, meteorologists, environmental experts, and data analysts to ensure a comprehensive and accurate assessment of the collected data.

Overall, this research will contribute to the broader goal of improving air quality monitoring and management strategies, with the potential to inform regulatory decisions and foster international cooperation in tackling air pollution issues.

1.11 Research gaps

Research gaps for the current scenario

- Studies related to Sources of fine particulates and their health impacts are extremely limited in India.
- This may be possibly due to inappropriate particulate source profiles, limited emission inventories, and differences in adopted methodologies.
- Application of back trajectory analysis for identification of regions contributing to particulate pollution is not well reported in India
- Studies on satellite data for air quality studies varied from region to region. Limited studies are reported for the Hyderabad region.
- Limited studies are reported on the long-range transport of $PM_{2.5}$ from different regions and on altitude analysis.

Based on these specific identified research gaps, the Objectives of the thesis were formulated as specified in section 1.13

1.12 Objectives

The following objectives are obtained from the research gaps

1) Assessment of health impacts caused by $PM_{2.5}$ bound heavy metals using Hazard Quotient and Hazard index.
2) Application of back trajectory analysis for identification of regions contributing to $PM_{2.5}$ bound heavy metals.

3) Studies on the use of satellite data (MODIS AOD) for missing data retrievals and prediction of $PM_{2.5.}$
4) Application of back trajectory analysis in conjunction with Concentration Weighted Trajectory (CWT), Potential Source Contribution function (PSCF), and cluster analysis to arrive at potential source regions for Hyderabad and Warangal.

1.13 Organization of the thesis

The thesis has been composed of 6 chapters, as mentioned:

Chapter 1: The "Introduction" chapter deals with the research background such as the atmospheric pollution due to the particulate matter and the$PM_{2.5}$ bond heavy metals. The health impact associated with the heavy metals, as well as the satellite retrievals of AOD to predict the ground level $PM_{2.5}$ concentrations. However, the identification of source regions based on the back trajectory analysis simplifies the long-range transport of pollutants towards the receptor location and Importance of the study, and aim and scope of the thesis

Chapter 2: The "Literature Review" chapter overview the studies available in the literature that are relevant to the present investigation. It has elaborated International and National status on $PM_{2.5}$ and heavy metals, aerosol sources and dispersion of the pollutants. Subsequently urban pollution influence on local meteorology relates with the aerosol concentration, as well as importance of the backward trajectory analysis, and a summary of literature and research gaps are well discussed.

Chapter 3: The “Materials and Methods “chapter outlines the analysis of major sources of air Pollution in the study area and the monitoring of the dust sample. Metal analysis using the MP-AES instrument instructions well discussed as well as non-carcinogenic and carcinogenic methodology for the health risk assessment, and the HYSPLIT model was assists in the identification of the source from the long-range transport of pollutants

Chapter 4: The title of this chapter is “Estimation of $PM_{2.5}$ and source contribution by Backward trajectory analysis over Warangal region." This chapter describes the Variation of the $PM_{2.5}$ concentration and its associated HMs as well as the correlation coefficient within the HM. Exposure dose assessment and non-carcinogenic health risks describe the

health impact possibility. Backward trajectory approach to compute the dominating HM source identification at the receptor location.

Chapter 5: The “Estimation of surface $PM_{2.5}$ with MODIS Aerosol optical depth and source identification using trajectory analysis: A case of Hyderabad City, India " chapter describes a case study of Hyderabad City and the variation of meteorology and the local $PM_{2.5}$ concentration. The satellite AOD retrievals are useful for the prediction of the ground level $PM_{2.5}$. Source identification of the different altitude layers and different seasonal contributions covered at receptor location.

Chapter 6: The “Summary and Conclusions " chapter addresses the Summary and Conclusions of the present research as well as a few recommendations.

Chapter 2 Review of Literature

2.1 General

Air quality modelling and management is critical in urban areas as a variety of complex sources are contributing to pollution. Monitoring pollution is a difficult preposition in many nations as it involves time and money. Several methods come to light in order to monitor air quality to overcome the challenges. In this chapter, literature pertaining to air quality in terms of $PM_{2.5}$ and related aspects of long-range transport of pollutants, health effects of heavy metals bound to $PM_{2.5}$, satellite AOD for air quality assessment, etc., are presented.

2.2 International and National Status on $PM_{2.5}$

$PM_{2.5}$ is a major air pollutant that poses significant risks to human health and the environment. It is generated by various sources such as industrial emissions, vehicle exhaust, and residential combustion. Both international and national efforts have been made to address the issue of $PM_{2.5}$ pollution and improve air quality. The WHO has set guidelines for $PM_{2.5}$ exposure levels to protect public health. According to the WHO Air Quality Guidelines, the recommended annual mean concentration of $PM_{2.5}$ is 5 μg/m³, and the 24-hour mean concentration should not exceed 15 μg (WHO 2021). These guidelines provide a benchmark for countries to assess and manage their air quality standards. Almost all the global population (99%) breathes polluted air exceeding WHO guideline limits. Low and middle-income countries face the highest exposure. Air quality is connected to the earth's climate and ecosystems worldwide. Ambient air pollution is reported to be responsible for around 4.2 million premature deaths worldwide (Murray et al., 2020). Implementing policies and investments that promote cleaner transport, energy-efficient homes, sustainable power generation, improved waste management, and access to clean household energy can effectively reduce outdoor air pollution.

The United States Environmental Protection Agency (EPA) in the United States has established the National Ambient Air Quality Standards (NAAQS) to regulate air pollutants, including $PM_{2.5}$. The current annual average standard for $PM_{2.5}$ is 12 μg/m³, while the 24-hour standard is set at 35 μg/m³. These standards are used to evaluate air quality across the country and guide pollution control measures. European Union (EU) has implemented air quality standards to control $PM_{2.5}$ pollution. The European Ambient Air Quality Directive sets a limit value for $PM_{2.5}$ at 25 μg/m³ for the annual average and 50 μg/m³ for the daily average. Member states are required

to report their air quality data, and actions are taken to improve air quality in areas where limits are exceeded.

Jahn et al., 2013, reported elevated $PM_{2.5}$ mass concentrations throughout Chinese megacity of Guangzhou's district, with ambient $PM_{2.5}$ levels that consistently exceeded the 24-h standards of the WHO. $PM_{2.5}$ pollution in Delhi averaged 150 $\mu g/m^3$ from 2012 through 2014, which is 15 times higher than the WHO annual-average guideline. Central Asian cities are air pollution hotspots with limited knowledge on air quality variation (Tursumbayeva et al., 2023). The study examined $PM_{2.5}$ levels and meteorological influences in six major cities (Almaty and Astana (Kazakhstan), Ashgabat (Turkmenistan), Bishkek (Kyrgyzstan), Dushanbe (Tajikistan), Astana and Tashkent (Uzbekistan). Results reveal severe air quality degradation, exceeding annual $PM_{2.5}$ limits by up to ten-fold with winter peaks at 3 locations (Almaty, Bishkek, and Astana). HYSPLIT model identified high $PM_{2.5}$ episodes due to regional pollutant transport. The study challenges previous emission inventory studies, revealing coal combustion as the primary $PM_{2.5}$ source. By analysing well-being surveys, particulate matter concentrations, and weather data, the study in the city of Ulaanbaatar (capital of Mangolia) reported a significant connection between air pollution and self-reported life satisfaction (Sanduijav et al., 2021). A multi-sensor characterization of the increasing pre-monsoon aerosol loading over northern India.

The new WHO global air quality guidelines aim to set even lower targets for reducing air pollution worldwide, encouraging significant decreases (WHO 2021). Achieving these guidelines will be challenging, especially for cities with high pollution levels, requiring several years of dedicated efforts. Simultaneously, the pressure to mitigate climate change and reduce fossil fuel usage has prompted many countries to establish temperature reduction goals in line with the Paris Agreement. This has resulted in an increase in clean energy generation and will eventually lead to widespread vehicle electrification in high-income countries by 2030. Burnett et al., (2018) estimates that the number of early deaths in India annually due to $PM_{2.5}$ could be more than two million. The Indo-Gangetic plain is known for having the largest number of brick kilns, which use outdated and inefficient combustion technology and rely on a combination of biomass and coal for fuel (Bhat et al., 2014). The states of Bihar, West Bengal, Jharkhand, Orissa, and Chhattisgarh are home to the country's largest coal mines and a cluster of power plants located in close proximity to these mines. During the 2010-11 period, 111 plants with a combined capacity of total electricity

generation capacity of 121 GW consumed 503 million tons of coal and generated an estimated 580 k tons of $PM_{2.5}$ particulates (Guttikunda et al., 2014). Additionally, the northern and north-eastern regions of India, particularly Punjab, Haryana, Delhi, and Uttar Pradesh, have several large power plants, making this area the most polluted part of the country. The geographical location of these cities in the north, being landlocked, exacerbates the impact of prevailing meteorological conditions on air quality, unlike some southern cities that benefit from land-sea breezes (Guttikunda and Gurjar, 2012).

In Jharia (Jharkhand State, India), the main contributors to air pollution were coal mining activities and active mine fires, with vehicular emissions playing a secondary role (Pandey et al., 2014). Additionally, wind-blown dust from unpaved roads also made a modest contribution to the overall air pollution levels and PCA recognized that coal mining and active mine fires (57.71% variance) are the main contributors of air pollutants in the study area Jharkhand. (Du et al., 2020) where poor air quality has caused a public health crisis. On average, 46% of population-weighted air pollution exposure originates from another state. Of the major sources, energy (75%) and industry (53%) see most of their emissions travel to another state. All sectors have 39% or more of their emissions travel across state boundaries in Indian states. The study in eastern India revealed elevated air pollution levels around clusters of coal-fired power plants (Tyagi et al., 2021). Results indicate that eastern India is becoming a new hotspot region for air pollution, with the highest levels recorded in India. Approximately 50% of residential $PM_{2.5}$ emissions are attributed to the <10% of households using cow dung as cooking fuel (Sharma et al., 2022). $PM_{2.5}$ emissions from open waste burning have seen minimal change from 2010 to 2020. Pollution levels in cities of varying sizes may be similar, despite differences in local activity levels. This similarity is attributed to the significant influence of the wider region on pollution levels, which currently plays a substantial role (Agrawal et al., 2021). Guttikunda et al., 2014 proposed two strategies for improving air quality in Indian cities. First, there is a need to raise public awareness and garner commitment to action from civic, commercial, and political sectors. Second, it is crucial to integrate air pollution mitigation efforts with broader social and economic development policies. For instance, addressing local challenges can involve implementing safer and more reliable public transportation systems, efficient waste management, dust-free roads, and promoting pollution-free industries and power plants. Investigate variations in indoor/outdoor concentrations of particulate matter during various activities. There is significantly a study in three different micro-

environments in Pakistan revelled higher levels of particulate matter in kitchens that use biomass fuels compared to other living areas (Colbeck et al., 2010). As a result, women and children are exposed to a greater extent as they spend more time in the kitchen. The urban concentrations observing the impact of traffic, it was evident that concerns regarding roadside $PM_{2.5}$ concentrations were more pronounced than non-roadside concentrations. A vertical dispersion experiment was conducted, demonstrating a significant decrease in $PM_{2.5}$ levels from 119.5 $\mu g/m^3$ at street level to 42.8 $\mu g/m^3$ on a third-floor rooftop. That the both horizontal and vertical dispersion of the pollutants exhibited sharp declines in $PM_{2.5}$ concentrations (Kinney et al., 2011).

Recent developments in remote sensing, global chemical-transport models, and improvements in coverage of surface measurements facilitate virtually complete spatially resolved global air pollutant concentration estimates. A recent study by Chatterjee et al., (2023) combining source-specific emission estimates to the grid simulations from a chemical transport model achieve the high-resolution hybrid PM2.5, and disease-specific mortality estimation was concluded the combined mortality burden associated with residential combustion (ambient) and household air pollution (HAP) in India is 0.72 million. However, primary data will be helpful for statistical modelling to evaluate the effectiveness of $PM_{2.5}$ emissions (Liu et al., 2012). Initial assessment of pollutants and spatial and/or temporal patterns of multiple pollutants in the ambient air are also attempted (Arku et al., 2008). Extensive evidence from past respiratory viruses and emerging research on COVID-19 demonstrated the harmful effects of air pollution on respiratory defense mechanisms, leading to more severe infections (Brauer et al., 2021). Taking decisive actions to reduce air pollution remains paramount to safeguarding public health and fostering a healthier future.

India has also been grappling with severe $PM_{2.5}$ pollution, particularly in densely populated cities. The Indian government has launched initiatives such as the National Clean Air Programme (NCAP) five-year action plan launched in 2019 to combat air pollution. The program aims to reduce $PM_{2.5}$ and PM_{10} concentrations by 20-30% by 2024. Implementation of measures such as stricter emission norms for industries and the promotion of electric vehicles is underway to achieve this goal (Broomandi et al., 2022). Despite significant efforts to reduce air pollution, the threat it poses to monuments and materials in East Asia remains severe and persistent. Exposure to ambient pollution, especially in urban areas, increases the vulnerability of World Heritage Sites to

degradation and corrosion. Therefore, special attention is needed to address this issue and protect these invaluable cultural treasures based on the dose-response calculations for material corrosion.

The following table represent some studies related to the air pollution sources in India, the developing cities which are increasing in the urban population as well as increase in the vehicles and daily activities of the human causes the air pollution in the urban regions. The Table 2.1 conclude the major sources dominating sectors from vehicles, industries, biomass burning and coal combustion.

Table 2.1 Studies related to the source identification over Indian region

Location	**Period**	**Data Source**	**Method**	**Main Result**	**Reference**
Delhi	2010-2014	CPCB monitors	CMB	Vehicles, biomass burning, and soil dust are the major sources of PM2.5	Sharma et al., 2017
Mumbai	2011-2012	CPCB monitors	PMF	Vehicles, sea salt, industrial emissions, and secondary aerosols are the major sources of PM2.5	Ramachandran et al 2017
Kolkata	2013-2014	CPCB monitors	PCA	Vehicles, coal combustion, biomass burning, and brick kilns are the major sources of PM2.5	Ghosh et al., 2018
Chennai	2014-2015	CPCB monitors	UNMIX	Vehicles, sea salt, industrial emissions, and secondary aerosols are the major sources of PM2.5	Kumar et al., 2016
Hyderabad	2015-2016	MODIS AOD	MLR	AOD can be used to estimate PM2.5 concentration	Shao, et al., 2017

				with moderate accuracy and uncertainty	
Warangal	2016-2017	Low-cost sensors	Kriging	PM2.5 concentration shows high spatial and temporal variability and exceeds the WHO guideline value	Kumar et al., 2017
Agra, India	January to December 2021	Fine particulate sampler(APM 550, Envirotech)	PCA	Carcinogenic risks of metals in PM2.5 is higher for adults than children.	Sah et al., 2023
Trombay (Mumbai, India)	2010 and 2011	Gent's dichotomous sampler	PMF	PM2.5 has major contributions from anthropogenic sources such as coal/biomass combustion (25.5%).	Police et al., 2018

2.3 International and National Status on Heavy Metals

In recent years, the presence of increased levels of heavy metals in urban ambient air is reported. Highways, an integral part of any urban development, only use a small percentage of urban land, however, they generate many types of combined pollutants, among which heavy metals, in particular Cadmium (Cd), Chromium (Cr), Copper (Cu), Nickel (Ni), Lead (Pb) and Zinc (Zn) are very common (Sankar et al., 2020; Wang and Zhang, 2018). Heavy metals are important environmental pollutants and are regarded as potential hazards to human health and natural ecosystems. Most of the heavy metals are dangerous to the human body since they tend to bio accumulate. The heavy metals derived from highways originate from diverse sources (Wang and Zhang, 2018). Studies indicated atmospheric deposition, input from traffic, carriageway breakup and surrounding land uses as the key sources of heavy metal pollution from roads (Sankar et al.,

2020; Wang and Zhang, 2018; Pal et al., 2018). The urban pollution impact associated with transportation has become an important issue as road traffic in India has increased rapidly. Aerosols are of immense scientific interest due to their complex nature and consequent effects on human health. Several researchers focused on human exposure to fine particulate matter and adverse impacts on human health. Fine particles penetrate deeper into the lung and reach up to the alveolar regions and thus their potential adverse health effect is much greater (Xing et al., 2016). Furthermore, these particles possess higher surface-to-volume ratios and are often generated through gas-to-particle conversion or combustion processes Many epidemiological studies have shown that both short-term and long-term exposures to fine particulate matter are associated with elevated rates of premature mortality (Bell et al., 2004; Woodruff et al., 2008; Tarín-Carrasco et al., 2021; Basith et al., 2022).

Primary elements generated from the Earth's crust (Al, Fe, and Ca) and anthropogenic sources (Pb, Ni, and Cd) were identified as major contributors to coarse and fine particles (Roy et al., 2023). PM-bound bacteria and the presence of potential respiratory pathogens indicated a significant risk to both human lung health and the environment. The heavy metals bound in the particulate matter are a major concern since they can induce polycyclic aromatic hydrocarbons and trace metals adsorbed to respirable particulate matter in higher concentrations (Kampa and Castanas, 2008; Singh et al., 2011).

Potential risk to children and adults from heavy metal exposure by calculating the average daily doses (ADD), non-cancer or hazard quotient (HQ), hazard index (HI), and cancer risk (CR) for ingestion, inhalation, and dermal contact pathways was attempted in a study in Pakistan (Khan et al., 2020). The results indicated that children had higher intake than adults, primarily through ingestion. The HI and CR values were observed within the acceptable limits (<1 and 10−4–10−6) of the US EPA. The removal of Topsoil and dust in urban areas are indicators of heavy metal contamination from atmospheric deposition (Krishna and Govil, 2007). Locations close to roads are severely polluted by heavy metals such as lead, zinc, copper, and chromium. Due to their non-volatile nature, heavy metals found in respirable particulate matter are less susceptible to chemical transformations. Consequently, they tend to persist in their emitted form without significant changes. Studies have shown that automobiles are the primary contributors to air pollution in urban areas, with a significant portion of heavy metals like Pb, Cd, Cu, Cr, and Ni being present in the

PM_{10} fraction (Pasha and Alharbi, 2015). These metals predominantly originate from anthropogenic vehicular activities associated with traffic.

CMB studies were reported by Gummeneni et al., (2011) for source identification of heavy metals bound to particulate matter. The study recommended controlling emissions from industries and automobiles and refuse burning. A similar study by Chaudhari et al., (2012) and Pasha and Alharbi, (2015) assessed heavy metals bound to $PM_{2.5}$ indicating industrial and automobile as major sources. Ambade, (2014) tagged Zn and Fe with natural sources and Pb, Cu, Cr, and Ni with anthropogenic sources. Several researchers reported the presence of heavy metals bound to particulate matter in their studies indicating industry, automobile, refuse burning, and other anthropogenic activities as sources of heavy metals (Kulshrestha et al., 2014; Bhuyan et al., 2018a; Ghosh et al., 2018; Alves et al., 2018).

Principal component analysis revealed that Cd, Cr, Ni, and Pb are associated with industrial sources whereas Zn and Cu are mainly contributed by vehicular traffic (Suryawanshi et al., 2016a). Contamination factor analysis showed that road dust samples are significantly contaminated by Zn and Pb. Step-wise linear regression model revealed that humidity and temperature significantly influence the mass concentration of $PM_{2.5}$ (Prabhu and Shridhar, 2019). Enrichment factor and principal component analysis revealed that anthropogenic activities such as vehicular emissions, road dust re-suspension, and biomass burning are the predominant sources of atmospheric $PM_{2.5}$. Particulate matter with Co, Cr, Ni, Cd, and Pb is reported to be carcinogenic while particulate matter with Mn, Fe, Cu, and Zn is non-carcinogenic (Pandey et al., 2017). Assessment of reliable fractions of heavy metals helps in the prediction of the degree of toxicity and pollution load. The exposure concentration (ng/m^3) was found highest for the industrial region followed by the residential. The health risk assessment of Cr, Mn, Co, Ni, Cu, As, and Cd provided useful information to the policymaker to frame regulation (Sah et al., 2019). They concluded the concentrations of Cr, Mn, Co, Ni, Cu, As, and Cd above the NAAQS and WHO limits, whereas those of Pb below the NAAQS and WHO 2014 limits and PM_{10} concentrations exceeded the annual mean standard set by the NAAQS in India, USEPA, and WHO Limits. Spatiotemporal variability of dust fall chemical constituents also provide important conclusions on the impact pattern of dust emissions on environmentally defined receptors (Gurugubelli et al., 2013). The dust fallout levels were found to be in the range of 13.73 ± 5.46 to 78.82 ± 34.81 g/m^2/month.

Overall air quality in the city of Kanpur was much inferior to other cities in India with respect to PM_{10} and $PM_{2.5}$. Also, heavy metals were almost 5–10 times higher than levels in European cities (Sharma and Maloo, 2005). (Gajghate et al., 2012a) This study demonstrates the re-suspension of dust released during traffic activities and soil erosion. However, the concentration and fluxes of Zn and V (anthropogenic elements) may be attributed to industrial emissions. Average individual trace element concentrations fluctuated between 0.003 $\mu g/m^3$ (Cr) and 3.43 $\mu g/m^3$ (Zn). CWT analysis indicated a higher influence of local sources during winter and post-monsoon (Chandra et al., 2014). Significant diurnal and seasonal variations were also reported. Enrichment Factor analysis indicated that Cd, Zn, Cu, Pb, and Ni were highly enriched relative to their crustal ratios with a substantial contribution from anthropogenic sources (Basha et al., 2010). Factor analysis, a receptor modelling technique has been used for identification of the possible sources contributing to the PM_{10} (Karar et al., 2006). Varimax rotated factor analysis identified four possible sources. Results of the correlation analysis showed that most of the metals exhibit moderate to weak relationships with each other. Seasonal distribution patterns indicate that most of the metals tend to exhibit maximum during the winter season, probably due to the temperature inversion. Health risks associated with heavy metals are reported by several researchers wherein exposure to heavy metal, exposure pathways, potential risk of cancer, vulnerable age groups, risk of long-term exposure, etc., were attempted (Sharma et al., 2008; Izhar et al., 2016; Dalal et al., 2013; Massey et al., 2013; Kulshrestha et al., 2009; Pervez et al., 2009).

2.4 Ambient Aerosol sources and dispersions

Atmospheric aerosol distributions are influenced by changes in precipitation, atmospheric mixing, and ventilation due to circulation changes. Emissions from natural aerosol sources strongly depend on climate factors like wind speed, temperature, and vegetation (Tegen and Schepanski, 2018). Several particle dispersion models are available which are used widely - Box models (AURORA, CPB, and PBM), Gaussian models (CALINE4, OSPM, CALPUFF, AEROPOL, AERMOD, UK-ADMS, and SCREEN3), Lagrangian/Eulerian Models (GRAL, TAPM, ARIA Regional), CFD models (ARIA Local, MISKAM, MICRO-CALGRID) and models which include aerosol dynamics (GATOR, MONO32, UHMA, CIT, AERO, RPM, AEROFOR2, URM-1ATM, MADRID, CALGRID, and UNI-AERO) (Holmes and Morawska, 2006). As well as deterministic methods are WRF-CMAQ, WRF-Chem, WRF/Chem-MADRID Operational Street Pollution Models (OSPM) and (CAMx) (Qi et al., 2023).

Primary aerosols are directly emitted into the atmosphere from specific sources. These can include natural sources such as dust and sea spray or anthropogenic sources such as industrial emissions, vehicle exhaust, and biomass burning. Primary aerosols are typically larger compared to secondary aerosols (Du et al., 2018; May et al., 2013; Mohr et al., 2009). Aerosol size distribution and chemical composition are crucial parameters that determine their dynamics in the complex atmosphere (Colbeck and Lazaridis, 2010). The aqueous-phase reaction presented a more complex effect on secondary aerosol formation at different relative humidity conditions. The formation efficiencies of secondary aerosols were enhanced during the lockdown as the increase of atmospheric oxidation capacity (Tian et al., 2021). Domestic energy use by the burning of solid biofuels is the largest contributor to ambient black carbon, primary organic aerosols, and anthropogenic secondary organic aerosols globally (Chowdhury et al., 2022). The variation in biomass burning contribution was inferred to be driven mainly by agricultural fires with relatively low combustion efficiencies (Cheng et al., 2021). Mechanical dispersion occurs when solid particles are mechanically generated and dispersed into the air. This mechanism is often associated with activities like construction, mining, and agricultural practices (Yan et al., 2023). These processes can generate dust particles that become suspended in the air as aerosols. Indoor and outdoor air pollution studies revealed that the Indoor levels were generally lower than the corresponding outdoor (Diapouli et al., 2011). Haze and Non-haze episodes study in Indonesia reported that the main cause of air pollution was uncontrolled biomass and peat burning. There was no consistent pattern for particle number concentrations during the haze period as compared to the non-haze period (Xu et al., 2015).

It is important to note that the sources of ambient aerosol and dispersions are complex and interconnected. Multiple processes can contribute to the overall aerosol composition and concentrations in the atmosphere, and their relative importance can vary depending on the location, season, and specific environmental conditions. Even though, heavy metals are known to enter the atmosphere from both natural and anthropogenic sources at trace levels, most of them are also introduced into the atmosphere by various anthropogenic activities only (Tian et al., 2015). The primary human-caused origins of pollutants include emissions from burning coal and oil, vehicle traffic and movement, stirring up of road dust, natural crustal materials, metallurgical processes, incineration, wind-blown dust from soil, piping, construction and demolition operations, waste incineration, components of various products, industrial and human activities, as well as industrial

point sources like ongoing and past mining activities, foundries, and smelters (Gummeneni et al., 2011; Kalaiarasan et al., 2018; Morantes et al., 2021; Patil et al., 2013).

2.5 Natural vs. Anthropogenic source's Influence on Urban Pollution

The contribution of each source varies depending on the type of activity like natural vs anthropogenic. The source-resolved model is compared to the results of chemical mass balance models (CMB) for Pittsburgh and multiple urban/rural sites, evidence that the organic PM emissions from natural gas combustion are overestimated (Lane et al., 2007). Regarding the natural and anthropogenic sources of aerosols in the northeastern Mediterranean area, Total Ozone Mapping Spectrometer (TOMS) -Absorbing Aerosol Index (AAI) one of the most useful space-borne data sets, offering long-term daily and global information on UV absorbing aerosol distributions.

The data is utilized as a proxy for the dust source, while the difference between MODIS and TOMS AOT is employed as an indicator of the anthropogenic aerosol component. The sources attributed to road traffic, while smaller contributions come from vegetative detritus, wood smoke, natural gas, coal, and dust/soil (Kubilay et al., 2005; Herman et al., 1997).

In order to assess the contribution of natural sources to $PM_{2.5}$ levels in North-West Germany, a one-year measurement project was conducted at two sites during the period from April 2008 to March 2009. Strong to moderate correlations between urban and regional areas were observed for factors categorized as aged marine aerosol, aged mineral dust, secondary sulfate, and fossil fuel combustion (Beuck et al., 2011). An integrated method combining Aerosol Robotic Network (AERONET) data, backward trajectories, and Potential Source Contribution Function (PSCF) modelling was used to identify probable transport pathways and magnitudes of source contributions for four characteristic aerosol types (Wong et al., 2013). The Hierarchical Bayesian Approach was used to estimate the contribution of urban growth to primary aerosols through statistical methods. The results suggested that The model performed moderately for most of Indian cities. The estimates were compared with the results of chemical transport models that provide more accurate but computationally expensive results, The approach is useful in locations without emission inventory (Misra et al., 2019).

2.6 Influence of Meteorology on Aerosol concentration

Aerosol concentration is significantly influenced by meteorological factors. Various aspects of meteorology, such as wind patterns, temperature, humidity, and atmospheric stability, play a vital role in the transport, dispersion, and accumulation of aerosol particles in the atmosphere. Wind patterns determine the direction and speed of air movement, affecting the spread of aerosols over large distances. Strong winds can disperse aerosols widely, while weak or stagnant winds can lead to localized accumulation. Temperature and humidity have an impact on the chemical reactions and physical properties of aerosols. Higher temperatures can increase the evaporation of water droplets containing aerosols, resulting in higher particle concentrations. Humidity levels also influence the growth of aerosols, affecting their size and composition. Atmospheric stability refers to the vertical profile of temperature and moisture in the atmosphere. Stable atmospheric conditions can trap aerosols near the surface, leading to higher concentrations. Conversely, unstable conditions promote vertical mixing and dispersion, resulting in lower aerosol concentrations. Moreover, meteorological conditions can interact with anthropogenic pollutant emissions, such as industrial processes, vehicle exhaust, and biomass burning. Temperature inversions, for instance, can trap pollutants close to the surface, causing elevated aerosol concentrations in urban areas. Meteorology plays a crucial role in shaping the spatial and temporal variations in ambient aerosol concentrations, thereby impacting air quality, climate, and human health.

Kumar et al., (2020) investigated the impact of meteorological parameters, including temperature, wind speed, and relative humidity at Varanasi, India. Temperature showed an insignificant relationship during the pre-monsoon period, but during winter months, it exhibited a negative trend with concentration. Wind speed exhibited a negative correlation throughout the observation period. Relative humidity showed a weak positive correlation with $PM_{2.5}$ and PM_{10} during winter months, while $PM_{2.5}$ did not show any significant relationship during the pre- and post-monsoon periods. The pollutants were reported to originate from various industrial activities, biomass burning, and vehicular emissions. The findings from these analyses provide valuable insights for future urban development planning and climate studies.

In India, assessment of the $PM2_{.5}$ concentration is challenging due to limited coverage, inconsistent data availability, and spatial-temporal gaps (Chelani, 2018). To address this, satellite-

based observations using MODIS were utilized in this study to estimate ground $PM_{2.5}$ levels in five cities in Maharashtra, India, from January 2016 to May 2017. The model incorporated meteorological parameters to enhance accuracy. Multiple linear regression (or) Multiple regression involves employing multiple explanatory variables to forecast the outcome of a response variable. A combination models, merging MLR and MLR residuals, was developed to derive more accurate estimates. The effectiveness of this approach was evaluated for two types of time series one with infrequent missing data and the other with frequent missing data. Spatial analysis revealed elevated AOD levels in Mumbai. Notably, integrating meteorological factors into the regression equation improved the MLR model's performance. Ultimately, the combination model outperformed MLR by considering the residuals of the MLR model. Tariq et al., (2021), focused on the analysis of aerosol optical properties using MODIS datasets, including AOD at 550 nm, Angstrom exponent (AE) at 440/870 nm, and enhanced vegetation index (EVI) over Pakistan. The goal was to gain a comprehensive understanding of aerosol variability and its relationship with meteorological variables such as temperature, relative humidity (RH), and wind speed (WS). The evaluation of Aqua-AOD against AERONET-AOD shows coefficients of determination (R^2) of 0.6724 over Lahore and 0.7678 over Karachi. Additionally, Aqua-AOD was validated using AOD data from Terra, MISR, and SeaWiFS. Notably, high AOD values (0.8–1) and low AE values (0.4–0.8) indicated the presence of dust aerosols in south and south-western Pakistan. The study also revealed significant interannual variation in AOD, with the lowest values (0.22) in January and the highest (0.58) in July. Furthermore, a positive correlation ($R \geq 0.6$) was observed between AOD and temperature in south-western Pakistan. Investigation into the variation of AOD and its physical-optical properties was attempted in Dibrugarh, northeast India, from October 2001 to November 2010 (Pathak and Bhuyan, 2015). The focus was on the diurnal AOD and its relationship with meteorological parameters. AOD consistently showed higher values during forenoon (FN) hours compared to afternoon (AN) hours in most seasons. This variation is primarily influenced by prevailing meteorological conditions and the change in the ray path from polluted industrialized areas in the east and northeast of Dibrugarh during the forenoon to cleaner mountain regions and the Brahmaputra River in the afternoon. This indicated a prevalence of coarse-mode aerosols during the forenoon compared to the afternoon. However, the climatological mean difference between MODIS Terra and Aqua AOD is smaller than the mean difference observed between ground based AOD measurements. Atmospheric visibility was analysed to

assess air pollution globally from 1973 to 2012 (Qu et al., 2020). In densely populated regions characterized by lower surface wind speeds, there tends to be a correlation with increasing air pollution and diminished visibility. Conversely, higher relative humidity (RH) tends to promote secondary aerosol formation and hygroscopic growth, further impairing visibility. The interaction between meteorological factors and major aerosol components in different regions globally can influence aerosol and cloud formation, impacting the evolution of the atmospheric boundary layer and air pollution. In East Asia, India, and Southeast Asia, the decline in visibility was linked to increased anthropogenic emissions and a more stable atmospheric boundary layer (ABL) characterized by weakened surface winds and reduced diurnal temperature range. Higher aerosol loading and cloud cover contribute to decreased solar radiation reaching the surface, further stabilizing the ABL and exacerbating air pollution.

The mass and optical properties of $PM_{2.5}$ were assessed in an ecologically sensitive zone in Central India (Sunder Raman and Kumar, 2016). The concentration of fine PM ranged from 3.2 μg/m³ to 193.9 μg/m³, with a median concentration of 31.4 μg/m³. The attenuation coefficients at different wavelengths and the scattering and absorption coefficients were also measured. The relationship between fine PM mass and attenuation coefficients varied seasonally, with the strongest correlation observed during the post-monsoon season. Fine PM mass exhibited the highest correlation ($r^2 = 0.81$) with a scattering coefficient at 550 nm during the post-monsoon season. However, monitoring optical properties alone as a surrogate for fine PM mass throughout the year was deemed unsuitable for the study location. MLR models were fitted for each season to assess the relationships between fine PM mass, optical properties, and meteorological parameters. The MLR model for the post-monsoon season explained over 88% of the variability in fine PM mass. However, the MLR models performed less effectively during the pre-monsoon and monsoon seasons, explaining only 31% and 32% of the variability, respectively. In the winter season, the MLR model accounted for 54% of the variability in $PM_{2.5}$. Variations in Black carbon (BC) mass concentration were studied at a high-altitude urban site, Srinagar (north-western Himalaya, India) in 2013 (Bhat et al., 2017). The study aimed to analyse temporal variations, meteorological influences, source contributions, and radiative forcing of BC. The highest mean monthly BC concentration (13.6 μg/m³) was observed in November, while the lowest (3.4 μg/m³) was in April. Autumn had the highest mean BC concentration (9.2 μg/m³), while spring had the lowest (3.5 μg/m³). The annual average BC concentration (6 μg/m³) was higher than other high-altitude

stations. Wind speed, minimum temperature, and total precipitation showed a negative correlation with BC, while evening relative humidity showed a positive correlation. Biomass burning was the main source of BC during autumn, spring, and winter, while both fossil fuel and biomass burning contributed equally during summer. Back trajectory simulations indicated the transport of BC from various regions to Srinagar, with westerly air masses being dominant except during summer.

Aerosol optical properties (AOPs) and particulate matter were measured continuously at an urban site in Delhi, India during the winter period (December 2011 to March 2012) (Tiwari et al., 2015). Higher values of scattering and absorption coefficients were observed in December, while lower values were observed in March and February. SSA was higher in January and lower in March. Bimodal distributions of scattering and absorption coefficients were observed during traffic rush hours and low boundary layer conditions, with lower values in the afternoon. Meteorological parameters such as wind speed, wind direction, visibility, and mixed layer depths were found to have a significant impact on AOPs and particle concentrations. There was a clear negative correlation between atmospheric visibility and scattering coefficient, absorption coefficient, and $PM_{2.5}$. AOPs and particle concentrations were significantly higher during foggy and dense foggy days, as well as when mixed layer depths were below 200 m and wind speed was below 1 m/s. The results indicate the crucial role of meteorological parameters in enhancing aerosol levels at ground level during the winter period in Delhi. Ravindra et al., (2022), investigated the impact of meteorological parameters and air pollutants on airborne pollen in Chandigarh, an urban city located in the Indo-Gangetic Plains. From June 2018 to June 2020. Temperature and wind were found to be the most influential parameters, showing a positive correlation with the annual pollen integral of Cannabis Sativa, Parthenium hysterophorus, Poaceae, and total pollen concentration. The study highlighted the distinct responses of each pollen taxon to meteorological parameters and air pollutants. It emphasizes the importance of examining pollen response at the taxon level and using long-term data to understand the relationships and trends among meteorology, air pollutants, and aerobiology for future scenarios and environmental changes. Guttikunda and Gurjar, (2012), attempted to study the role of meteorology in Delhi's pollution using the Atmospheric Transport Modelling System. The harsh and highly polluted winters in Delhi, a megacity, have significant impacts on health and transportation. Pollution levels during winter are two to three times higher than in summer, leading to delays and accidents. The pollution contribution was mainly from a combination of manmade factors, such as fuel burning,

and natural factors influenced by meteorology. Despite efforts to control pollution, fine particulate matter remains a major concern, averaging 80 to 100 μg/m^3 daily in 2009. The results show that tracer concentrations were consistently 40% to 80% higher in winter (November, December, and January) and 10% to 60% lower in summer (May, June, and July) compared to the annual average.

2.7 Satellite retrievals for Aerosol optical properties

Satellites collect the different types of remote sensing data which can be used for several purposes including estimation of aerosol concentrations. These instruments observe the Earth's surface and the atmosphere from space, capturing the interaction of sunlight with aerosols. The retrieval process involves analysing the radiance measurements acquired by the satellite sensors and comparing them to radiative transfer models. These models simulate the interaction of sunlight with aerosols and the atmosphere, considering factors such as scattering, absorption, and the influence of surface reflection. Through a series of algorithms and inversion techniques, the satellite data is processed to estimate the AOD values at different locations on the Earth's surface.

This retrieval process considers various factors, including satellite geometry, atmospheric properties, and surface characteristics. Satellite retrievals for AOD provide valuable information about the spatial and temporal distribution of aerosols on a global scale. This data is used for studying air quality, climate research, understanding aerosol sources and transport patterns, and validating atmospheric models. It's important to note that different satellite instruments and retrieval algorithms may have variations in the accuracy and spatial resolution of AOD measurements. Therefore, it is essential to consider the specific satellite platform and retrieval methodology when utilizing satellite-derived AOD data for scientific analysis and applications. Most of the researchers utilized AOD as one of the components to suit the purpose of the study.

Kumar, 2014, used AOD values at 550 nm from NASA's Terra and Aqua satellites' MODIS sensors. The study was carried out for the period 2003-2012 in Delhi, Northern India. The results indicated a notable increase in AOD values exceeding 25% in Delhi, India over the study period. Yearly mean AOD values derived from Terra/Aqua data showed a gradual increase at rates of approximately 0.005/0.009 per year. Winter mean AOD values exhibited a slightly higher increasing trend at rates of about 0.012/0.007 per year. Sharma and Kulshrestha, 2014, investigated the relationships between MODIS-derived AOD and SPM, NO_2, and SO_2 levels. In this study, SPM concentrations were analysed across different regions of India. Central and northern districts

generally exhibited higher SPM concentrations than the south. Nine out of the top ten districts with high SPM pollution were in Uttar Pradesh state. Zeeshan and Kim Oanh, 2014, carried out correlation studies between satellite AOD and ground monitoring PM considering synoptic patterns and meteorological factors. The correlation (R^2) between MODIS and Sun photometer AODs was above 0.8. The radiative and climatic impacts of the observed AOD variations for Bangalore were attempted in a study (Sreekanth, 2013). AOD values at 550 nm, derived from NASA's Terra and Aqua satellites' MODIS sensor were used for the study. Monthly mean AOD values show an increasing trend from January to May, with a secondary peak in July, and a minimum in December. The highest AOD values were reported in the monsoon season, lowest AOD values were reported in winter. Yearly AOD values increased mainly due to higher summer AOD. The results are compared with previous studies and other Indian locations.

MODIS data from the Terra satellite was used to analyse the spatial and temporal variations of aerosol particles in the North Eastern region of India (Kumar, 2013). The study revealed an increase of over 15% in aerosol optical depths across the North Eastern part of India during the last decade. The mean AOD values during summer were observed to be 0.60±0.07, while during the post-monsoon season, the mean AOD values were 0.07±0.02. The highest annual mean increase in AOD (>79%) was found in Guwahati. Furthermore, the study investigated the relationship between AOD and five cloud parameters, including water vapor, cloud fraction, cloud top temperature, cloud top pressure, and cloud optical depth, in order to enhance the understanding of aerosol-cloud interactions in the North Eastern part of India.

Spatial and temporal variations of aerosol particles in Southern India were explored using MODIS data from the Terra satellite (Balakrishnaiah et al., 2012). High AOD values were observed during the summer season in most regions, and the monsoon season in Pune, Visakhapatnam, and Hyderabad. The relationship between AOD and cloud parameters (water vapour, cloud fraction, cloud top temperature, and cloud top pressure) was analysed. Positive correlations were found between AOD and cloud fraction in some cities, while AOD showed negative correlations with cloud top pressure and cloud top temperature in Southern Indian regions. The correlation between AOD and cloud fraction was strongest for some cities while some of them indicated a weak correlation. Additionally, a strong positive correlation was observed between AOD and water vapour for all cities studied. However, there was a negative correlation

between AOD and cloud-top pressure as well as cloud-top temperature in the Southern Indian regions.

The impact of biomass burning and wildfires on atmospheric aerosol concentrations was analysed using satellite data in Greece (Kaskaoutis et al., 2011). The study examined various aerosol parameters, including Aerosol Optical Depth (AOD), effective radius, Angstrom exponent, mass concentration, cloud-condensation nuclei (CCN), OMI Aerosol Index (AI), single scattering albedo, absorption, and extinction optical depths. Smoke plumes from the fires were observed traveling southwards over thousands of km, affecting the central Mediterranean and North African coastal regions.

Agricultural residue burning in the Indo-Ganges region was found to significantly contribute to greenhouse gas emissions and aerosols (Vadrevu et al., 2011). This study utilized MODIS data to examine fire intensity, seasonality, variability, fire radiative energy (FRE), and aerosol optical depth (AOD) during the residue burning season. Fire counts exhibited two peaks in April-May and October-November, corresponding to wheat and rice residue burning. FRE variations aligned with the amount of burnt residues. The average AOD from 2003 to 2008 was 0.60. Increased AOD during winter correlated with the rice residue burning season. However, the AOD-fire relationship was weak during the summer. These findings underscore the importance of a comprehensive assessment of greenhouse gases and aerosols to address air quality concerns in the region.

Kharol et al., (2011), examined the use of remote sensing to analyse aerosols and their role in global warming and climate change in Hyderabad, India. Specifically, it compares aerosol optical depths (AOD550) obtained from Level 2 (10 × 10 km) and Level 3 (1° × 1°) Terra/Aqua MODIS (C005) data with ground-based measurements using the MICROTOPS-II sun photometer. Correlation coefficients (R^2) between Level 3 MODIS and ground-based AOD550 range from 0.30 to 0.46 across all seasons. Lower correlations were observed when utilizing Level 2 MODIS data (R^2 = 0.16-0.30). Level 3 MODIS AOD550 underestimates ground-based AOD550, whereas Level 2 AOD550 values surpass those of Level 3. Assessing Terra/Aqua MODIS AOD550 at a regional scale, particularly over urban/industrial areas with significant diurnal aerosol variation. Results indicated a relatively strong correlation (R^2 ~ 0.6-0.7) for the Level 3 dataset, but Level 2 data exhibit substantial scatter and weak correlations. Mean seasonal AOD550 values are similar, with

Terra AOD550 being higher than Aqua. Both satellite and ground-based measurements demonstrated increasing trends in AOD over Hyderabad, and the same was attributed to urban expansion, population growth, motor vehicle emissions, and local pollution.

A multispectral empirical model was developed using Landsat 8 Operational Land Imager satellite data to estimate the concentration of PM_{10} in Delhi, India (Saraswat et al., 2017). Ground monitoring stations in New Delhi provided PM_{10} concentration data that corresponded to the acquisition dates of the Landsat 8 satellite data. The visible bands of Landsat 8 imagery were used to calculate atmospheric reflectance, which was then correlated with PM_{10} measurements from the ground stations. The proposed algorithm's feasibility was assessed based on the correlation coefficient and root mean square error value. The results indicated that the suggested multispectral PM_{10} model can predict particulate matter concentrations with an acceptable level of accuracy. Multi-satellite observations and ground-based measurements are used to analyse a dust storm event in the Persian Gulf and Arabian Sea region on February 19-24, 2008 (Badarinath et al., 2010). The study utilized Indian geostationary satellite KALPANA-1 VHRR data and ground observations to analyse the temporal variation of the dust event, with the strongest intensity observed on 22 February. The OMI Aerosol Index (AI) was also examined to assess dust presence and plume location independently. The study observes a significant increase in Terra/Aqua MODIS AOD550 (> 1.0) and AURA-OMI-AI during the dust event. Additionally, AODs derived from sun photometers at six AERONET sites in South Asia confirm the presence of dust and its west-to-east transport.

Sreekanth et al., (2017), addressed the need for high-resolution data on PM_{10} mass concentrations for health and epidemiological studies in India. The results established empirical relations between AOD and PM_{10} mass concentrations in five Indian megacities. The goal is to predict surface $PM_{2.5}$ concentrations using high-resolution columnar AOD datasets. The study utilizes multi-city public domain $PM_{2.5}$ data and MODIS AOD data spanning almost four years. Positive correlations between $PM_{2.5}$ and AOD were found, with spatially varying regression coefficients observed through station-wise linear regression analysis. Multiple regression analysis indicated the impact of day-to-day variability in local meteorological conditions on the AOD-$PM_{2.5}$ relationship. A cross-validation approach using three years of data as a training dataset and one year as a validation dataset yielded an R^2 value of approximately 0.63. The performance of

MODIS Collection 6 AOD retrieval algorithms was evaluated for the Indo-Gangetic Plain (IGP) of South Asia (Mhawish et al., 2017). The study examined the Dark Target (DT) AOD at 3 km and 10 km resolutions, Deep Blue (DB) AOD at 10 km, and the merged DT-DB AOD at 10 km. The evaluation compared collected Aqua MODIS C6 AOD data with AOD measurements from six AERONET stations over the IGP from 2006 to 2015. The study investigated the impact of aerosol heterogeneity, including aerosol loading and type, on the uncertainty of satellite based AOD retrieval. Findings indicated that the DT algorithm at both resolutions over estimated AOD by 14-25%, with only 51.37-61.29% of retrievals falling within the expected error range. The DT 3 km algorithm under estimated surface reflectance compared to DT 10 km, which performs better in terms of collocation numbers and retrieval accuracy, especially in urban areas. DT 3 km performs the poorest.

Yan et al., (2021), made an attempt to study the importance of fine-mode AOD (fAOD) as an indicator of column-integrated anthropogenic particulate pollutants. The study developed a retrieval algorithm based on the latest global-scale MODIS aerosol product (Collection 6.1) to generate a 10-year global fAOD product. The product was validated by comparing it with fAOD derived from Aerosol Robotic Network (AERONET) measurements. The resulting root-mean-square error (RMSE) of 0.22 indicates good agreement between satellite-derived and AERONET. Ground-level RSPM was estimated using satellite remote sensing AOD data and ground-based meteorological measurements for Jaipur, a semi-arid region in North-western India (Soni et al., 2018). Multi-regression statistical models were developed using satellite MODIS Level 2.0 AOD to estimate RSPM values in the study area. The models considered factors such as the Height of the Planetary Boundary Layer (HPBL) and meteorological parameters to optimize the representation of MODIS AOD. The performance of the regression models was evaluated using statistical measures including Normalized Mean Square Error (NMSE), Correlation (R), and Fractional Bias (FB). The nonlinear multi-regression model performs the best for the study period and region, with a correlation of 0.80, and NMSE of 0.01. The coefficients obtained from MODEL V were also applied to Jodhpur and found to be effective. Mangla et al., 2020, compared AOD measurements from multiple satellites (MISR, MODIS, and OMI) with ground-based observations over the IGP region (2010-2017). The results showed a higher correlation with MODIS (R^2 = 0.7 at Gandhi College), followed by MISR and OMI AOD. MISR exhibited the highest percentage (58%) of data points within the error envelope. Both MISR and OMI consistently displayed a

negative bias trend for higher AOD, while MODIS showed a negative bias only over the Jaipur region. Seasonally, the IGP region exhibits higher AOD in summer due to dust storms. Comparing MODIS and MISR, MODIS generally exhibits higher seasonal AOD. The spatial correlation between MODIS and MISR was high during summer and winter seasons. However, the OMI sensor's performance in the IGP region does not match existing patterns. These findings provide valuable insights for selecting reliable satellite AOD products in future studies.

The impact of environmental attributes on the uncertainty in satellite-based AOD retrieval compared to AERONET measurements was assessed at 21 sites in North Africa, California, and Germany from 2007 to 2017 (Falah et al., 2021). The effects of spatial and temporal averaging techniques were examined. MAIAC AOD was then analysed based on different environmental attributes, including aerosol loading, dominant particle size, vegetation cover, and prevailing particle type. The expected retrieval error varied across these attributes, with more accurate AOD retrievals observed in highly vegetated areas. Retrieval accuracy was found to be sensitive to aerosol loading and particle size, with larger biases between MAIAC and AERONET AOD during high aerosol loading of coarse particles. (Kaskaoutis et al., 2009; Moorthy et al., 2005; Quinn, 2002; Tripathi, 2005 also reported similar findings from their research on AOD and satellite observations.

2.8 Source-Receptor modeling

Source-receptor modelling is a technique used to understand the relationship between the emission sources of pollutants and the locations where these pollutants are observed or measured. It involves analysing the transport and dispersion of pollutants from their sources to the receptor’s location, allowing for the identification and quantification of the contributions of different emission sources to the observed pollution levels. Source apportionment techniques are used to attribute the contributions of different emission sources to the observed pollution levels. This can be done through statistical methods, receptor modelling, or other data analysis techniques. Source-receptor modelling is valuable for understanding the spatial and temporal variations in pollutant concentrations and identifying the major emission sources responsible for pollution in specific regions. This information can be used for developing effective air quality management strategies, implementing pollution control measures, and assessing the impacts of different emission sources on air quality and public health.

Source Apportionment (SA) studies over different geographical divisions of IGP, Delhi, western, eastern, and central India indicated that more than 50% of the studies are focused on the Delhi National Capital Region (NCR) and IGP (Yadav et al., 2022). Based on the database is available on chemical characterization of ambient aerosols, only 49 offline and 16 online SA studies. The most studied size fractions are PM_{10} (34%) and $PM_{2.5}$ (28%) followed by 11% studies on PM_1 and only 5% on size-segregated SA of aerosols in India. The contributions of $PM_{2.5}$ emission sources were quantified in Busan, South Korea (Jeong et al., 2017). Three receptor models (PCA/APCS, PMF, and CMB) were used to analyse the data. The results showed that the secondary formation of $PM_{2.5}$ was the dominant contributor (45-60%) to $PM_{2.5}$ levels in Busan. Ship emissions were found to be a non-negligible contributor (up to 10%) according to PMF and PCA/APCS, but negligible according to CMB. The different models produced varying estimates of source contributions due to their limitations. Analysis of potential source contribution function and concentration-weighted trajectory revealed that long-range transport from sources in eastern China and the Yellow Sea significantly influenced $PM_{2.5}$ levels in Busan Dutta and Chatterjee, 2022, assessed aerosol pollution in India, focusing on long-term trends, source apportionment, and future projections for each state. Results indicated that most states in the Indo-Gangetic Plain are highly vulnerable, while central, western, and southern states are considered vulnerable. The study identified coal-fired thermal power plants, vehicular emissions, solid fuel/waste, and biomass burning as major aerosol sources.

2.9 Source identification based on backward trajectory analysis

Backward trajectory analysis utilizes atmospheric science to trace the origin and transport history of air masses or pollutants by calculating the trajectories of air parcels or particles in reverse from their current location back to their source region. This analysis aids in understanding the pathways, sources, and potential influences on the air masses or pollutants being studied. By analysing meteorological data and identifying source regions, researchers gain insights into long-range pollutant transport, the contribution of different regions to local pollution, and the influence of meteorological conditions and transport mechanisms. Backward trajectory analysis plays a crucial role in air quality studies, atmospheric pollution research, climate investigations, and understanding atmospheric transport and dispersion processes. However, studies on source identification based on trajectory are limited in India (Banerjee et al., 2015b)

Chandra et al., 2017 investigated trace metals associated with PM_{10} aerosols and their variations during different times of the day and different seasons in 2012. Principal Component Analysis (PCA) identified five components that explained 86.8% of the cumulative variance. PC1 represented 30% of the variance and was associated with metals of anthropogenic origin, while PC2 explained 28% of the variance and consisted of metals of crustal origin. These trace metals exhibited distinct seasonal and diurnal patterns. Cu, Pb, and Cd concentrations were higher during the night in all seasons, while Fe had higher concentrations during the daytime except in the monsoon season. During the post-monsoon season, Cu, Cd, Zn, and Pb had the highest mean values, likely due to winds carrying pollutants from waste/biomass burning and industrial activities in Punjab and Haryana regions. Concentration-weighted trajectory analysis indicated that metals of crustal origin were transported over long distances, while metals from anthropogenic and industrial sources originated from regional/local areas. Positive matrix factorization (PMF) and potential source contribution function (PSCF) analysis were used for identifying the sources of aerosols in the Indian Ocean Experiment domain (Bhanuprasad et al., 2008). Surface aerosol measurements and emissions inventory information was utilized to identify co-located sources from PSCF. PMF analysis identified six factors, including biomass combustion, industrial emissions, and two dust factors. These factors effectively predicted measured submicron PM concentrations. Probable source regions beyond India, such as Africa, West Asia, the Arabian Peninsula, and Southeast Asia were identified. These sources affected particulate matter concentrations in the INDOEX domain covered by the Ron Brown cruise.

Source identification and human health risks associated with elements in fine $PM_{2.5}$ over Agra, India were attempted by Sah, 2023. The average annual $PM_{2.5}$ concentration exceeded air quality guidelines, measuring 144.32 ± 57.18 $\mu g/m^3$. Winter exhibited the highest $PM_{2.5}$ concentration, followed by post-monsoon, summer, and monsoon seasons. Si had the highest concentration among the analysed elements, while V had the lowest. The concentrations of Cr, Ni, As, and Cd exceeded WHO limits, while V, Mn, and Pb concentrations were below the limits. Significant seasonal variations in element concentrations were observed. The HI for studied metals was 7.02 for both age groups. Carcinogenic risks due to Pb for both children and adults and due to Cd for children were lower than 1×10^{-6}. Carcinogenic risks for other studied metals exceeded 1×10^{-6}. The total carcinogenic risks for adults and children surpassed the acceptable limit of 1×10^{-6}. Hourly data was analysed to study NO_2 and O_3 levels at an urban background site in Seoul,

Korea (Vellingiri et al., 2016). The trajectory analysis was used to examine the contributions of variables in special cases with high NO_2 and O_3 levels (>60 ppb). A potential source contribution function with a grid size resolution of 0.25° × 0.25° was utilized to identify potential external sources of NO_2 and O_3 in the study area. The results indicated that both the northern China region and local emission sources were major contributors to the increase in NO_2 concentration at the site. For O_3, the influential source pathways included the oceanic and mountainous regions of China and Japan.

Air mass back trajectories in Toronto were analysed using cluster analysis and a neural network (Owega et al., 2006). The two techniques utilized different similarity criteria but yielded similar results regarding $PM_{2.5}$ emission sources and pollution levels associated with various air transport patterns. Both methods highlighted the cleaner nature of northerly and north-westerly patterns compared to southerly and south-westerly ones, as well as the impact of stagnant air masses. The conventional PSCF method was compared with the proposed 3D-PSCF-CONC method for the assessment of air pollution in the Metropolitan Area of São Paulo in Brazil (Dos Santos and Hoinaski, 2021). Using backward trajectories from the HYSPLIT version 4 model, a total of 1825 trajectories with the three models were analysed. The analysis suggested that vehicular sources near the receptor site contribute significantly to air pollution, while long-range transport of industrial emissions and biomass burning associated with sugarcane production also play a role. Overall, the 3D-PSCF-CONC method provides a valuable tool for understanding the air pollution process and identifying pollution sources accurately. Previous studies also reported results of back trajectory analysis and effective origin source regions and long-range transport of pollutants (Conte et al., 2020; Hong et al., 2019).

2.10 Summary of Literature

The summary presents a comprehensive overview of the widespread issue of $PM_{2.5}$ pollution and its bound Heavy Metals (HMs) associated with health impact. The global efforts to combat this problem, with various countries and international organizations setting air quality standards and guidelines. The World Health Organization (WHO) guidelines serve as a benchmark for evaluating and managing air quality, but despite these efforts, almost all global populations still breathe polluted air exceeding these limits, particularly affecting low and middle-income countries. The literature summary delves into specific case studies from different regions,

showcasing the severity of $PM_{2.5}$ pollution and its sources. India, in particular, faces significant challenges due to factors like coal mining, industrial emissions, and biomass usage for cooking, leading to severe air pollution levels. Furthermore, the study emphasizes the importance of addressing long-range sources of $PM_{2.5}$ pollution, recognizing the significant impact on public health, especially for vulnerable groups like adults and children. It highlights the critical need for comprehensive strategies to mitigate air pollution, integrating air quality efforts with broader social and economic development policies. To combat air pollution, various countries, including the United States and European Union, have established regulatory standards to control $PM_{2.5}$ emissions, and India has launched initiatives like the National Clean Air Programme (NCAP) to reduce pollution levels. However, despite these efforts, the persistent threat of $PM_{2.5}$ pollution on cultural heritage sites in East Asia remains a significant concern, emphasizing the need for special preservation measures. Recent developments in remote sensing and global as well as regional chemical-transport models provide valuable data to estimate ground-level pollutant concentrations, facilitating a better understanding and evaluation of $PM_{2.5}$ emissions and their impacts on public health. In recent years, there's been a documented rise in the presence of heavy metals, which are hazardous pollutants posing potential threats to both human health and natural ecosystems., as they tend to bio-accumulate in the human body. The heavy metals emitted from highways come from various sources, such as atmospheric deposition, traffic emissions, carriageway breakup, and surrounding land use. Urban pollution from transportation has become a crucial concern due to the rapid increase in road traffic in many countries, including India.

Studies have identified both primary elements from the Earth's crust (Al, Fe, and Ca) and anthropogenic sources (Pb, Ni, and Cd) as major contributors to coarse and fine particles in urban areas. The manmade sources are dominating sources in the urban areas. Particulate matter can also harbor bacteria and potential respiratory pathogens, posing risks to lung health and the environment. Researchers have attempted to assess the potential risk of heavy metal exposure to children and adults through various pathways. Overall, children tend to have higher intake levels than adults, however, the exposure levels were found to be within acceptable limits according to the US EPA guidelines. The atmospheric aerosol distributions are influenced by various factors such as precipitation, atmospheric mixing, and ventilation due to circulation changes. Emissions from natural aerosol sources are influenced by climate factors like wind speed, temperature, and vegetation. Several particle dispersion models are available and widely used to study aerosol

dynamics and distribution in the atmosphere. Mechanical dispersion is a process where solid particles are mechanically generated and dispersed into the air. This mechanism is often associated with activities like construction, mining, and agricultural practices, which can release dust particles into the air as aerosols. In some regions, haze episodes are caused by uncontrolled biomass and peat burning. However, the sources of ambient aerosol and their dispersions are complex and interconnected, with multiple processes contributing to the overall aerosol composition and concentrations in the atmosphere. Understanding the sources and dynamics of aerosols in the atmosphere is essential to address air pollution and its impacts on human health and the environment. The interplay of various factors, both natural and human-induced, influences the presence and distribution of aerosols, including heavy metals, in the atmosphere. Effective strategies and regulations are required to mitigate air pollution and protect air quality.

Overall, these studies highlight the importance of understanding the sources of aerosols in different regions and the methods used to assess their contributions. Accurate knowledge of aerosol sources is essential for developing effective strategies to mitigate air pollution and its impacts on human health and the environment. Several studies explore the relationship between aerosol concentration and meteorological factors in various regions. Meteorological factors significantly influence aerosol concentration wind patterns, temperature, humidity, and atmospheric stability play vital roles in the transport, dispersion, and accumulation of aerosol particles in the atmosphere. These factors affect the spatial and temporal variations in ambient aerosol concentrations, impacting air quality, climate, and human health. In general temperature showed a negative trend with concentration during winter months, while wind speed exhibited a negative correlation. Relative humidity showed a weak positive correlation with $PM_{2.5}$ and PM_{10} during winter months. A combination model incorporating meteorological parameters enhanced accuracy in estimating ground $PM_{2.5}$ levels. AOD showed significant interannual variation, with a positive correlation with temperature. AOD consistently showed higher values during forenoon hours compared to afternoon hours, influenced by prevailing meteorological conditions and pollution sources. The lower surface wind speeds and higher relative humidity tend to worsen air pollution and reduce visibility in heavily populated areas.

Overall, studies highlight the importance of considering meteorological factors in understanding and predicting aerosol concentrations. The compilation of various research studies

and their findings related to Satellites, AOD estimation, and its applications. These satellites collect remote sensing data, including information on aerosol concentrations. Retrieving AOD values involves analyzing radiance measurements from satellite sensors for AOD are used for studying air quality, climate research, understanding aerosol sources and transport patterns, and validating atmospheric models. Studies assessed the impact of environmental attributes on the accuracy of satellite-based AOD retrieval, indicating the importance of considering factors like aerosol loading, particle size, and vegetation cover. Studies highlight the significance of satellite-derived AOD data in various applications and the need to consider different factors affecting AOD retrieval for accurate analysis and interpretation. Source-receptor modelling is a valuable technique used to understand the relationship between pollutant emission sources and their locations of observation or measurement. It involves analysing how pollutants are transported and dispersed from their sources to receptor locations, allowing for the identification and quantification of different emission sources' contributions to observed pollution levels. This information is crucial for developing effective air quality management strategies, implementing pollution control measures, and assessing the impacts of various emission sources on air quality and public health. Studies on source-receptor modelling have been conducted in different geographical regions, with a significant focus on the NCR and IGP.

A study in India assessed aerosol pollution in each state, focusing on long-term trends, source apportionment, and future projections. The IGP states were found to be highly vulnerable to aerosol pollution, while central, western, and southern states were considered vulnerable. Major aerosol sources identified in India include coal-fired thermal power plants, vehicular emissions, solid fuel/waste, and biomass burning. Overall, source-receptor modelling plays a crucial role in understanding pollutant sources, and their impacts, and devising effective pollution control strategies to safeguard public health and improve air quality. Backward trajectory analysis is a powerful technique in atmospheric science used to trace the origin and transport history of air masses or pollutants by calculating the trajectories of air parcels or particles in reverse from their current location back to their source region. This analysis provides valuable insights into long-range pollutant transport, the contribution of different regions to local pollution, and the influence of meteorological conditions and transport mechanisms. Overall, backward trajectory analysis is a valuable tool in various atmospheric studies, providing essential information for air quality

management, pollution control strategies, and understanding atmospheric transport and dispersion processes.

Overall, the summary emphasizes the importance of comprehensive strategies for $PM_{2.5}$ pollution, including addressing the outdoor sources and integrating with satellite AOD and meteorological parameters to predict the ground level of $PM_{2.5}$. The long-range transport of the aerosol pollutants from the source regions an indirect effect on the social and economic development policies and implementing effective regulations and mitigation measures to protect human health and the environment.

Chapter 3 Materials and Methods

3.1 Study Area

One of the study areas is Warangal, in the southern part of India, hosting a population of 983000 as per the 2021 census. It is the second-largest municipality in Telangana state, next to the state capital, Hyderabad, which is the second study location. Warangal located at 18.0°N and 79.58°E, records an average temperature of 34.5°C during summer and an average temperature of 22.4°C during winter. Tropical climate prevails in the area with an annual average precipitation of 945 mm. Air samples were collected at the institute campus by adopting prescribed procedures. The index map of the study area with the sampling location is presented in Figure 3.1. The sampling location was situated on the roof (~15 m above ground level) of the Chemistry Department building.

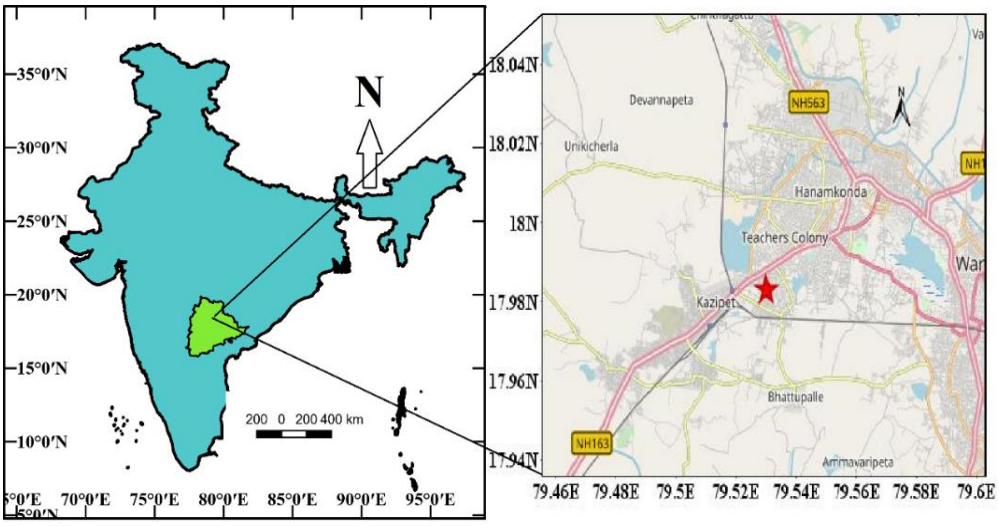

Figure 3.1 Sampling Location in the study area at Warangal.

The second study area was the Hyderabad, a city with a rich history spanning 400 years, proudly serves as the state capital of Telangana. It is nestled on the Deccan Plateau, approximately 500 meters above sea level, situated at a latitude of 17° 23′ 13.704” N and a longitude of 78° 29′ 30.0624″ E (Figure 3.2). The city extends over an area of around 650 km^2 along the banks of the Musi River. Hyderabad shares its glory with its twin city, Secunderabad, and together, they form the fifth-largest urban agglomeration in India. According to the 2011 census, the metropolitan population was around 0.97 crores. During the monsoon season, from June to October, the

southwest monsoon graces the city with heavy rainfall, contributing significantly to its annual precipitation.

The climate in Hyderabad is generally pleasant, with an average annual temperature of 26.6 °C. However, temperatures can fluctuate from 21 to 33 °C throughout the year. The hottest month, with temperatures reaching 36–39 °C, is May, while December and January experience cooler weather, ranging from 14.5 to 28 °C. With a thriving industrial sector and numerous research centers, Hyderabad has emerged as a prominent high-tech hub in southeast India. This remarkable growth has attracted a substantial influx of people, resulting in a high population density of approximately 17,000 individuals per km^2. The rapid urbanization and increased economic activities have led to significant migration to the twin cities, resulting in a surge in personal, public, and para transit vehicles, as well as industrial output. This growth has also placed a considerable burden on the cities' infrastructure. Hyderabad, together with the neighbouring ten Municipalities, constitutes the Hyderabad Urban Development Area (HUDA). The region has been expanding at an average annual rate of 9%, further solidifying its position as one of the fastest-growing cities in India.

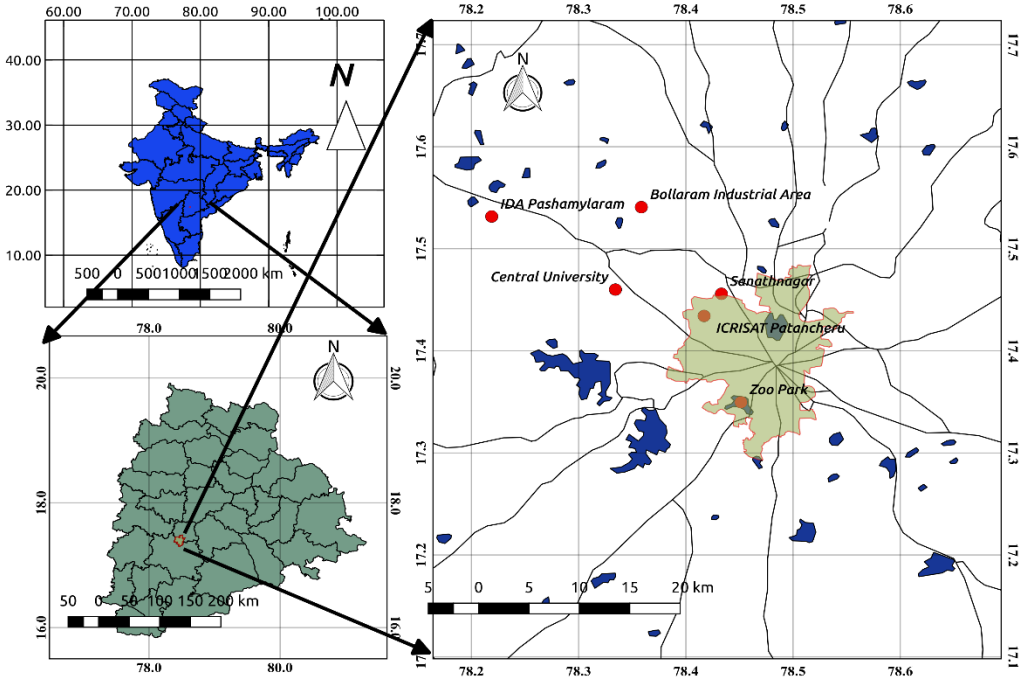

Figure 3.2 Meteorological data locations and CPCB monitoring sites considered in this **S**tudy at Hyderabad region

3.2 Major Sources of Air Pollution

Warangal is a typical town with mixed land uses dominated by residential, commercial, and transportation activities with no major industrial sources within a 3-4 km radius. The sampling location is in the institute campus extending 240 acres with academic and residential buildings and a population of about 7000 residing on the campus. Transportation and daily cleaning activities can be considered as the major sources of air pollution in the college campus. Construction activity is another source on the campus that contributes to particulate matter in the air. The sampling location is close to Warangal - Hyderabad National Highway (about 300 m to the North) with high traffic density is also a major dominating source of pollution. Direct vehicular emissions, road dust, and dust resuspension in particular contribute to air pollution. Open burning nearby areas is another source that contributes to particulates in the air. The campus is surrounded by residential with mixed activities influencing air pollution. In summary, local and non-local sources influence the pollution levels at the location. The non-local sources include industries, biomass burning, and coal mining activities.

Hyderabad, a bustling metropolis in southern India, grapples with a myriad of pollution sources that contribute to its environmental challenges. Vehicular emissions stand out as a significant contributor, given the city's burgeoning population and rapid urbanization. The increasing number of vehicles on the roads releases pollutants, including particulate matter and greenhouse gases, impacting air quality. Industrial activities, prevalent in and around the city. Bollaram located in the Medchal-Malkajgiri district of Telangana, India, is recognized for its industrial importance. It houses diverse industrial estates and manufacturing units, playing a pivotal role in the economic landscape. Over recent years, Bollaram has undergone substantial development, becoming a magnet for businesses and making significant contributions to the overall economic advancement of the neighboring region.

Central University Hyderabad Situated in Gachibowli, Hyderabad, Telangana, India, it is also recognized as the University of Hyderabad and finds itself amidst a burgeoning IT and business hub. Gachibowli, positioned in the western part of Hyderabad, has evolved into a prominent district hosting technology companies, educational institutions, and research centers. The environmental quality around the university campus plays a role in influencing pollution levels in the campus region.

Industrial Development Area (IDA) Pashamylaram, positioned on the outskirts of Hyderabad, Telangana, is an industrial development area near Pashamylaram. Falling under the jurisdiction of the Hyderabad Metropolitan Development Authority (HMDA), Pashamylaram is renowned for its industrial estates, situated northwest of Hyderabad city. Within the IDA of Pashamylaram, diverse industrial units, manufacturing facilities, and businesses thrive. The purpose of its development is to foster industrial growth and contribute significantly to the economic advancement of the region. The specific location within Pashamylaram can vary, contingent upon the specific industrial zone.

International Crops Research Institute for the Semi-Arid Tropics (ICRISAT) resides in Patancheru, on the outskirts of Hyderabad, Telangana, India. Patancheru, a dynamic industrial and residential zone on Hyderabad's periphery, is strategically positioned. It accommodates a mix of industrial estates, educational institutions, and residential complexes, contributing significantly to Hyderabad's economic landscape. This area is home to manufacturing units, research centers, and IT companies, exemplifying its industrial importance. ICRISAT's presence underscores its pivotal role in global agricultural research. Despite its industrial vibrancy, Patancheru embraces natural beauty, with lakes and green spaces enhancing its surroundings.

Sanathnagar located in the western part of Hyderabad, Telangana, India, Sanathnagar is a vibrant locality renowned for its industrial and residential zones. The area boasts a blend of commercial establishments, manufacturing units, and residential neighbourhoods. Sanathnagar has experienced substantial urban development and enjoys excellent connectivity to other parts of the city. Its significance lies in hosting industrial estates that contribute significantly to Hyderabad's economic activities. However, the region faces environmental challenges, particularly related to traffic density and ongoing construction activities.

The Nehru Zoological Park, commonly known as Zoo Park, is situated in the Bahadurpura area of Hyderabad, part of the Old City with a rich historical and cultural heritage. Next to the zoo lies Lumbini Park, featuring a delightful musical fountain, providing visitors with a pleasant recreational space. The ancient Mir Alam Tank, a reservoir nearby, enhances the natural beauty of the surroundings and serves as a habitat for diverse bird species. The vicinity of the zoo has witnessed urban development, with the emergence of residential neighbourhood’s, commercial establishments, and educational institutions, creating a diverse and vibrant locale.

Table 3.1 Air quality monitoring stations over Hyderabad

S.No	Stations	Latitude and Longitude
1	Bollaram Industrial Area, Hyderabad - TSPCB	17.54089, 78.358528
2	Central University, Hyderabad - TSPCB	17.460103, 78.334361
3	IDA Pashamylaram, Hyderabad - TSPCB	17.5316895, 78.218939
4	ICRISAT Patancheru, Hyderabad - TSPCB	17.512414, 78.2753706
5	Sanathnagar, Hyderabad - TSPCB	17.4559458, 78.4332152
6	Zoo Park, Hyderabad - TSPCB	17.349694, 78.451437

3.3 Respirable dust sampler

$PM_{2.5}$ particles were collected using a Respirable dust sampler as shown in Figure. 3.3. For proper control of $PM_{2.5}$, a flow win impactor and silica gel were used. The dust sampler flow rate was 16.67 ± 5% liters per minute (LPM) and an accuracy of ±2% was maintained throughout the sampling period. 12 hours of samples were collected separately during the day and night. A total of 130 samples were collected for six months starting from September 2018 to February 2019. Prescribed glass-fiber filter paper was used for the filtration of samples (Bhuyan et al., 2018; Chaudhari et al., 2012b; Satsangi et al., 2014). The weight of dry filter paper before and after sampling was recorded with the help of mass balance and subsequently, $PM_{2.5}$ concentrations were calculated. A desiccator was used to control the influence of atmospheric moisture on filter papers. The collected samples were stored in the refrigerator for subsequent metal analysis using the Agilent Microwave Plasma Atomic Emission Spectrometers (MP-AES) model was Agilent 4210 MP-AES.

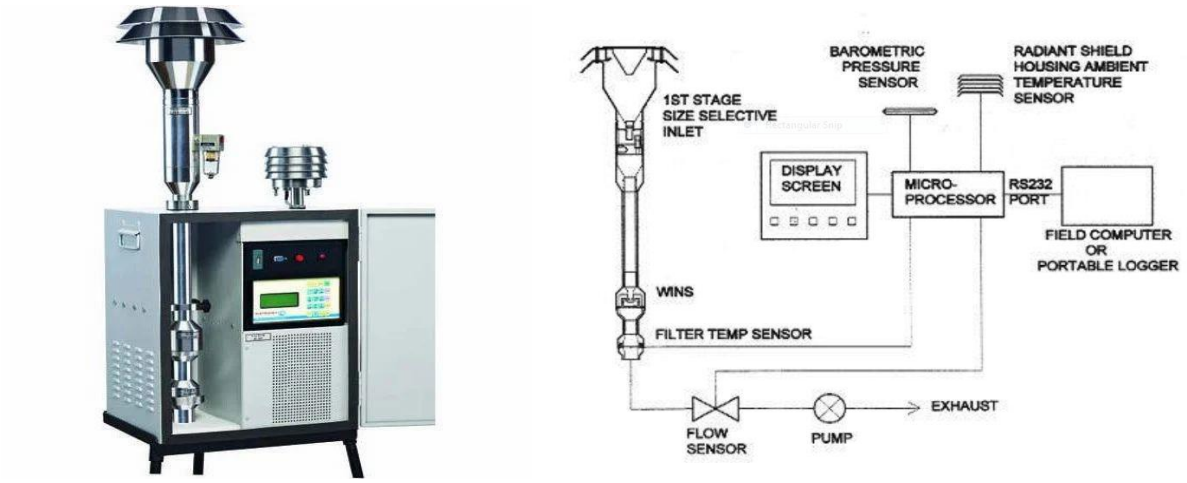

Figure 3.3 Configuration of Respirable dust sampler

3.4 MP-AES heavy metals analysis

The Agilent 4210 MP-AES offers a superior alternative to flame Atomic Absorption Spectroscopy (AAS) with high sensitivity and accuracy. Unlike AAS, it uses a microwave plasma and operates on air, allowing for flexible installation in labs or remote locations. With detection limits down to ppb levels, it provides excellent sensitivity while eliminating the need for sample pretreatment. The 4210 MP-AES delivers cost-effective analysis without compromising accuracy or sensitivity.

The heavy metal analysis on the filter paper was conducted using the following method: The glass-fiber filter papers underwent acid digestion with 20 ml concentrated HNO_3 solution for 2-h on the hot plate (Chakraborty & Gupta, 2010; Kamala et al., 2014). The solution was maintained at 180°C until the acid got evaporated completely. The residual liquid was then filtered through a 0.22 μm Teflon filter and diluted to 100 mL with Milli-Q water (resistivity 18.2 mΩ) for subsequent elemental analysis. A blank filter was digested following the same procedure as the sample filters. The blank filters were analysed separately and the values were subtracted from the total weight after filtration to get the weight of the retentived. The reference standard solutions for MP-AES were prepared for calibration to find the concentration of metals in the samples (Kamala et al., 2014).

The analytical performance of MP-AES is similar to that of AAS, but MP-AES can measure more elements more rapidly across a broader concentration range. The detection limit in

MP-AES is a crucial factor determining the instrument's capacity to identify and measure trace quantities of elements within a sample. Ensuring a low detection limit is indispensable for applications demanding heightened sensitivity. Detection limits parameters influence the signal-to-noise ratio the signal from the analyte emission lines needs to be clearly distinguished from the background noise. A higher signal allows for the detection of lower concentrations. Spectral Interferences from other elements or compounds in the sample can affect the accuracy of detection. Methods such as collision or reaction cells may be employed to reduce spectral interferences and improve the detection limits. Accurate calibration of the instrument using standards of known concentrations is essential. A well-calibrated instrument provides a reliable basis for determining the detection limit. The following table presented the detection limits for the element analysis (pang 2014).

Table 3.2 MPAES instrument detection limits for elemental analysis.

Element/Heavy Metal	**Detection Limit (µg/L)**
Aluminum (Al)	0.1
Arsenic (As)	0.01
Cadmium (Cd)	0.005
Chromium (Cr)	0.05
Copper (Cu)	0.01
Iron (Fe)	0.1
Lead (Pb)	0.01
Manganese (Mn)	0.2
Nickel (Ni)	0.01
Zinc (Zn)	0.01

3.5 Enrichment Factor analysis

The enrichment factor (EF) is generally used to identify the pollutant originating from the earth's crust and non-crustal sources. Equation 3.1 may be used for the determination of EF. In most studies (Das et al., 2015; Zhang et al., 2009), Fe and Al are used as reference elements as these elements exhibit stable chemical properties. Therefore, in this study, Fe was used as a reference element. The standard crustal composition reported by Rudnick and Gao, (2003), was used in the present study. However, there is no thumb rule for selecting reference elements.

$$EF = \frac{\left(\left(\frac{X}{CC_{ref}}\right)_{sample}\right)}{\left(\left(\frac{X}{ref}\right)_{crust}\right)} \qquad \text{Eq. 3.1}$$

Where X is the concentration of the element being examined and "C_{ref}" is the reference element concentration, with respective sample and crust. The relation between EF and the level of enrichment is given in Table 3.1.

Table 3.3 Interpretation of EF (Zhang et al., 2009)

EF	Level of Enrichment
< 2	Minimal enrichment
2–5	Moderate enrichment
5–20	Significant enrichment
20–40	very high enrichment
EF > 40	extremely high enrichment

3.6 Non-carcinogenic and carcinogenic health risk assessment

The health risk assessment for adults and children was analysed based on heavy metals associated with $PM_{2.5}$. Exposure to ambient metals occurs through inhalation, ingestion, and skin. In the present study, the exposure assessment methodology developed by the U.S. EPA (US EPA 2009a; US EPA 2009b) has been adopted. Ambient heavy metals are inhaled through the nose and mouth; ingested through food and absorbed through skin pores. Risk Assessment methodologies have been reported in a few studies (Han et al., 2016; Hu et al., 2012; Wei et al., 2015) and the

health risk assessment framework includes the identification of pollutants and the exposure assessment based on dose-response assessment.

3.6.1 Average Daily Dose

US EPA considers the Average Daily Dose (ADD) (mg/kg/day) for exposure dose assessment of the risk posed by metals to humans. The potential exposure through three different pathways for each metal separately is computed in the present study with the help of equations 3.2, 3.3, and 3.4) (Ferreir & Miguel, 2005; Hu et al., 2012; Kong et al., 2012).

$$ADD_{ing} = \frac{C \times IngR \times EF \times ED \times CF}{BW \times AT} \quad \text{Eq. 3.2}$$

$$ADD_{der} = \frac{C \times SA \times AF \times ABS \times EF \times ED \times CF}{BW \times AT} \quad \text{Eq. 3.3}$$

$$ADD_{inh} = \frac{C \times InhR \times EF \times ED}{PEF \times BW \times AT} \quad \text{Eq. 3.4}$$

Where ADD_{ing}, is the average daily dose by ingestion (mg/kg/day).

ADD_{der} is the average daily dose by dermal contact (mg/kg/day).

ADD_{inh} Average daily dose by inhalation (mg/kg/day).

C is the heavy metal concentration (mg/kg).

IngR is Ingestion rate (mg/day) 30_adults, 60_children (US EPA 2007);

EV is Events frequency that occurs every day at once.

EF is Exposure frequency, 180 days for a year.

ED is Exposure duration, 24 years for adults, 6 years for Children.

CF is a Conversion factor 10^{-6} kg/mg.

BW is Body weight - 70kg for adults, 15kg for children.

SA is Skin surface area - 5700 cm^2 for adults, 2800cm^2 for children.

AF is the Adherence factor of soil to the skin - 0.07 (mg/cm^2/event) for adults, 0.2 (mg/cm^2/event) for children.

ABS is Dermal absorption fraction - 0.001 (US EPA 2004b);

InhR is Inhalation rate 7.63m^3/day for adults, 20m^3/day for Children.

PEF is Particle emission factor - 1.36 X 10^9 m^3/kg (US EPA 2009a);

AT is Averaging time for Non carcinogens (AT = ED X 365 days/year) and Carcinogens (AT = 70 years X 365 days/year) (Du et al., 2013).

In the present study, standard parameter values as given by US EPA (US EPA 2004b; US EPA 2004c; US EPA 2007; US EPA 2009a; US EPA 2009b) were used.

3.6.2 Hazards Quotient and Hazards Index

The non-carcinogenic health risk assessment was calculated based on Hazard Quotient (HQ) and Hazard Index (HI). HQ and HI were determined using Eq. 3.5 and 3.6 respectively. HQ value of less than 1 indicates there is no significant health impact, while HQ value of more than 1 indicates an adverse effect on human health (Zheng et al., 2010). HQ value was found based on the reference dose (RFD) of each element. HI is the sum of all the Hazard Quotients (Ferreira & Miguel, 2005; Zheng et al., 2010). HI value of less than 1 indicates that there is no significant non-carcinogenic impact, while HI value greater than 1, indicates chances of significant non-carcinogenic impact (Zheng et al., 2010).

$$HQ = \frac{ADD}{RfD} \qquad \text{Eq. 3.5}$$

$$HI = \sum_{1}^{n} HQ_i \qquad \text{Eq. 3.6}$$

3.6.3 Excess Cancer Risk Assessment

Excess Cancer Risk (ECR) is a measure of the incremental cancer risk over the lifetime (Hu et al., 2012). ECR is calculated using Eq. 3.7. The inhalation unit risks of the metals are provided by US EPA IRIS (Integrated Risk Information System) (US EPA, 2009). A zero value indicates that there is no cancer risk, while higher values indicate a higher chance of cancer risk. The US EPA methodology provides only the inhalation unit risk. However, other pathways and associated risks are not provided. When the ECR value falls within the range of 10^{-6}-10^{-4} indicates carcinogenic risk (Hu et al., 2012; Qi et al., 2019) was minimal.

$$ECR = \frac{C \times ET \times EF \times ED \times IUR}{AT} \qquad \text{Eq. 3.7}$$

Where C is pollutant levels in mg/m^3; ET is the exposure time taken as 8 h/day; EF is Exposure frequency 180 days for a year; ED is Exposure duration: 24 years for adults, 6 years for children; IUR is inhalation unit risk in mg/m^3, AT is Average time for carcinogens 70 year 365 days/year 24 h/day).

3.7 MODIS AOD data product

AOD is derived from atmospheric radiance observations by the MODIS instruments aboard the Terra and Aqua. Collection 6.1. The MODIS Aqua and Terra retrievals are obtained from NASA's Level-3 and Atmosphere Archive & Distribution System (LAADS) Distributed Active Archive Center (https://ladsweb.nascom.nasa.gov). The MODIS AOD product available in two algorithms which are Dark Target (DT) and Deep Blue (DB). DT is designed to retrieve AOD at various wavelengths over relatively "dark" targets in the visible, such as water bodies or vegetation. In contrast, DB is designed to address the retrieval of AOD over more reflective surfaces, such as sand. For this study, two resolution data was analysed terra/aqua products 3km and 10km aerosol product. Here on words representation of all four MODIS products as the MODIS terra 3km (MOD04_3K), MODIS terra km (MOD04_L2), MODIS aqua 3km (MYD04_3K), MODIS terra 3km (MYD04_L2). The 3 km product tends to be noiser than the 10 km product. Comparisons of the global mean AOD from the two products shows that the 3 km AOD is 0.01 to 0.02 higher over land (Levy et al., 2015). MODIS product files are stored in Hierarchical Data Format (HDF-EOS). To extraction of the HDF data files python scripts are developed. Terra crosses the equator southward about 10:30 local solar time (LST), whereas Aqua northward about 13:30 LST. Because of the difference in direction, the mid-latitude time differences between Terra and Aqua are approximately 1.5 h in the northern Hemisphere and 4.5 h in the southern Hemisphere (Kaufman et al., 2005), while for Hyderabad this time interval is about 2.5 h. The above four data sets are adapted in this study, and following the Interquartile Range (IQR) method, the method stands out as a robust approach for pinpointing outliers in a dataset. It achieves this by examining the range between the first and third quartiles. The higher AOD values are represent the haze days due to the cloud interaction in the atmosphere, similar data causes the uncertainty in the predictions of PM2.5. To this extent data was excluded from the analysis.

3.8 Meteorological data

The meteorological data was obtained from CPCB (https://app.cpcbccr.com/ccr/#/caaqm-dashboard-all/caaqm-landing) six monitoring locations over Hyderabad. The six monitoring locations are presented in the Table 3.1. The meteorological parameters considered Temperature (AT), Relative Humidity, pressure (BP), Solar Radiation (SR), Wind speed (WS) and direction (WD) and PM2.5 data collected over the period of May 2017 to May 2019 (two years) was used in the study. For further analysis, the analysis encompasses all available parameters and data

available days only, to reduce the uncertainty in the model. All the datasets removed outliers using the IQR method. The all the meteorological parameters and AOD data ready for the further model analysis to predict the PM2.5.

Ensuring the quality of data is crucial in air quality monitoring stations, particularly as decisions hinge on results obtained through the CPCB's air quality monitoring program. Various pollution control activities rely on these outcomes. To guarantee acceptable data quality, the CPCB conducts exercises such as visiting monitoring stations and holding meetings. Regular calibration, servicing, and repair of field devices are imperative to maintain data quality at a high standard.

3.9 Multiple linear Regression model

Multiple linear regression (MLR) as established for $PM_{2.5}$ and MODIS AOD Terra/Aqua products along with meteorological parameters. MLR equation shown in Eq.3.1 was adopted. However, b_0 represents the model intercept, and the b_1, b_2... and b_7, represent the model parameters to be estimated. The $\boldsymbol{\alpha}$ represents the error term that individual outcomes will vary about that mean. The assumption was error terms are normally distributed and homoscedastic, that is, the variance of the errors is the same across all levels of the independent variables.

$$PM_{2.5} = b_0 + b_1(AOD) + b_2(AT) + b_3(RH) + b_4(WS) + b_5(WD) + b_6(SR) + b_7(BP) + \alpha \ldots \quad \text{Eq. 3.8}$$

The meteorological data were obtained from CPCB (https://app.cpcbccr.com/ccr/#/caaqm-dashboard-all/caaqm-landing) for Air Quality Monitoring Stations (AQMs) considered in the study. The meteorological parameters Temperature (AT), Relative Humidity (RH), Pressure (BP), Solar Radiation (SR), wind speed (WS) and direction (WD), and PM2.5 data collected for the period between May 2017 and May 2019 (two years) were used in the study. 80% of the data was used for model development and 20% of the data was used for model validation. The interquartile range (IQR) method was used to exclude external outliers from the data. The best option model was used to predict the PM2.5 and validate the observed data at six locations in Hyderabad. Hybrid Single-Particle Lagrangian Integrated Trajectory (HYSPLIT) model

The National Oceanic and Atmospheric Administration (NOAA) Air Resources Laboratory (ARL) proposed the Hybrid Single-Particle Lagrangian Integrated Trajectory model (HYSPLIT) (Draxler and Hess, 1998). The HYSPLIT atmospheric dispersion model was used to simulate daily wind-aided dispersion with a focus on long-range transportation and initial establishment (Chapple et

al., 2012; Westbrook et al., 2011). HYSPLIT continues to be one of the most extensively used atmospheric transport and dispersion models in the atmospheric sciences community to establish source–receptor relationships (Draxler and Hess, 1998; Fleming et al., 2012). The major contribution of fireworks and their species identification on back trajectory analysis using the NOAA–HYSPLIT model was reported by Pathak et al., (2015). The study indicated the existence of the transported aerosols. The applications based on the HYSPLIT model were used for forecasting and to assess the influence of the radioactive material (Connan et al., 2013) and to study the suspicious non-identified wildfire smoke (Rolph et al., 2009). AOD and solar irradiance revealed higher spatial variation of AOD during the summer season leading to the dispersion of particles in Delhi (Bhardwaj et al., 2017). Freitag et al., (2013), investigated the conditions for the formation and expanding airborne gas and aerosol measurements based on the HYSPLIT model.

3.10 Model Performance Evaluation

Performance of the models is assessed using commonly used statistical performance measures, including correlation coefficient (R) is a statistical measure that quantifies the degree to which two variables are related or associated. It gauges both the strength and direction of a linear relationship between two variables. The closer the correlation coefficient is to 1 or -1, the stronger the correlation. The normalized mean bias (NMB) is a statistical metric used to assess the accuracy of a model or measurement by quantifying the average tendency of the model or measurement to overestimate or underestimate a variable of interest. A positive NMB indicates a systematic overestimation by the model or measurement, while a negative NMB suggests a systematic underestimation. A NMB close to zero suggests minimal bias. Normalized mean bias is useful for comparing model outputs to observations and understanding the overall bias in a system. The root mean squared error (RMSE) is a commonly used metric to assess the accuracy of a predictive model or measurement by quantifying the average magnitude of the errors between predicted and observed values. It provides a measure of how well the model's predictions align with the actual observed values. RMSE calculates the square root of the average squared differences between predicted and observed values. The result is in the same units as the variable being measured, providing a clear understanding of the magnitude of errors. A lower RMSE indicates better model performance, as it signifies smaller errors between predicted and observed values. The index of agreement (d) is a statistical metric used to assess the agreement or similarity between observed and modelled or predicted values in a dataset. The Index of Agreement ranges from 0 to 1, with a

value of 1 indicating perfect agreement between observed and predicted values. Higher values suggest better agreement, while lower values indicate poorer agreement. It provides a comprehensive measure of the overall performance of a model or prediction compared to the observed data.

$$R = \frac{\sum(Cp-\overline{Cp})(Co-\overline{Co})}{\sqrt{\sum(Cp-\overline{Cp})^2 \sum(Co-\overline{Co})^2}} \ldots\ldots\ldots\ldots \quad 3.9$$

$$NMB = \frac{\sum(Cp-Co))}{\sum Co} \ldots\ldots\ldots \quad 3.10$$

$$RMSE = \sqrt{\frac{\sum(Cp-Co)^2}{n}} \ldots\ldots\ldots \quad 3.11$$

$$d = 1 - \frac{\sum(Cp-Co)^2}{\sum(|Cp-\overline{Co}|+|Co-\overline{Co}|)^2} \ldots\ldots\ldots \quad 3.12$$

where Cp and Co represents the predicted and observed concentrations of PM2.5 respectively whereas n represents number of samples.

3.11 Meteoinfo

MeteoInfo is a flexible framework designed primarily for the meteorological community, providing support for GIS applications and scientific computations (Wang, 2014). MeteoInfo Map is a GIS application that enables users to visually explore and analyse spatial and meteorological data in multiple formats (Wang, 2019). MeteoInfo Lab is a powerful scientific computation and visualization environment that leverages Jython scripting. It provides advanced features, including multi-dimensional array calculations and comprehensive 2D/3D plotting capabilities.

3.11.1 Trajstat

TrajStat, a GIS-based software, utilizes statistical analysis of air mass back trajectories and long-term air pollution measurements to identify pollution sources(Wang et al., 2009). It visualizes, analyses, and clusters trajectories, and calculates the potential source contribution function (PSCF) and concentrated weighted trajectory (CWT) using measured data.
The HYSPLIT model calculates trajectories that can be converted into ESRI "PolylineZ" shape files, representing three-dimensional endpoint data with properties based on longitude, latitude, and air pressure. Trajectories can be visualized in various spatial patterns, such as two-dimensional figures using level or height coordinates, or three-dimensional plots combining longitude, latitude,

and height. Long-term measurement data can be assigned to trajectories, and a query function helps identify polluted trajectories with high measurement concentration, estimating pollutant pathways. Cluster models like Euclidean distance or angle distance can be selected, with the maximum cluster number determined by comparing mean-trajectory maps visually. Cluster statistics calculate the mean pollutant concentration for each cluster, linking pollutant pathways to high-concentration clusters. Computation of PSCF and CWT values, along with a weight function for cells with limited endpoints, aids in identifying potential source regions with high PSCF or CWT values. The screenshot of MeteoInfo for analysis and flowchart is given in Figure 3.4. The step-by-step process for performing the Trajstat tool is given below.

Following are the steps to implement in the Trajstat tool:

1. Add the proposed station to the tool.
2. Calculate 7-day back trajectories during the PM_{10} data measurement period.
3. Converting trajectory files to the .tgs files.
4. Then join all .tgs files into one combined file which will represent the all trajectory.
5. Convert the combined .tgs file to the shape file and then add the shape file to the project.
6. Add measurement data into the trajectories.
7. Create grid polygon shape layers of PSCF and CWT.
8. PSCF and CWT analysis.
9. Cluster calculation to the trajectories.

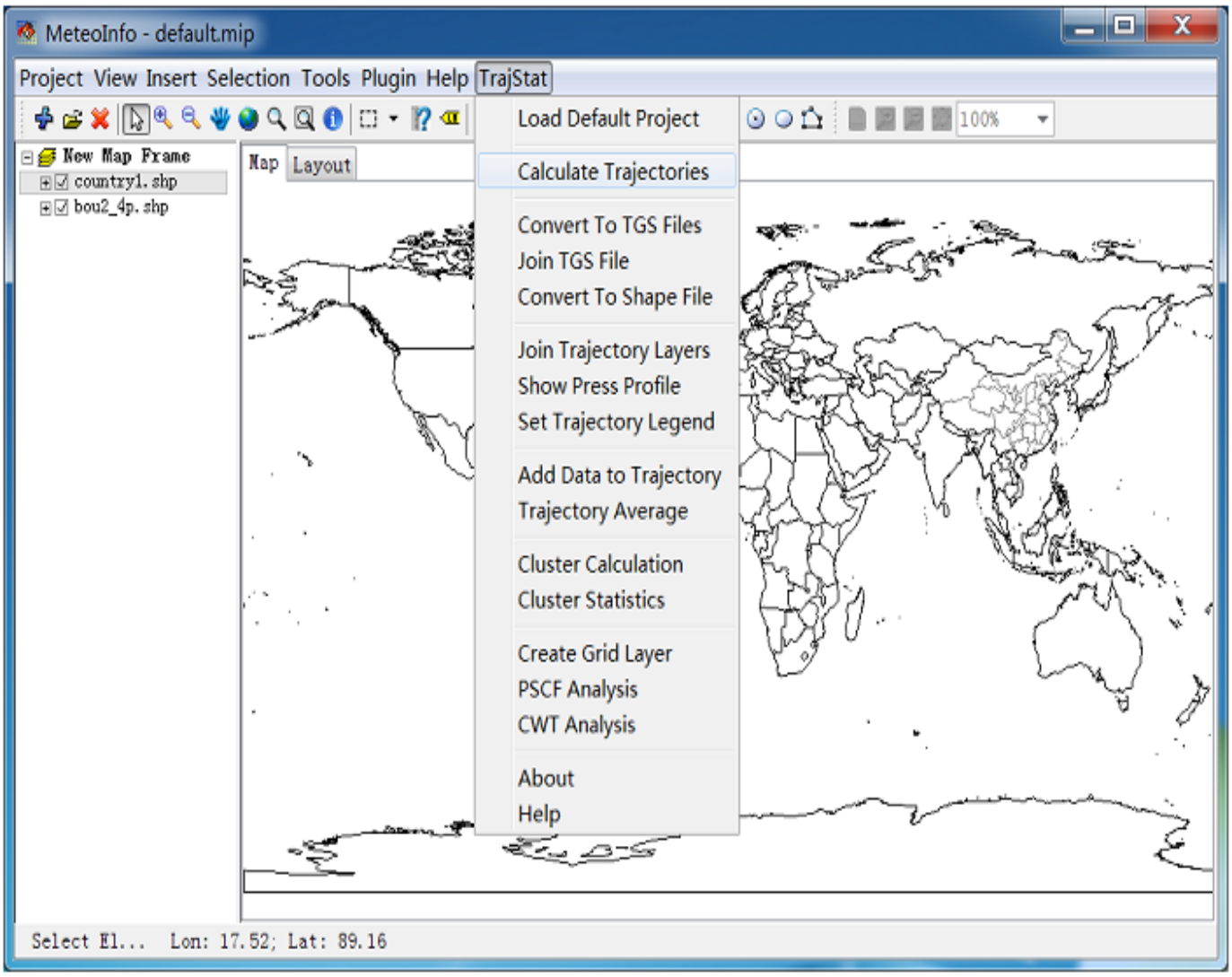

Figure 3.4 Meteoinfo interface for Trajstat plug-in tool

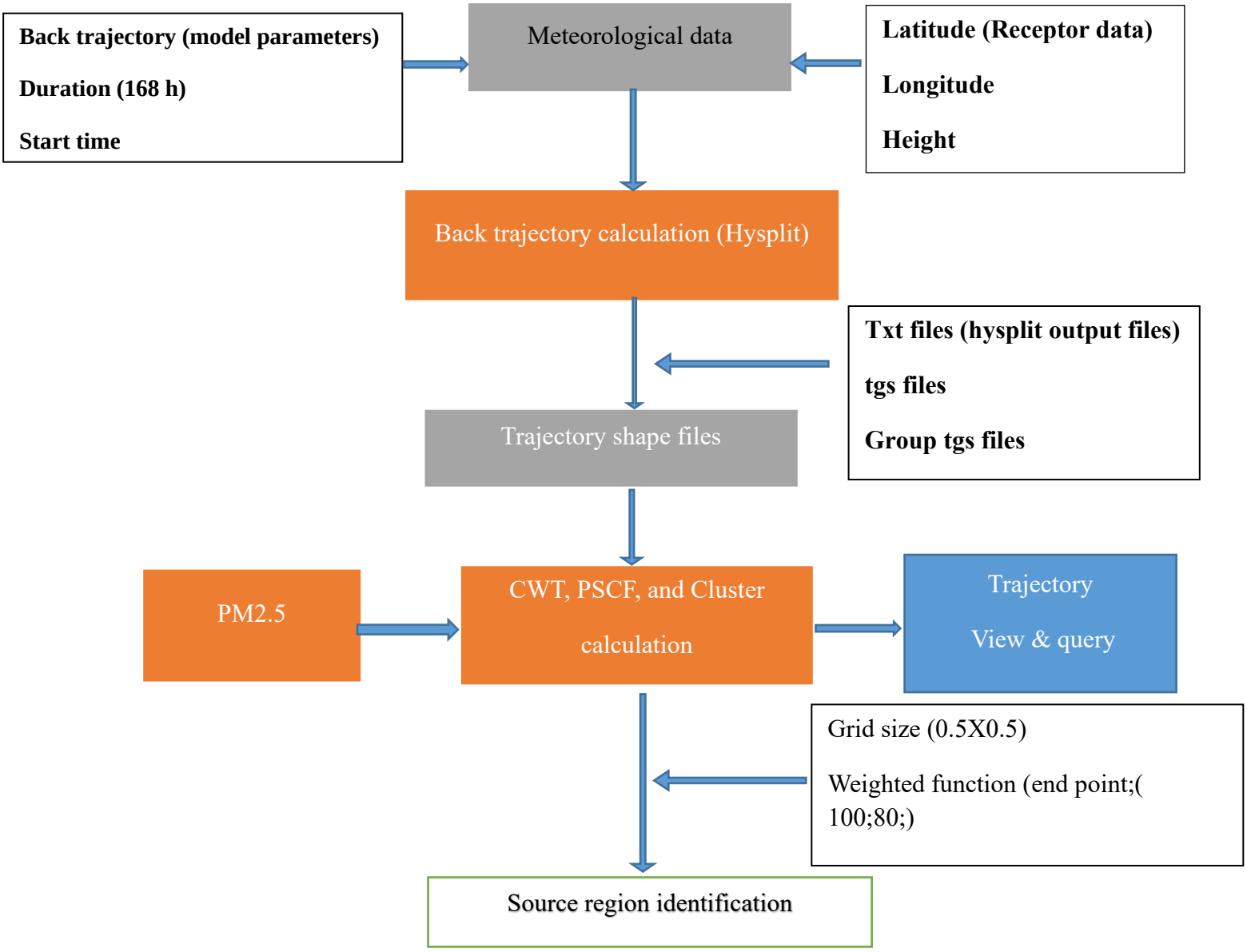

Figure 3.5 CWT analysis flow chart for back trajectory.

The source identification was done based on CWT, PSCF, and Cluster analysis. MeteoInfo tool and GIS-based software were used for meteorological data visualization and analysis (Wang, 2014). The PSCF, CWT, and Cluster analysis were analyzed using the plugin TrajStat tool (Wang et al., 2009), for conducting source analysis.

3.11.1.1 Concentration Weighted Trajectory Analysis

CWT analysis shows the long-range pollutants at the receptor site and the strength of the source (Cheng et al., 2013). CWT model can locate the regional sources that can affect the receptor region.

In CWT analysis, each cell in the grid is assigned a weight by averaging the pollutant concentration (Seibert et al., 1994). The trajectory endpoint time in the grid cells has been weighted by the corresponding $PM_{2.5}$ trajectory. The concentration of each grid cell was calculated using Eq. 3.9 (Chen et al., 2018). In this study, the spatial resolution 0.5°×0.5° was considered to find the source paths.

$$CWT_{ij} = \frac{\sum_{l=1}^{L} c_l \tau_{ijl}}{\sum_{l=1}^{L} \tau_{ijl}} \qquad \text{Eq. 3.9}$$

Where C_l is the observed mean concentration of pollutant; l denotes the associated backward trajectory; τ_{ijl} each segment endpoints in 0.5^o x 0.5^o grid cells (i, j); L presents the total number of backward trajectories considered in this study.

3.11.1.2 Potential Source Contribution Function Analysis

The Potential source contribution function (PSCF) was used to indicate the probability of the impact of sources on the receptor (Negral et al., 2020). PSCF values may be calculated using the following equation 3.10.

$$PSCF_{ij} = \frac{M_{ij}}{N_{ij}} W_{ij} \qquad \text{Eq. 3.10}$$

Where, M_{ij} is the total number of back trajectories with grid cell (i, j), N_{ij} is the total number of back trajectories with respective each grid cell (i, j); W_{ij} denotes the weighting function of back trajectory segment endpoints in a grid cell (i, j) (Fu et al., 2012). A weight function (W_{ij}) was established for each grid to overcome the uncertainty in N_{ij} (Zeng and Hopke, 1989).

3.11.1.3 Cluster Analysis

The clustering technique shows the average trajectory paths for each cluster. There are two clustering options with Euclidean distance or angle distance. The Euclidean distance cluster technique is extensively used for studying air mass trajectories representing pollutant pathways. When the Euclidean distances were used, shorter trajectories were more likely to be assigned to the same cluster, and longer trajectories were more likely to be assigned to different clusters. In the present study, the Euclidean distance was adopted for clustering the back trajectories as given in Eq. 3.11.

$$d_{12} = \sqrt{\sum_{l=1}^{n}((X_1(i) - X_2(i))^2 + (Y_1(i) - Y_2(i))^2)} \quad \text{Eq. 3.11}$$

Where $X_1(Y_1)$ and X2(Y2) reference backward trajectories 1 and 2, respectively.

The angle distance between two backward trajectories was defined by Eq. 3.12

$$d_{12} = \frac{1}{n}\sum_{i=1}^{n} COS^{-1}(0.5\frac{(A_i + +B_i - C_i)}{\sqrt{A_i B_i}}) \quad \text{Eq. 3.12}$$

Where

$$A_i = (X_1(i) - X_0)^2 + (Y_1(i) - Y_0)^2$$

$$B_i = (X_2(i) - X_0)^2 + (Y_2(i) - Y_0)^2$$

$$C_i = (X_2(i) - X_1(i))^2 + (Y_2(i) - Y_1(i))^2$$

The variables X0 and Y0 define the position of the site. d12 varies between 0 and π. The two extreme values occur when two trajectories are in the same and opposite directions, respectively. d12 is the mean angle between the two backward trajectories, as seen from the studied site.

3.12 Quality Assurance and Quality Control

Quality Assurance (QA) is a systematic process or set of activities designed to ensure that processes meet specified standards and fulfil the target requirements. The primary goal of QA is to prevent errors and to consistently deliver high-quality results. QA encompasses a range of activities that focus on establishing and maintaining processes to ensure the reliability and quality of the end results. Quality Control (QC) is a systematic process or set of activities designed to regulate the quality of products. The primary goal of QC is to identify deviations from established standards, ensuring that the final output meets specified requirements. Unlike QA, which focuses on preventing defects, QC involves inspection and testing activities to detect and address issues during or after the production or implementation phase.

QA/QC are essential for ensuring the accuracy, precision, and reliability of data generated by the MP-AES instrument. Here are considerations for QA/QC in the context of MP-AES, the main

consideration was calibration. The regularly calibrate the MP-AES instrument using certified reference standard samples to establish accurate calibration curves. Ensure that calibration standards cover the concentration range of interest. The internal standards to correct for variations in sample introduction, plasma stability, and detector response. This helps improve the precision and accuracy of quantitative measurements. Blank samples were introduced in the analytical sequence to identify and correct for any contamination during sample preparation or analysis. Monitor background noise levels. Quality control samples incorporate of known concentrations into each analytical run. Regularly analyse QC samples to assess the accuracy and precision of the MP-AES instrument. Reproducibility and Precision assess the reproducibility and precision of the MP-AES instrument by running replicate analyses of the same sample. Low variability among replicates indicates high precision. Instrument regularly check and maintain the MP-AES instrument. Verify the stability of the plasma source, assess detector efficiency, and ensure the integrity of optical components. Implement thorough data validation procedures to identify and address anomalies in the analytical data. Check for outliers, confirm adherence to calibration curves, and ensure results fall within acceptable limits. Ensure that analysts are well-trained in the operation, maintenance, and troubleshooting of the MP-AES instrument. Regular training updates contribute to the reliability of analytical results. By adhering to these QA/QC practices, in the laboratories enhance the reliability and accuracy of data generated by the MP-AES instrument. These are the crucial for meeting regulatory standards, ensuring data integrity, and providing trustworthy results for various applications.

QA/QC are essential in handling and analysing data, including MODIS Aerosol Optical Depth (AOD) data and data from the Central Pollution Control Board (CPCB). Here are considerations for QA/QC in the context of these datasets, Confirm the data source of the MODIS AOD and meteorology data, ensuring it comes from reputable and authoritative sources. Check for quality flags or indicators in CPCB data that highlight potential issues, such as missing values or data gaps. Understand the calibration procedures for instruments used by CPCB. Verify that instruments are regularly calibrated, and any issues with calibration are addressed. Document and review the steps involved in processing MODIS AOD data, ensuring transparency and reproducibility. Check for temporal and spatial consistency in the MODIS AOD data. Verify that the data aligns with the expected patterns.

Chapter 4 Estimation of $PM_{2.5}$ and source contribution by back trajectory analysis over Warangal region

4.1 Assessment of Particulate Matter

The monthly mean mass concentrations of $PM_{2.5}$ are presented in Figure 4.1 (a) at Warangal. During the study period, the monthly mean $PM_{2.5}$ concentrations were found to be in the range of 8.3-29.6 µg/m^3, with the highest daily concentration of 58.3 µg/m^3, and the lowest daily concentration of 4.7 µg/m^3. During the monsoon period, maximum, minimum, and mean concentrations of $PM_{2.5}$ were 41.6, 24.9, and 29.6 µg/m^3 respectively. Concentrations of $PM_{2.5}$ were observed to be higher during the weekend as compared to the concentration during weekdays. This is perhaps due to the proximity of the highway to the monitoring station, and the fact that the highway caters to higher volumes of traffic during the weekends compared to weekdays.

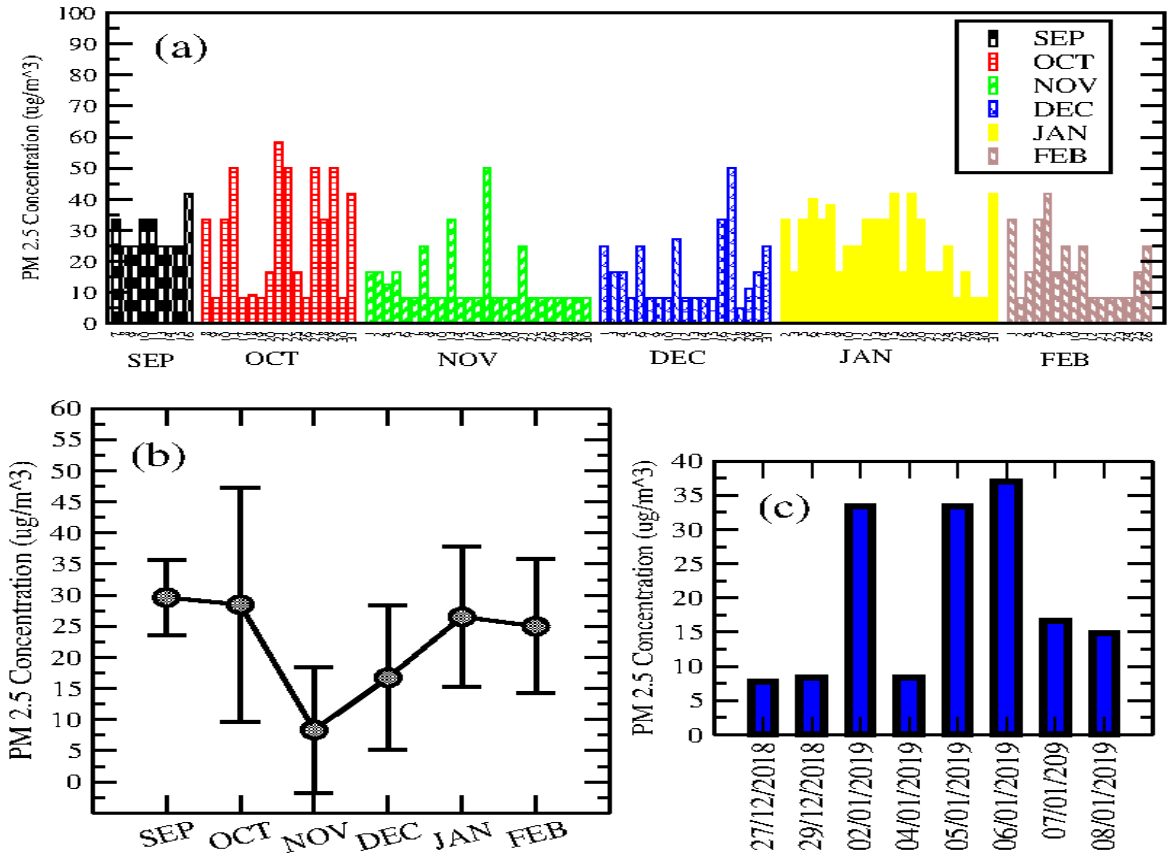

Figure 4.1(a) Diurnal Concentration of $PM_{2.5}$ (b) Monthly variation of $PM_{2.5}$

(c) Night-time concentration of $PM_{2.5}$

During the post-monsoon period, maximum, minimum, and mean concentrations of $PM_{2.5}$ were 58.3, 8.33, and 19.5 $\mu g/m^3$ respectively. During the winter, maximum, minimum, and mean concentrations of $PM_{2.5}$ were 49.9, 4.7, and 21.2 $\mu g/m^3$ respectively (Figure 4.1 (b)). As per the National Ambient Air Quality Standards (NAAQS), the $PM_{2.5}$ concentrations were below the standard levels (40 $\mu g/m^3$ for $PM_{2.5}$ annually and 60 $\mu g/m^3$ for 24 hours). The $PM_{2.5}$ during the night presented in Figure 4.1 (c), is considered as background concentration. The night-time (06:00 PM-06:00 AM) concentrations were observed to be lower than daytime (06:00 AM-06:00 PM) concentrations. The night maximum, minimum, and mean concentrations were 38.45, 8.33, and 20.51 $\mu g/m^3$ respectively. Wind profiles and temperature influence the movement of particles. Low concentrations during nighttime are attributed to minimum traffic volumes during the night. The results of the present study were similar to the reported values in other places (Bhopal, Nagpur) dominated by vehicular and urban activities (Das et al., 2015; Karar & Gupta, 2006; Nirmalkar et al., 2021). In Nagpur city, the concentration $PM_{2.5}$ value is 52 $\mu g/m^3$ due to road dust on highways (Chaudhari et al., 2012b). At Dongargarh, Chhattisgarh India, the $PM_{2.5}$ concentration was reported to be 64 $\mu g/m^3$ mostly due to vehicular emissions (Ambade, 2014b). In Kolkata city, $PM_{2.5}$ concentration was reported as 83 $\mu g/m^3$ at a location where construction activities and road dust were major contributors to air pollution (Das et al., 2015). In Hyderabad city, $PM_{2.5}$ was reported as 45 $\mu g/m^3$ (Gummeneni et al., 2011). In Agra city, $PM_{2.5}$ was 104.9 $\mu g/m^3$ mainly due to industrial emissions and anthropogenic activities (Kulshrestha et al., 2009).

The number of daily deaths due to air pollution varies among cities and is correlated with their respective population sizes. Shimla records the lowest daily death count (4.2 ± 2.7), whereas Mumbai reports the highest (225.6 ± 30.7) (Dholakia et al., 2014). While all the cities have different pollution levels arising from different sources, the common sources of $PM_{2.5}$ in the urban atmosphere are road dust, construction activities, small industries, and vehicular emissions. Most of the deaths due to the air pollution in India during 2019 were from ambient particulate matter pollution (0·98 million [0·77–1·19]). The economic loss as a proportion of the state Gross domestic product (GDP) varied 3·2 times between the states (Pandey et al., 2021).

4.2 Assessment of heavy metals

The samples collected during the study were analysed for heavy metals using MP-AES and presented in Figure 4.2 (a) and (b). Some metals like Zn, Cu, and Fe were higher when compared

with other metals. Average concentrations of Zn, Fe, Cu, Ni, and Cd were 1.25, 0.65, 0.35, 0.005, and 0.0025 $\mu g/m^3$ respectively. Metals in ambient air bound to $PM_{2.5}$ reported by various researchers for studies conducted in India are presented in Table 4.1. For obvious reasons, the concentrations of metals vary with location depending on the sources dominating in that location. Metallic contaminants like Fe, Cu, Ca, Zn, Pb, etc, are generally released predominantly from anthropogenic sources in inland regions (Nair et al., 2006). Trace metal contributions from long-range transport of polluted air masses were reported at receptor locations (Sudheer and Rengarajan, 2012).

Table 4.1 Studies on Ambient Heavy metal over India

S.no	**Author**	**Region**	**Heavy metals**
1	Abhishek (2010)	Kanpur Region	Zn, Fe, As, Cu, Cd, Ca, Cr, Mg, Pb, Ni, Se, V
2	Kulshrestha (2009)	Agra, India	Pb, Zn, Ni, Fe, Cr, Mn, Cu
3	Ambade (2014)	Dongargarh, Central India	Fe > Zn > Pb > Cu > Ni > Cr > Cd
4	Chaudhari (2012)	Nagpur	Zn > Fe > Pb > Ni > Cd > Cr 2006
5	Kamala (2014)	Hyderabad	Al, As, B, Ba, Ca, Cr, Cu, Fe, K, Mn, Na, Ni, Pb, Zn
6	Das (2015)	Kolkata	Zn, Cr, Ni, Mo, Cu, Sn, Sb, V, Co, Cd, Pb, Ca, Al, Mg, Sc, Ti, Mn and Fe
7	Vijayanand (2008)	Tamil Nadu	Zn, Fe, Cu, Pb, Ni and Cr) Cd
8	Habil (2016)	Agra	Fe, Pb, Mn, Cu, Ni, Cr, Zn, Cd
9	Massey (2013)	Agra	Fe, Pb, Ni, Cr, Cd, Cu, Mn
10	Monika (2016)	central Delhi	K > Zn > Mg > Fe > Mn > Cu > Cd.
11	Pant(2017)	New Delhi	Si*, Ca, Fe, Ti, Mn, Ni, Cu, Zn, Pb

12	Poonam Pandey (2017)	Lucknow	Fe>Pb>Ni>Cu>Cr>Cd
13	Ghosh (2018)	Bolpur	Mn, Zn, Cd, Pb, Ni, Co,

The variations of heavy metals during the study period concluded that the post monsoon season concentrations are high as compared to the monsoon season concentrations presented in Figure. 4.2. . These metals are perhaps released from automobiles, construction activities, and other urban activities. Literature suggests that Fe, Si, Al, and Ti originate from the earth's crust (Pant et al., 2016). Zn and Pb concentration levels correlate well with non-exhaust traffic emissions (Nirmalkar et al., 2021; Piscitello et al., 2021), industrial sources (Zhao et al., 2021), and solid waste burning (Wang et al., 2016). Ni et al,. (2017) concluded that open biomass burning and industrial pollution results in Fe, Zn, Pb, and K emissions. Cd, Cr, Ni, and Pb are associated with industrial sources whereas Zn and Cu are associated with traffic emissions. The use of Zn for protective coating on iron, steel, etc, by the industries results in a higher concentration of this heavy metal (Vijayanand et al., 2008). Road dust is commonly associated with high concentrations of Cd and Pb (Massey et al., 2013; Suryawanshi et al., 2016b). Mn, Zn, Pb, Fe and Cu emissions from lubricants oil, brake pads, and tires are the main sources (Garg et al., 2000; Grigoratos & Martini, 2015; Ntziachristos et al., 2007; Pakkanen et al., 2003; Wang et al., 2016). The concentration of Zn and Fe is attributed to industrial emission, crustal trace element concentrations, and fluxes due to the re-suspension of dust released during traffic activities and soil erosion (Gajghate et al., 2012b). Increased concentration of Cd was reported to be contributed by solid waste combustion, refinery, and fossil fuel burning (Banerjee., 2003; Chinnam et al., 2006).

The Heavy Metals (HMs) transport was dominated by the Suspended Particulate Matter (SPM) load over Caohai, China. The reported HMs were attributed to agriculture and industry regions (Li et al., 2023). In Isfahan City, Iran, the concentrations of As, Cd, and Ni were in a range of 23–36, 1–12, and 5–76 ng/m^3 and all of them were above the US-EPA standards (Soleimani et al., 2018). The most important sources of HMs are fossil fuel combustion, abrasion of vehicle tires, and industrial activities. A research (Harrison, 2020) finding suggests that the heavy metals in the particulate matter increase with a decrease in the particle size. Literature suggests that the coarse particulate matter contains heavy metals from natural origin, while the fine particles host heavy metals emitted from anthropogenic sources (Soleimani et al., 2018). However, heavy metals bound to particles are capable of long-range atmospheric transportation (Chang et al., 2018; Githaiga et

al., 2020). Around 57-64% of heavy metals like Pb, Zn, and Cu are found in soil dust particles smaller than 10 μm due to their lower densities and higher surface area per unit volume. The finer fraction is easily re-suspended and they result in a high impact on human health. They linger in the air for longer periods and have a greater tendency to adhere to the skin. Metals bound to finer fractions can readily be adsorbed and accumulate in the upper respiratory tract of humans during inhalation (Valiulis, 2008). In-depth studies lead to fingerprinting the sources and their apportionment.

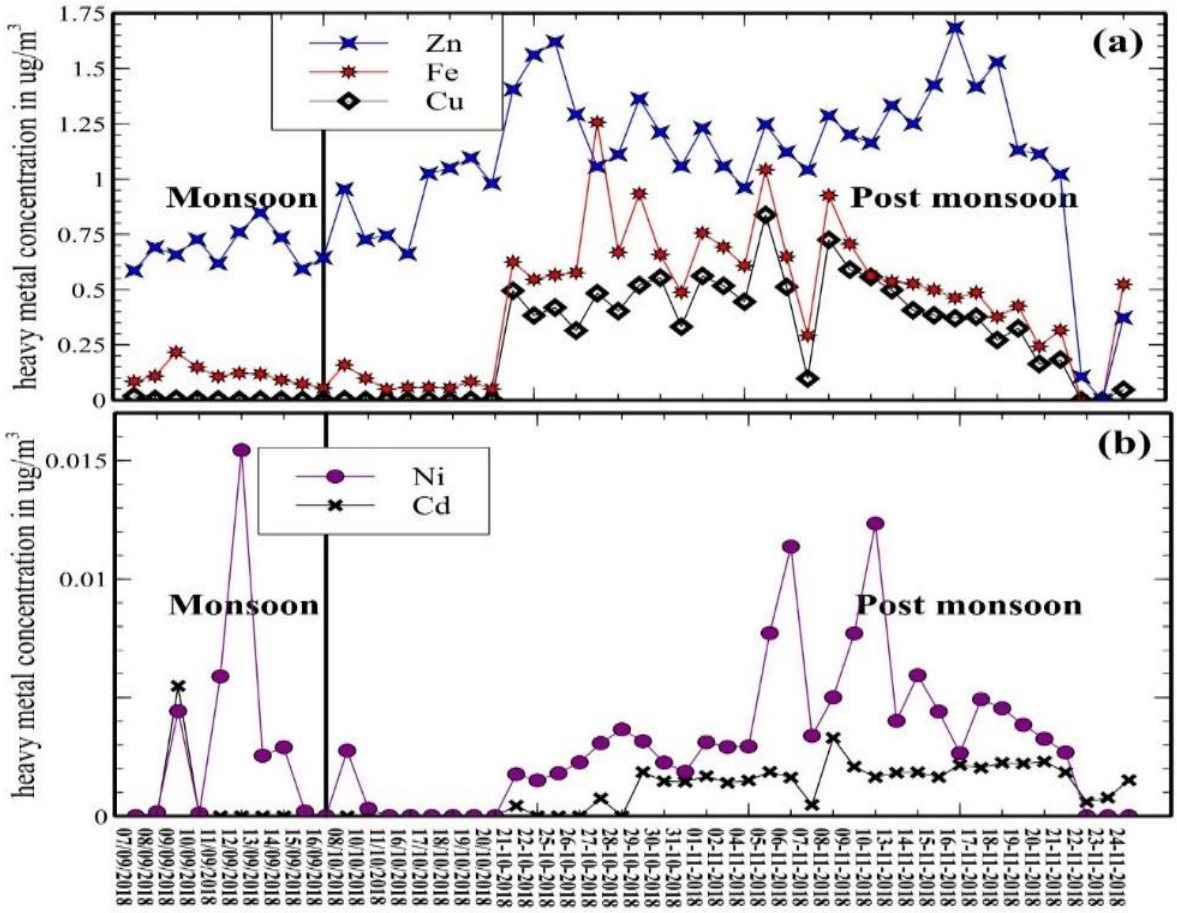

Figure 4.2 Variation in heavy metal concentration

The average concentrations of heavy metals in Warangal region as presented in the Figure 4.3. The order of Zn>Fe>Cu>Ni>Cd observed from the Figure 4.3(a). the HM concentration of the two seasonal differences in monsoon and post monsoon (Figure 4.3(b)) variations, the analysis clearly shows that the monsoon and the post-monsoon concentrations are decreasing trend from one

season to another season. The sudden variation due to the wet deposition of the ambient particulate matter observed in monsoon (Mamun et al., 2022), and the increase in the post-monsoon season will be due to the resuspension of the particulates in the atmosphere. It may cause due to meteorological variations. In the monsoon season, only two elements are in the detectable range (Zn, Fe) but the other elements are not detectable range. In the post-monsoon season, three elements (Zn, Fe, Cu) are detectable and two are not detectable range elements (Ni, Cd). The possibility of the difference would be the anthropogenic activity involved in the post-monsoon season it could be related to Cu emissions.

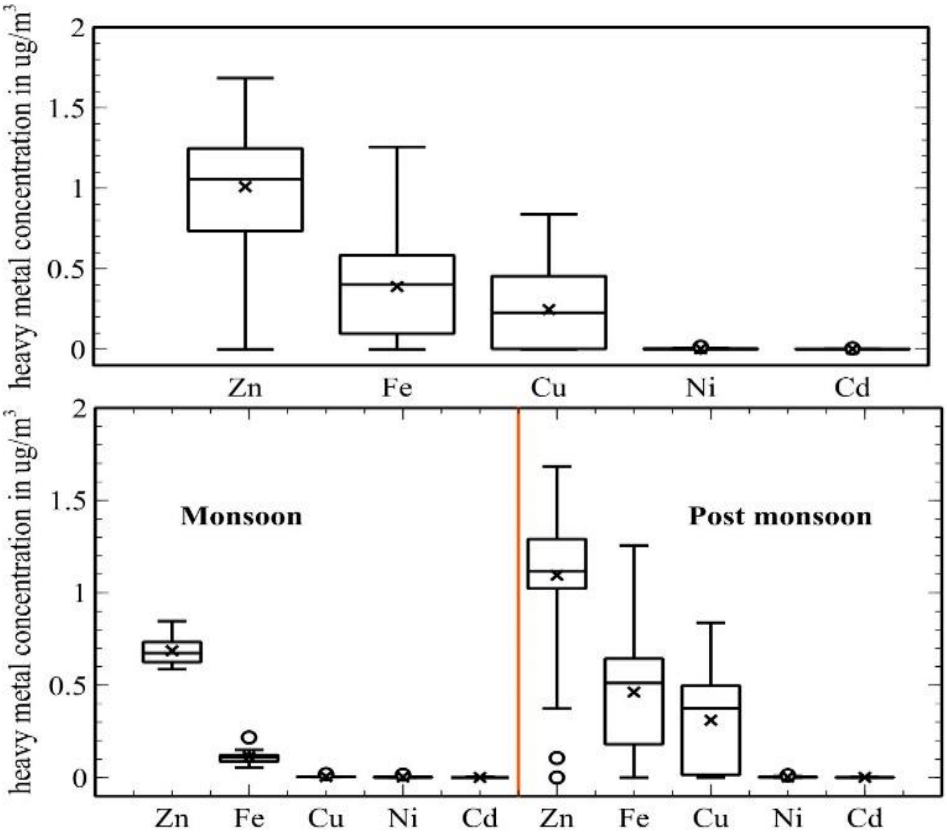

Figure 4.3 Monsoon and Post monsoon Seasonal change in heavy metal concentration

4.3 Pearson's correlation between heavy metals and PM $_{2.5}$

Results of Pearson's correlation analysis performed are presented in Figure. 4.4. Results indicate that Fe and Cu were strongly correlated when compared with other metals. Other significant correlations exist between Zn and Cu, and Zn and Fe and are all predominantly related to traffic emissions. The other correlations among the heavy metals were moderate during the study. Similar results were reported by Fang et al., (2000) indicating traffic as an important source

of heavy metals in urban environments. Chandra et al., 2017, also identified vehicular pollution as the main source of heavy metals. Fe is generally associated with rock weathering and dust from minerals (Cheng et al., 2005; Xia & Gao, 2011), however, in the present study, it was not a dominating source.

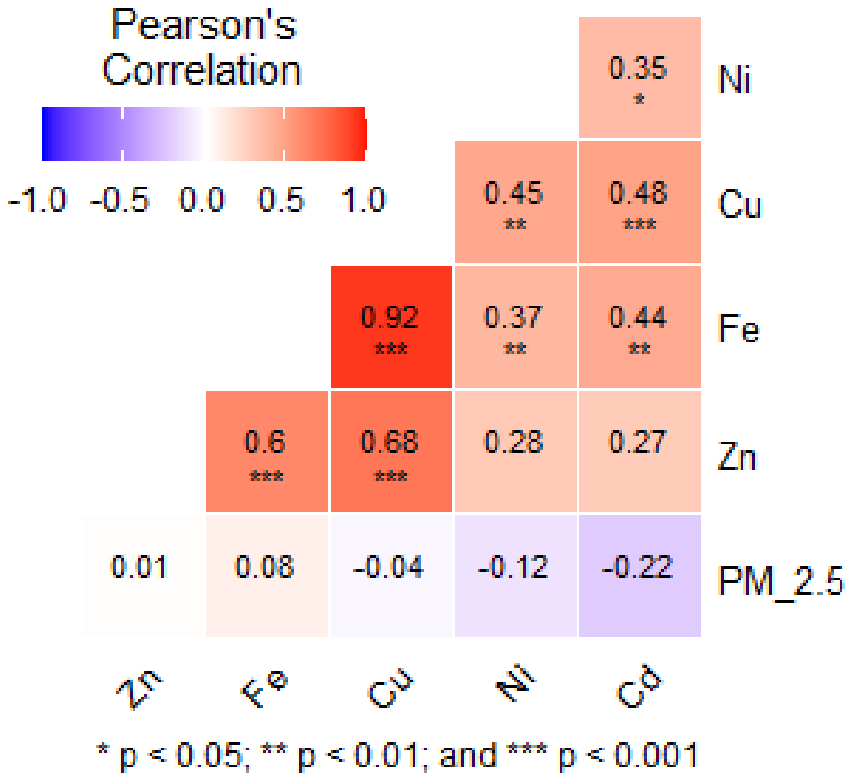

Figure 4.4 Pearson's correlation between various metal elements

4.4 Enrichment Factor analysis

The enrichment factor indicates whether the source of emission is natural or anthropogenic. EF values obtained are depicted in Figure 4.5. EF values for Zn, Cu, Ni, and Cd are above 10. EF value for Ni falls in the moderately enriched bracket indicating nearby industries as possible sources. EF values of Zn, Cu, and Cd were greater than 100 and hence fall in the highly enriched category. Similar results of high enrichment for Zn were reported by Zhang et al., (2010). These emissions are perhaps due to combustion and related activities originating from the automobile and industrial sectors. Ambade, (2014) reported that Ni, Cu, and Cr are emitted from anthropogenic activities while Fe and Zn are generally emitted from natural sources.

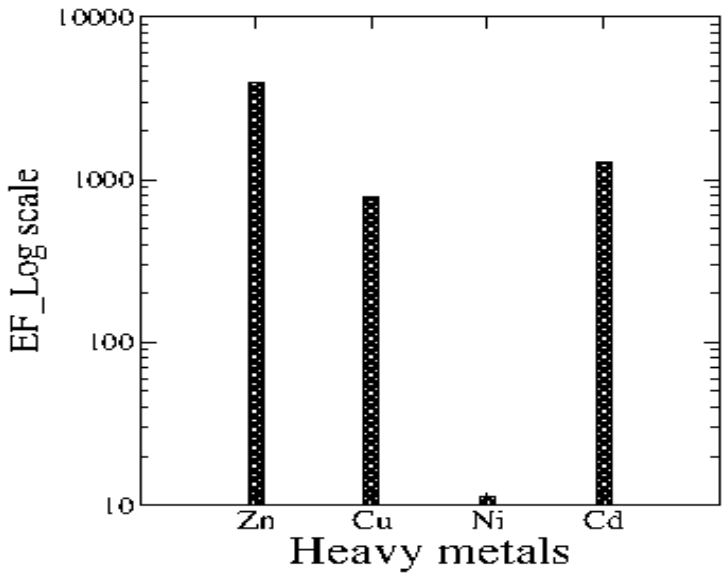

Figure 4.5 Enrichment Factor for heavy metals

4.5 Health Risk Assessment

4.5.1 Exposure Dose Assessment

The exposure assessment evaluation based on Average Daily Dose (ADD) for ingestion, inhalation, and skin contact is presented in Figure 4.6. The results indicated a similar trend variation in ADD for all the exposure pathways in both children and adults. Zn exhibited higher values for all three exposure pathways, while Cu and Fe showed moderate ADD values. Ni and Cd exhibited negligible ADD values for all the pathways. The total average daily dose is presented in Figure 4.7(a) and the order of impact of exposure of metals may be observed to be as follows: Ingestion > Dermal > Inhalation. Zheng et al., (2010) also reported that the ingestion pathway of HMs is a dominant route of exposure followed by dermal contact. Literature reports the significant impact of the resuspension of dust particles and construction activities on ADD values (Kong et al., 2011; Mitra & Das, 2020). Both resuspension of dust due to traffic activity and construction activities dominate the study area.

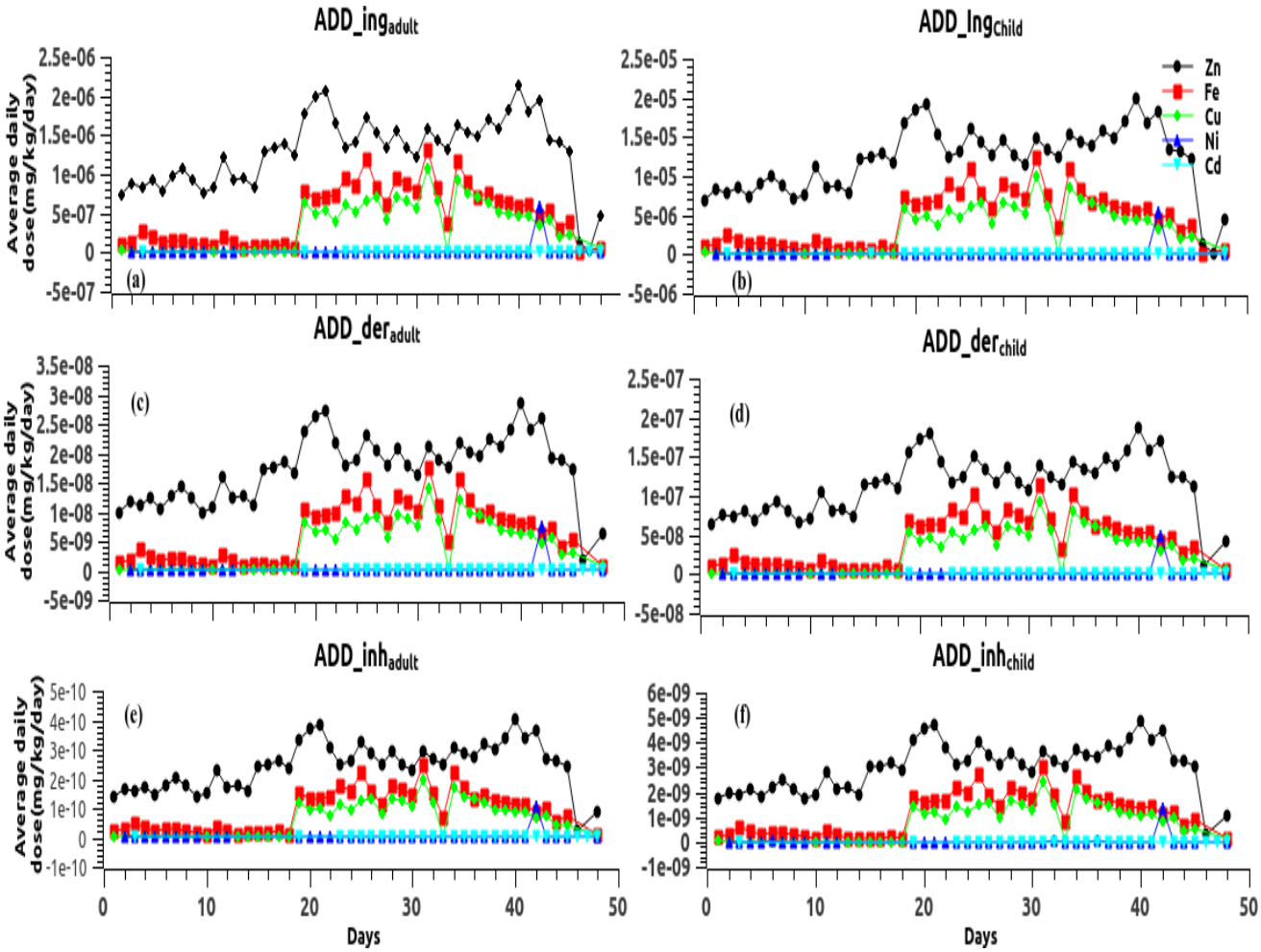

Figure 4.6 ADD for children and adults for ingestion, dermal, and inhalation pathways

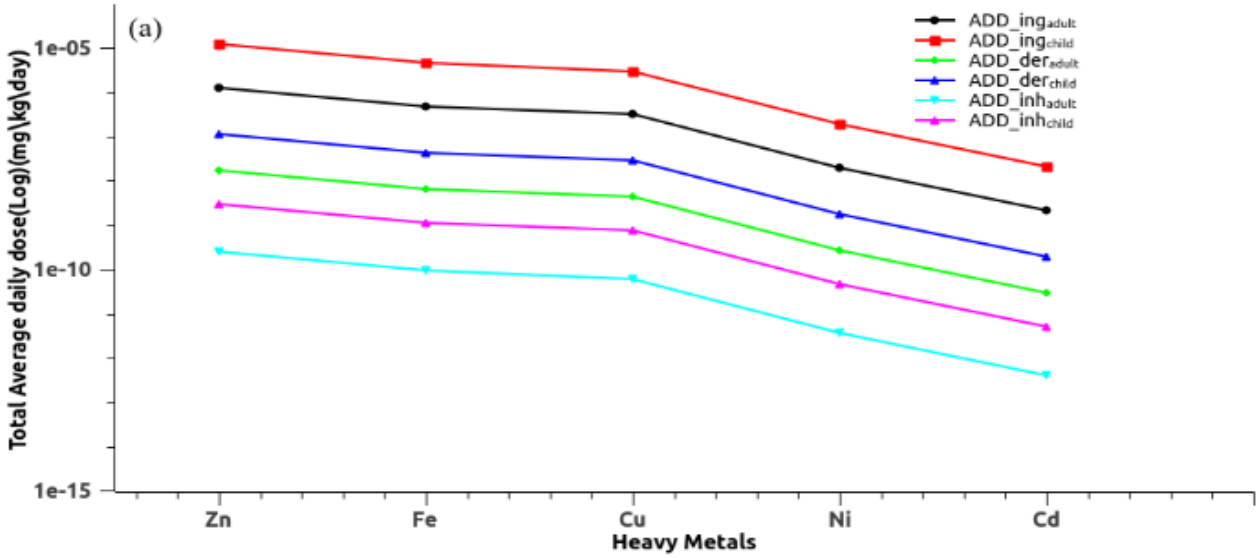

Figure 4.7 Total Average Daily Dose

4.5.2 Non-Carcinogenic Health Risk

Hazard Quotient (HQ)obtained during the study is presented in Figure 4.8. The HQ results obtained were in the following order: HQ_{ing}>HQ_{der}>HQ_{inh}. The trend is similar to that of risk of exposure. Izhar et al., (2014) reported a similar trend in their study on health risks posed by particle-bound metals. For HQ_{der} the following order of metals was observed: Cd > Zn > Cu>Ni, whereas for HQ_{inh} order of metals was: Cu > Zn > Ni > Cd for both children and adults. Though the values were slightly different from one another, the HQ_{ing} trend in both adults and children (Figure 4.8) was observed to be: Cu > Zn > Cd > Ni. HQ index was observed to be below 1 for all pathways.

The HI index is the sum of HQs and the values obtained in the study are presented in Figure 4.9. As RfD values for Fe, Se, and Ca metals have not been specified by USEPA. The results signify that non-carcinogenic threat was negligible for both children and adults since HI (Figure 4.9) values are below 1. However, a higher risk was reported when we consider the injection pathway and derminal contact. Also, the risk for children was more when compared to that of adults. Pongpiachan et al., (2018) also similar HI values (below 1) were reported in the study indicating that that these have non-carcinogenic risks. Ni, Cd, Co, Cr, and Pb are considered carcinogenic metals while Fe, Cu, Zn, and Mn are considered non-carcinogenic metals that generally originate from anthropogenic activities (Pandey et al., 2017).

The HQ_{child} values for all pathways were almost higher values than the HQ_{adult} are appears in this study. It appears reasonable to mention that children are more vulnerable than adults to the noncancerous health effects. The situation can be attributed to their mouthing behaviours and the children’s hand-to-mouth activities are the major exposures.

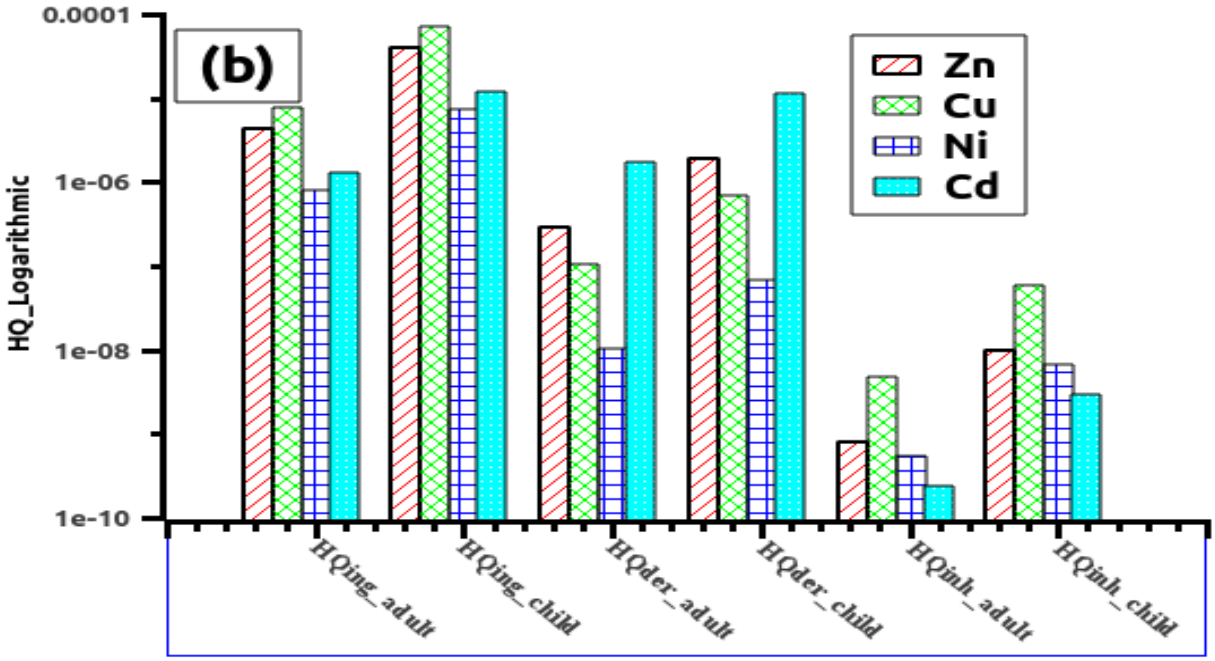

Figure 4.8 HQ Index for heavy metals

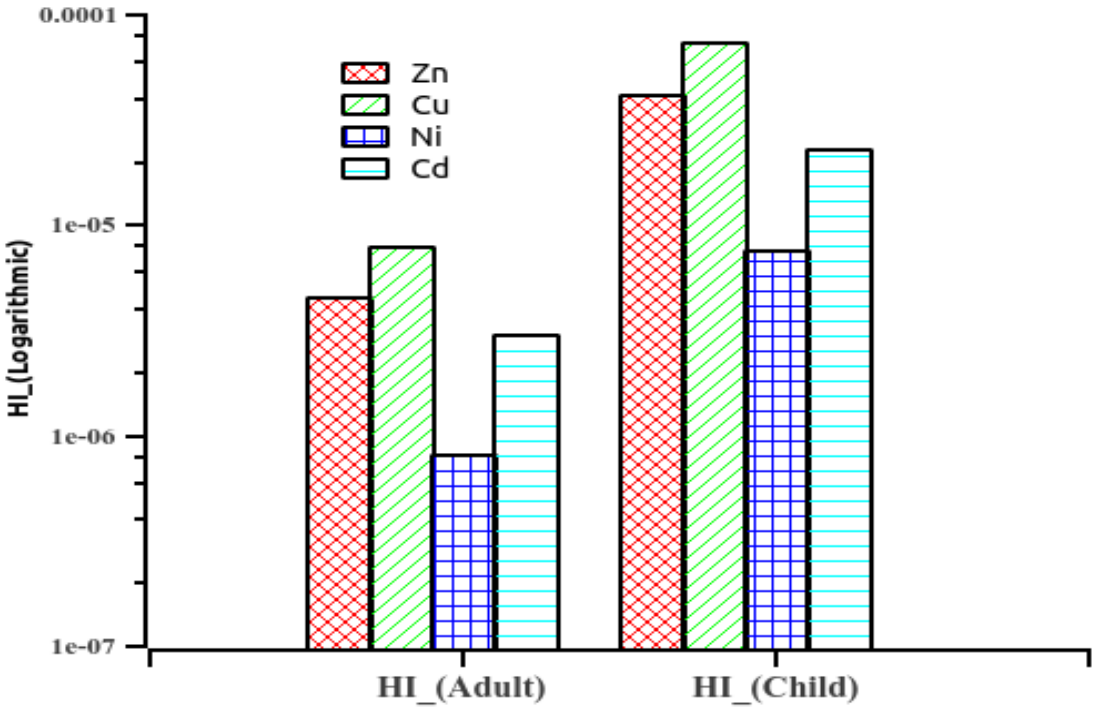

Figure 4.9 Hazard Index associated with heavy metals for adults and children

4.5.3 Excess Cancer Risk Assessment

Results of the study show that the concentration of Ni was higher than Cd when considering the two carcinogenic elements for children and adults. The cancer risk in adults with Ni was 1.02

$x10^{-6}$ and with Cd was 6.12 x 10^{-7}. The ECR in the case of children with Ni and Cd was 1.18x 10^{-6} and 7.15x10^{-6} respectively. The results obtained in the study were within the acceptable limits of 10^{-6} to 10^{-4}. Similar trends in non-carcinogenic and carcinogenic risk assessment for both adults and children were reported in Nanjing, China (Hu et al., 2012). The non-carcinogenic and carcinogenic risks are in general reported to be higher for children than adults (Das et al., 2020; Hu et al., 2012; Mitra & Das, 2020; Sah et al., 2019; Xie et al., 2020).

4.6 Source identification

The back trajectory analysis was used to trace the path of the air mass arrivals at the receptor location. The 7-day back trajectory involves accessing the source regions at the receptor location. The trajectories for September, October, and November (2018) are presented in Figure 4.10. The trajectory for September month indicates the influence of the Western region of India, while the trajectories of October and November were influenced by Indo Gangetic Plain (IGP). Few trajectories were observed from the Bay of Bengal (BOB) in October. The changes in the trajectories can be attributed to changes in season and variations in wind and temperature profiles. However, most trajectories were observed to be from the north-eastern (NE), northern (N), and western (W) regions of India. HYSPLIT back trajectories analysis has also been used by other researchers for the identification of source regions at receptor locations (Yusup et al., 2016).

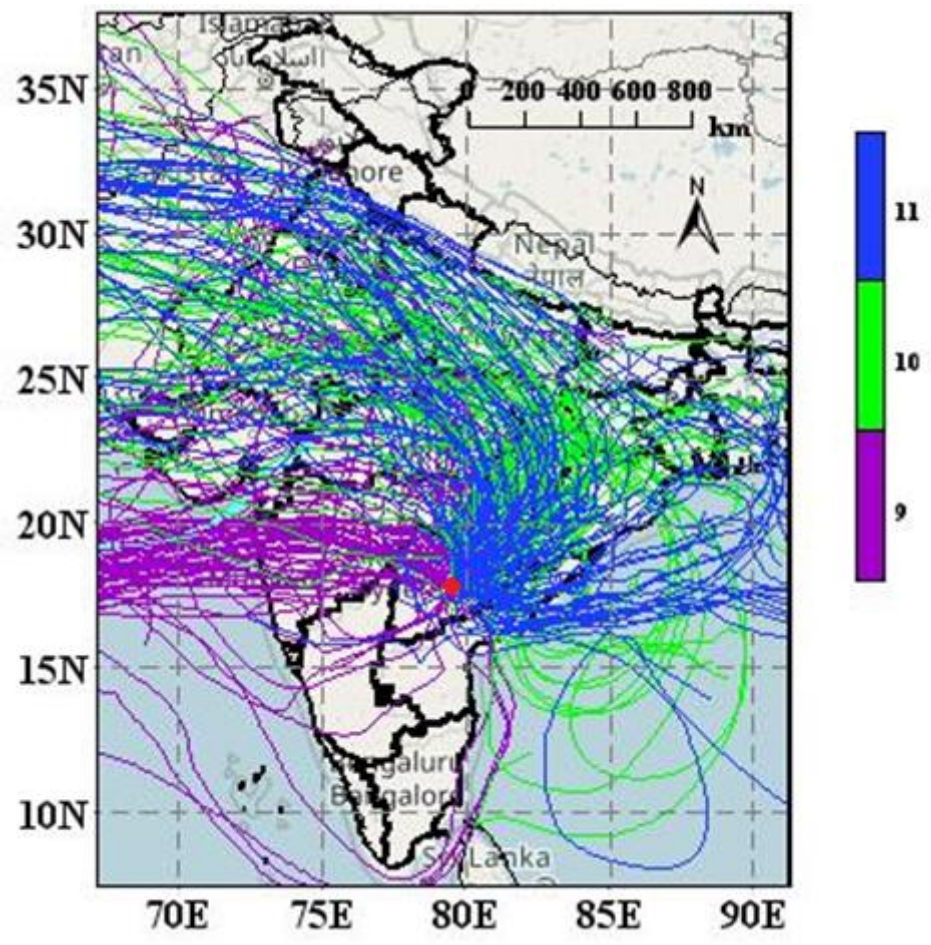

Figure 4.10 HYSPLIT back trajectory for September, October, and November

4.6.1 Concentration Weighted Trajectory Analysis

The CWT analysis shows the contribution of the majority of trajectory regions at receptor or sampling location. The heavy metal transformations at the receptor location are presented in Figure 4.11. Each trajectory coupled with respective metal concentrations using the MeteoInfo software. The meteoinfo is an intergrated framework both for GIS application and scientific computation. Results show that Zn is contributed from NE regions especially Odisha and Chhattisgarh and parts of Central India (mainly Madhya Pradesh). This can be attributed to significant coal mining and biomass burning in these regions. Fe, Cu, Ni, and Cd are contributed by local anthropogenic activities and dust resuspension due to wind currents. (Mukherjee and Agrawal, 2018) reported a significant contribution of $PM_{2.5}$ from north-western (NW) regions of India using CWT and Cluster Analysis. Rai et al., 2020, identified that the pollutants moving toward the receptor, (Darjeeling in their case) originate mainly from Nepal apart from the IGP and the BOB.

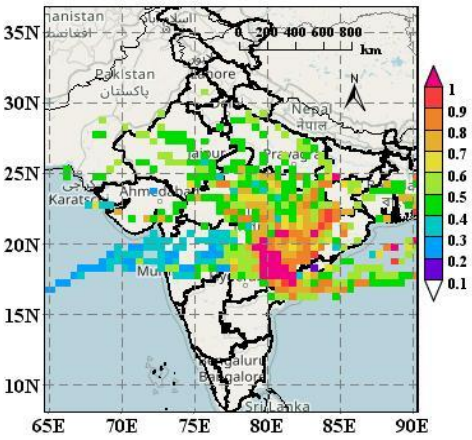

(a) Zinc(Zn)

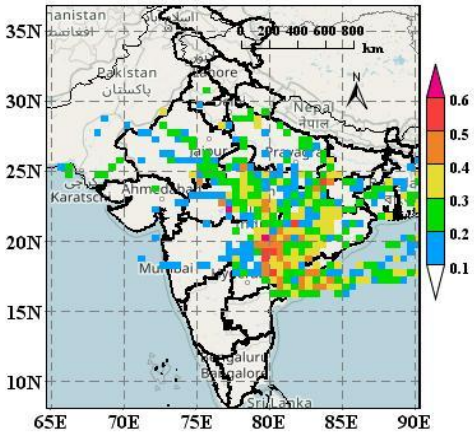

(b) Iron(Fe)

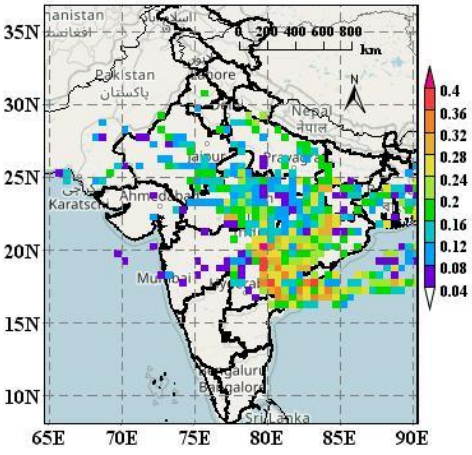

(c) Copper(Cu)

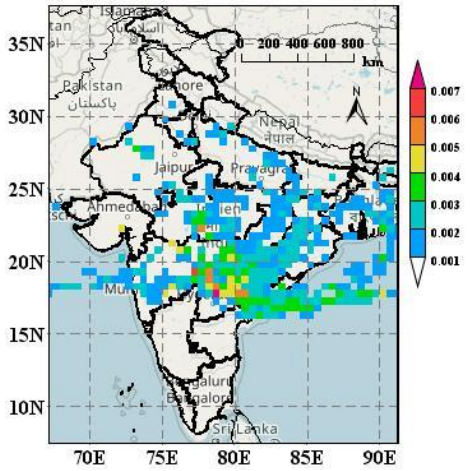

(d) Nickel(Ni)

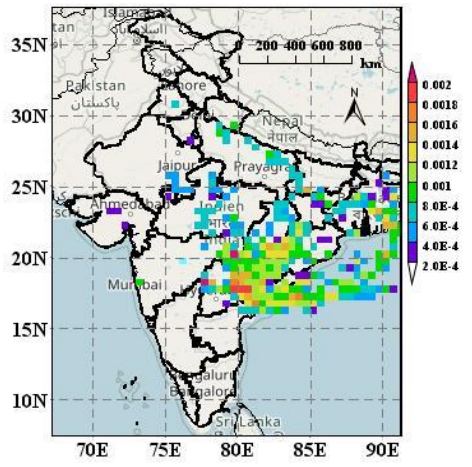

(e) Cadmium(Cd)

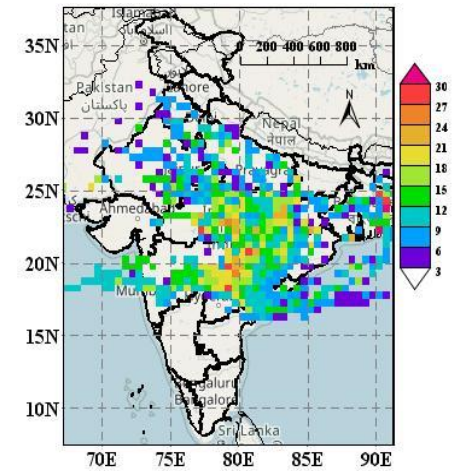

(f) PM $_{2.5}$

Figure 4.11 CWT analysis for September October and November(a) Zn (b) Fe (c) Cu (d)Ni (e) Cd (f) $PM_{2.5}$

4.6.2 Potential Source Contribution Function Analysis

NE regions (Odisha, Chhattisgarh, and Jharkhand) and IGP regions contribute Zn and the same was evident in WPSCF analysis (Figure 4.12). As these regions are dominated by mining activities and the burning of fossil fuels, Zn contributions will likely be significant. Similar findings have been reported by Chinnam et al., 2006. Fe, Cu, and Ni were mainly contributed by nearby local sources. The NE coastal region was a moderate contributor (0.7-0.8 significance levels) for all metals. The majority of the potential source regions fall upwind towards the receptor location. It may be noted that the transformation of pollutants from upwind to downwind causes a transboundary particle moment from most east coastal states and some central states. The transport and accumulation of pollutants are based on the geographical location of the existing region (Kong et al., 2020; Qiao et al., 2019).

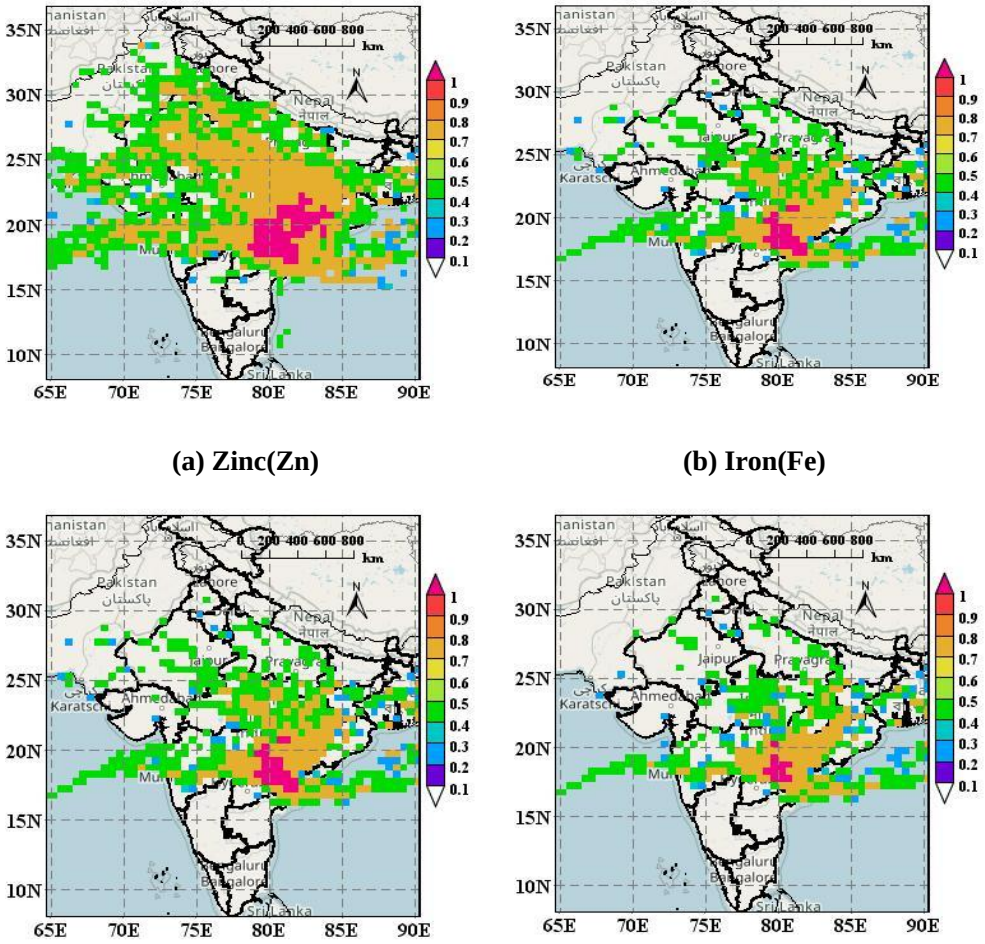

(a) Zinc(Zn) **(b) Iron(Fe)**

(c) Copper(Cu) **(d) Nickel(Ni)**

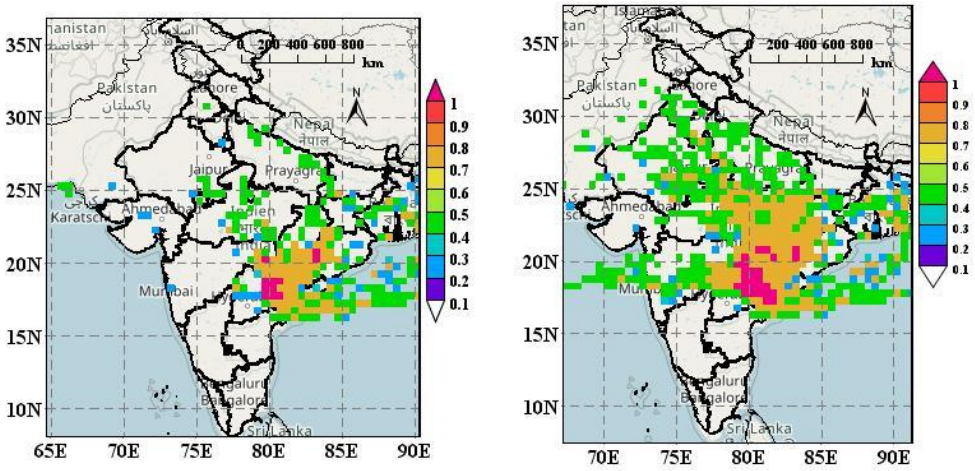

(e) Cadmium(Cd) **(f) PM $_{2.5}$**

Figure 4.12 PSCF analysis for (a) Zn (b) Fe (c) Cu (d) Ni (e) Cd (f) PM $_{2.5}$

4.6.3 Cluster analysis

The clustering of all 7-day back trajectories at receptor location observed during the study is shown in Figure 4.12. Cluster 4 was observed to contribute 27.11% of trajectories from the NW region of India, while Cluster 2 was observed to contribute 22.34% of trajectories from Odisha, Chhattisgarh, and part of Madhya Pradesh. Cluster 3 contributed about 20.15% from parts of Madhya Pradesh, Rajasthan, and Western parts of the world on Indian border. Clusters 1 and 5 contributed about 10.62 and 8.79% from part of Maharashtra and the Arabian sea mostly. Cluster 6 contributed 10.99% of trajectories from the BOB indicating the influence of sea salt origin at the receptor location. In cluster analysis, it was noticed that Odisha and Chhattisgarh contribute significantly due to mining activities, thermal power plants, and associated industries. Similar findings related to transport in the lower layer and from nearby local regions were reported by Hong et al., (2019); Kopas et al., (2020). Luo et al., (2020) also reported 5 clusters from their investigations based on 48-h mass back trajectory studies. The tracers for CO and $PM_{2.5}$ were identified as fire emissions in the regional air quality forecasting system. The modelling framework indicates that stubble-burning fires contributed up to 30-35% of Delhi's air pollution during October-November 2021(Govardhan et al., 2023).

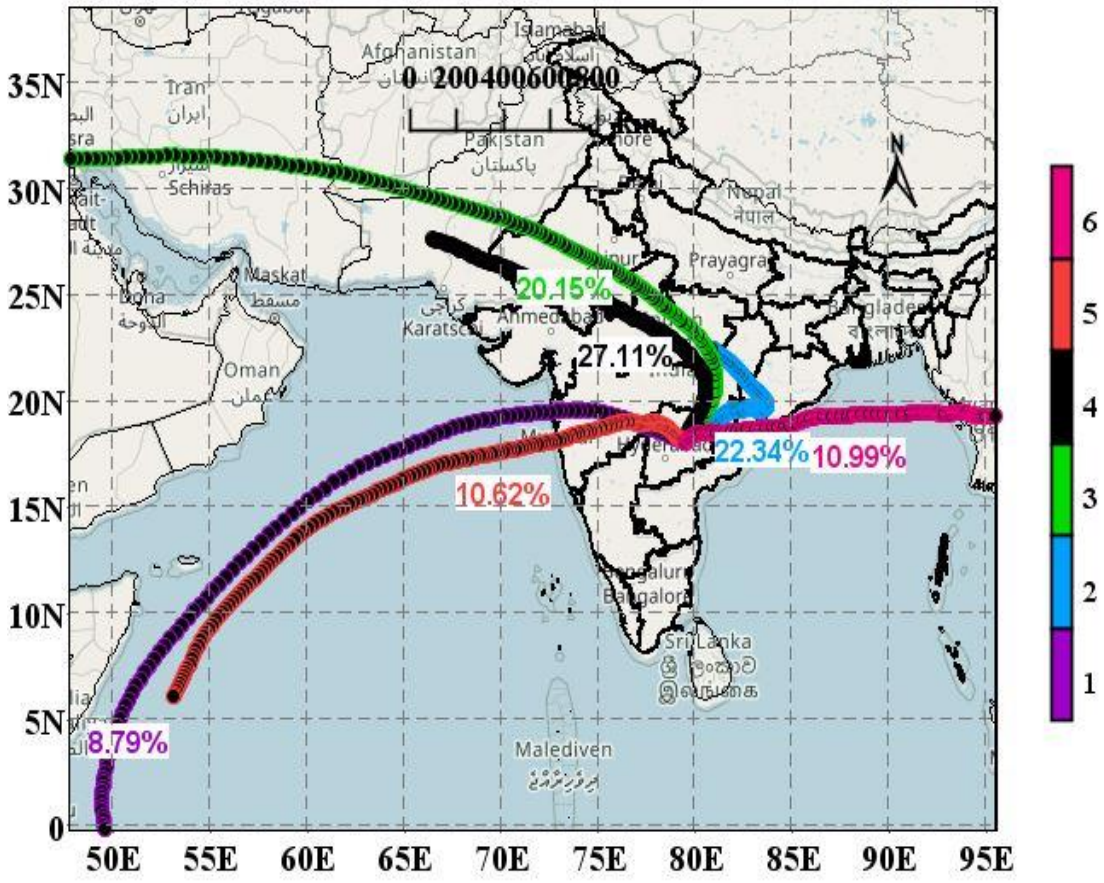

Figure 4.13 Cluster analysis

4.7 Summary

Based on the analysis of $PM_{2.5}$ during the study, concentrations of $PM_{2.5}$ and heavy metals are high in the post-monsoon season. However, the $PM_{2.5}$ concentrations observed were lower than the standards prescribed by NAAQS. Pollution due to heavy metals bound to $PM_{2.5}$ was significant due to emissions from traffic and anthropogenic activities in urban areas. It was evident that from the CWT, PSCF and cluster analysis indicate the pollution was significantly contributed by long-range transport. Zn, Fe, and Cu concentrations in $PM_{2.5}$ were significantly higher compared to the concentrations of Ni and Cd. The order of occurrence of heavy metals in descending order was found to be: Zn>Fe>Cu>Ni>Cd. Long-term sampling may help in better understanding the variation in $PM_{2.5}$ and metal concentrations. EF values of Zn, Cu, and Cd are high indicating association with combustion and industry. Health risk assessment showed that the ingestion pathway dominates over the dermal and inhalation pathways. Based on HQ and HI index, it may be concluded that there is no significant non-carcinogenic and carcinogenic risk from the observed

metals in the study region. However, the risk for children was higher when compared to that for adults.

From the CWT, PSCF, and cluster analysis, it may be concluded that the contributions from the western and North-Western regions of India dominate at the given receptor location. Since heavy metals bound to PM2.5 were analysed in this study, the presented results from health assessment and source identification can be used in planning air pollution control strategies and for framing appropriate regulations.

Chapter 5 Estimation of ground level $PM_{2.5}$ with MODIS Aerosol optical depth and source identification using trajectory analysis over Hyderabad region

5.1 Variation of meteorological parameters

Meteorology and air pollution are interconnected disciplines that explore the intricate interplay between the atmosphere and the presence of pollutants within it. Meteorological parameters influence the air quality and their transport in the atmosphere. Meteorology delves into the mechanisms and dynamics of the Earth's atmosphere, encompassing the analysis of weather patterns, atmospheric phenomena, and the behaviour of air masses. A comprehensive grasp of meteorological factors is pivotal in evaluating and forecasting levels of air pollution. Meteorological parameters namely – ambient temperature (AT), relative humidity (RH), wind speed (WS), wind direction (WD), solar radiation (SR) and barometric pressure (BP) variations are analysed over Hyderabad regions from the May 2017 to May 2019. The data adapted in this study from the CPCB secondary data and the variations are presented in Figure 5.1. Statistical parameters of the meteorological factors are given in Table 5.1. The temperature and relative humidity values are approximately to those reported in the Jaipur region reported by Soni et al. (2018). Temperature inversion leads to higher values of pollutants in the winter season at ground level (Yadav et al., 2019). The wind speed and direction are also important parameters in the dispersion and transport of particles. These particles move along with the wind from one region to far away regions depending on the strength of the wind and atmospheric stability conditions. Hence, the meteorological parameters are crucial for the identification of the particulate concentration at the receptor location (Das et al., 2021; Zhang et al., 2017). Higher variations are observed in BP and SR at all locations. Lower deviations in AT, RH, PM, and AOD are observed. This is perhaps due to the topography of the land and climatic conditions. In the present study, the mean temperatures recorded at all locations are typical of those found in tropical regions. However, the winter and summer temperature variations are significant.

The use of satellite data to estimate air quality is one of the indirect methods that is used in regions where data is scarce or temporal coverage is limited. Regional air quality assessment and modeling can use data obtained by satellite sensors. AOD and MODIS are widely used to assess air quality

at urban and local scales. The presence of particulates in the atmosphere will be reflected by AOD and the intensity of the light received by the instrument will reflect the columnar property of the atmosphere. Satellite-based AOD measurements are widely used to predict $PM_{2.5}$ and PM_{10} (Shao et al., 2017; Soni et al., 2018). The variations in $PM_{2.5}$ with AOD during the May 2017 to May 2019 period shown in Figure 5.1(d) and the statistical parameters are given in Table 5.1. The mean AOD variations in the ranges as follows at Bollaram (0.54±0.21), Central University (0.54±0.23), IDA (0.50±0.2), Patancheru (0.55±0.23) Sanathnagar (0.52±21) and Zoopark (0.47±0.22). High AOD was observed at Patancheru and the least AOD at the Zoopark location. The higher AOD values at Patancheru are perhaps due to concentrated industrial activity while Zoopark represents minimum anthropogenic activity. Higher AOD values indicate a significant contribution from submicron aerosols to columnar loading. Soni et al., (2018) reported the average AOD as 0.42 and the range as 0.02–1.67 in the Jaipur region. AOD values were higher during the pre-monsoon and winter with a subsequent decrease in the summer period. The study in an urban environment in Eastern India reported AOD in the range of 0.82 (winter) and 0.71 (summer) (Pani and Verma, 2014). The influence of climate change on particulate pollution and transboundary aerosols was reported by Deb and Sil (2019). However, the influence of climate change on particulate pollution is not attempted in the present study.

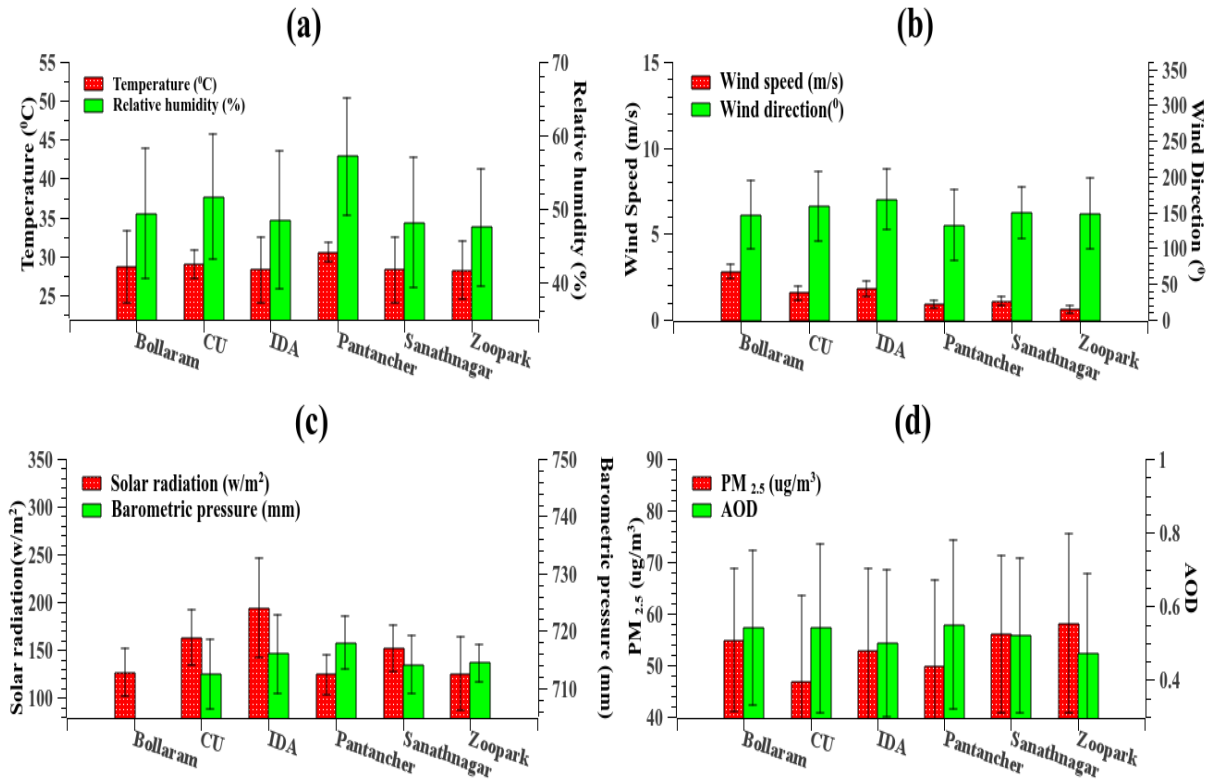

Figure 5.1 Meteorological variation of all locations (a) RH (%) and Temperature (^{0}C) (b) Wind speed (m/s) and Wind direction (degrees) (c) Barometric pressure (mm) and Solar radiation (W/m^2) (d) $PM_{2.5}$ (µg/m^3) and MODIS Terra AOD

Table 5.1 Variation of the meteorological parameters over six locations for May2017 to May 2019. **Source:** CPCB (2020a)

Location	**Parameters**	**Aerosol optical depth**	**Ambient temperature(^{0}C)**	**Relative humidity (%)**	**Wind speed(m/s)**	**Wind direction(degrees)**	**Solar radiation(W/m^2)**	**Barometric pressure(mm)**	**$PM_{2.5}$ (µg/m^3)**
Bollaram	Min	0.04	19.56	30.66	0.30	42.71	70.04	-	12.39
	Max	1.16	39.70	72.07	9.23	287.78	199.89	-	92.97
	Median	0.52	28.36	49.02	1.62	140.06	121.00	-	55.01
	Average	0.54	28.65	49.32	2.80	146.65	126.42	-	54.84
	Stdev	0.21	4.63	8.84	2.41	47.80	25.08	-	13.95
Central University	Min	0.04	25.79	33.34	0.60	45.94	76.75	700.97	13.17
	Max	1.23	33.52	74.06	2.63	259.34	237.78	731.50	96.84
	Median	0.51	28.45	51.41	1.53	153.56	162.07	713.39	43.00
	Average	0.54	28.98	51.62	1.54	159.00	163.02	712.39	46.77

	Stdev	0.23	1.83	8.54	0.39	48.43	28.61	6.04	16.78
IDA	Min	0.10	20.64	28.56	0.80	53.49	83.12	696.83	6.41
	Max	1.09	38.49	75.31	3.02	302.60	326.79	732.98	83.63
	Median	0.48	27.34	47.60	1.77	165.92	192.98	716.72	53.89
	Average	0.50	28.23	48.44	1.80	168.16	194.07	715.92	52.80
	Stdev	0.20	4.27	9.36	0.45	42.21	51.59	6.77	16.00
Patancheru	Min	0.05	28.59	41.45	0.52	27.00	66.78	711.62	0.94
	Max	1.22	34.03	79.68	1.56	268.41	167.96	731.43	78.78
	Median	0.52	30.05	58.59	0.87	121.97	121.49	716.80	50.50
	Average	0.55	30.51	57.14	0.91	132.29	124.03	717.87	49.76
	Stdev	0.23	1.22	7.99	0.22	49.72	20.75	4.61	16.77
Sanath Nagar	Min	0.05	20.24	30.11	0.58	86.11	83.86	701.79	15.57
	Max	1.10	38.80	72.86	1.94	261.25	216.87	725.47	91.69
	Median	0.50	28.19	47.27	1.04	145.52	152.12	714.63	54.71
	Average	0.52	28.23	48.06	1.08	148.86	151.39	714.10	56.02
	Stdev	0.21	4.27	8.84	0.29	35.94	24.52	5.16	15.16
Zoopark	Min	0.01	19.34	28.89	0.29	44.20	18.02	703.41	13.00
	Max	1.08	36.86	68.99	1.30	317.12	233.51	721.96	104.09
	Median	0.44	27.88	47.54	0.53	143.38	123.58	715.84	60.01
	Average	0.47	28.18	47.44	0.58	148.28	125.20	714.35	58.12
	Stdev	0.22	3.72	8.00	0.24	49.58	38.77	3.22	17.33

5.2 MODIS AOD for prediction of the $PM_{2.5}$

5.2.1 Variation of MODIS AOD over an urban region

The relation between MODIS products (MOD_3K, MOD_L2, MYOD_3K, and MYOD_L2) and $PM_{2.5}$ are shown in Figure 5.2. The relationships are established using the R language tool. In the present study, a weak positive correlation is observed between AOD and $PM_{2.5}$ at most locations for all MODIS products. The linear regression results between AOD and $PM_{2.5}$ results indicate a weak positive correlation in some locations with a relatively higher correlation at Bollaram. A single grid of each pixel was chosen for the study, the missing AOD data was replaced with an average AOD of 3x3 or 5x5 grid. The variations are perhaps due to the urban conditions and geographical differences. Local dominating sources also result in variations.

The relationship between AOD and $PM_{2.5}$ is based on the theoretical assumption that $PM_{2.5}$ is reflected in AOD captured by satellites. As such there is a correlation between AOD and $PM_{2.5}$ and it is either strong or weak depending on various factors. $PM_{2.5}$ represents the ground-level concentration of particles with a diameter of less than 2.5 μm, while AOD represents the visibility

in the atmospheric column from the ground surface to satellite height (in the order of numerous km). Furthermore, $PM_{2.5}$ reflects the dry weight of particles, and it is not affected by water vapor and other particles in the atmosphere, while AOD is affected by water vapor and other particles in the atmosphere as well. Hence, the relationship between AOD and $PM_{2.5}$ can be either weak or strong. The complicated relationship between AOD and $PM_{2.5}$ varies temporally and spatially depending on environmental conditions. The relationship is reflected in $PM_{2.5}$ retrievals. However, For retrievals, the study is useful for this region only as such, cannot address large-scale retrieval challenges. A comprehensive study over the larger area covering different cities and regions is required to establish relationships between $PM_{2.5}$ -AOD which subsequently can be used for retrievals. The AOD - $PM_{2.5}$ relation is stronger in some locations in India (Chelani, 2018). Other studies have also shown a similar trend where, coastal areas, the $PM_{2.5}$-AOD relation was weaker comparisons shown by Yang et al., (2019). Few studies indicated a positive and weaker correlation with the AOD - $PM_{2.5}$ (Chelani, 2018; Yang et al., 2019).

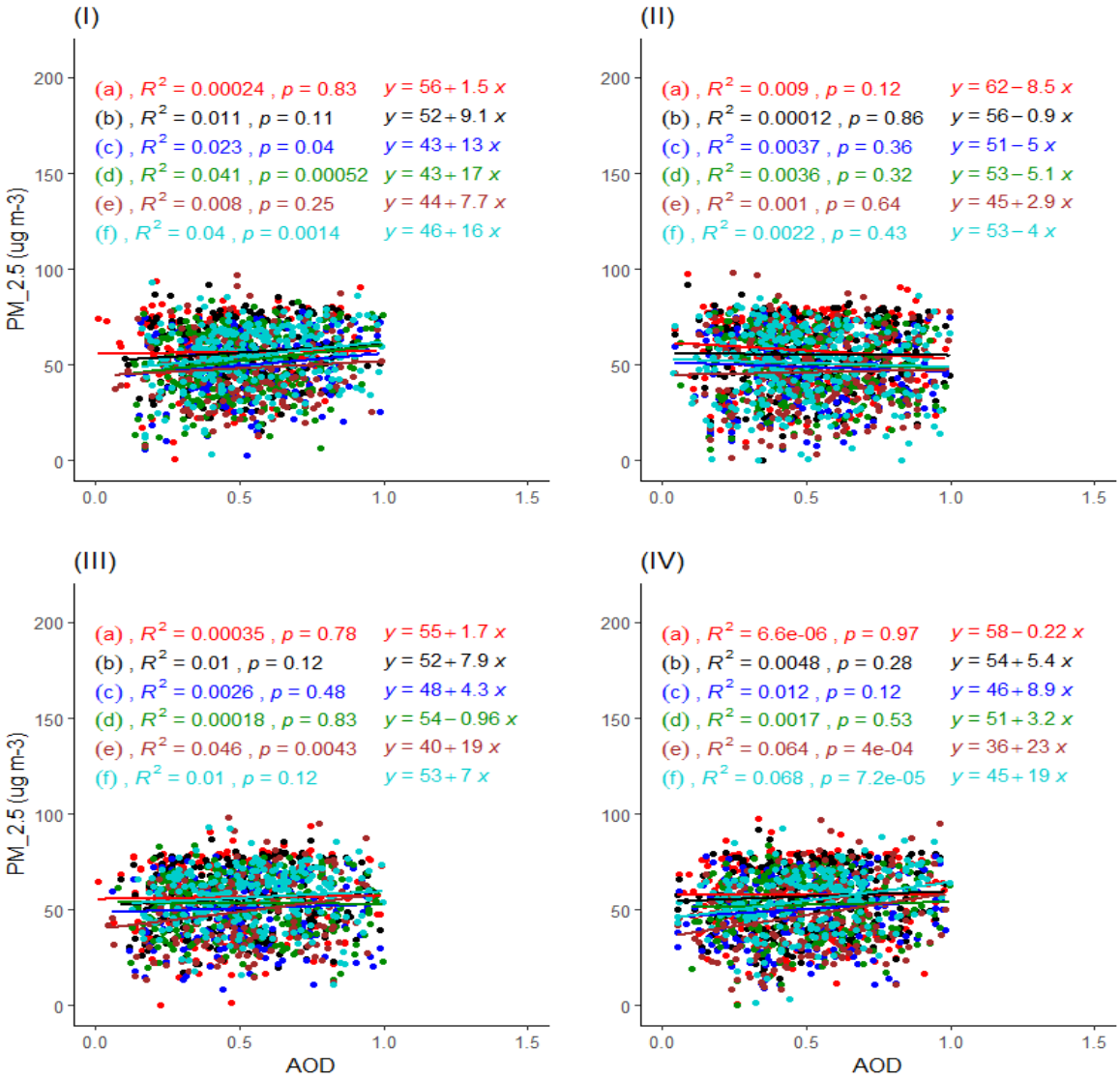

Figure 5.2 AOD - $PM_{2.5}$ correlation within MODIS product at all locations,

(I) MOD_3K (3km) (II) MOD_L2 (10km) (III) MYOD_3K (3km) (IV) MYOD_L2 (10km)
(a) Zoopark (b) Sanathnagar (c) Patancheru (d) IDA (e) Central University (CU) (f) Bollaram

5.2.2 Multiple linear regression model

For the prediction of ground-level $PM_{2.5}$ concentration, regression model was developed using AOD and meteorological parameters (temperature, RH, Wind speed, wind direction, solar radiation, and pressure). Statistical parameters (R, RMSE, d, and NMB) of the models are presented in Table 5.2. Results indicated relatively good agreement at Zoopark when compared to the other five locations. Also, the MOD_L2 product was observed to give better predictions when compared to others except for Patancheru. The variations in model predictions were observed from

location to location. Some of them gave good predictability which is reflected in terms of R ranging between (0.33-0.64) at the Zoopark location. Kharol et al., 2011 also reported similar correlation coefficients (0.30 to 0.46) between Level 3 Terra/Aqua MODIS and MICROTOPS-II, AOD550 in all seasons over Hyderabad.

The scatter plots between observed and predicted concentrations (for 3 km and 10 km resolution of Aqua and Terra product) for Zoopark are presented in Figure 5.3. Most of the predicted values fall within the 30% error line (black dotted line) indicating the applicability of the MLR model. Few points were observed within the 50% error line.

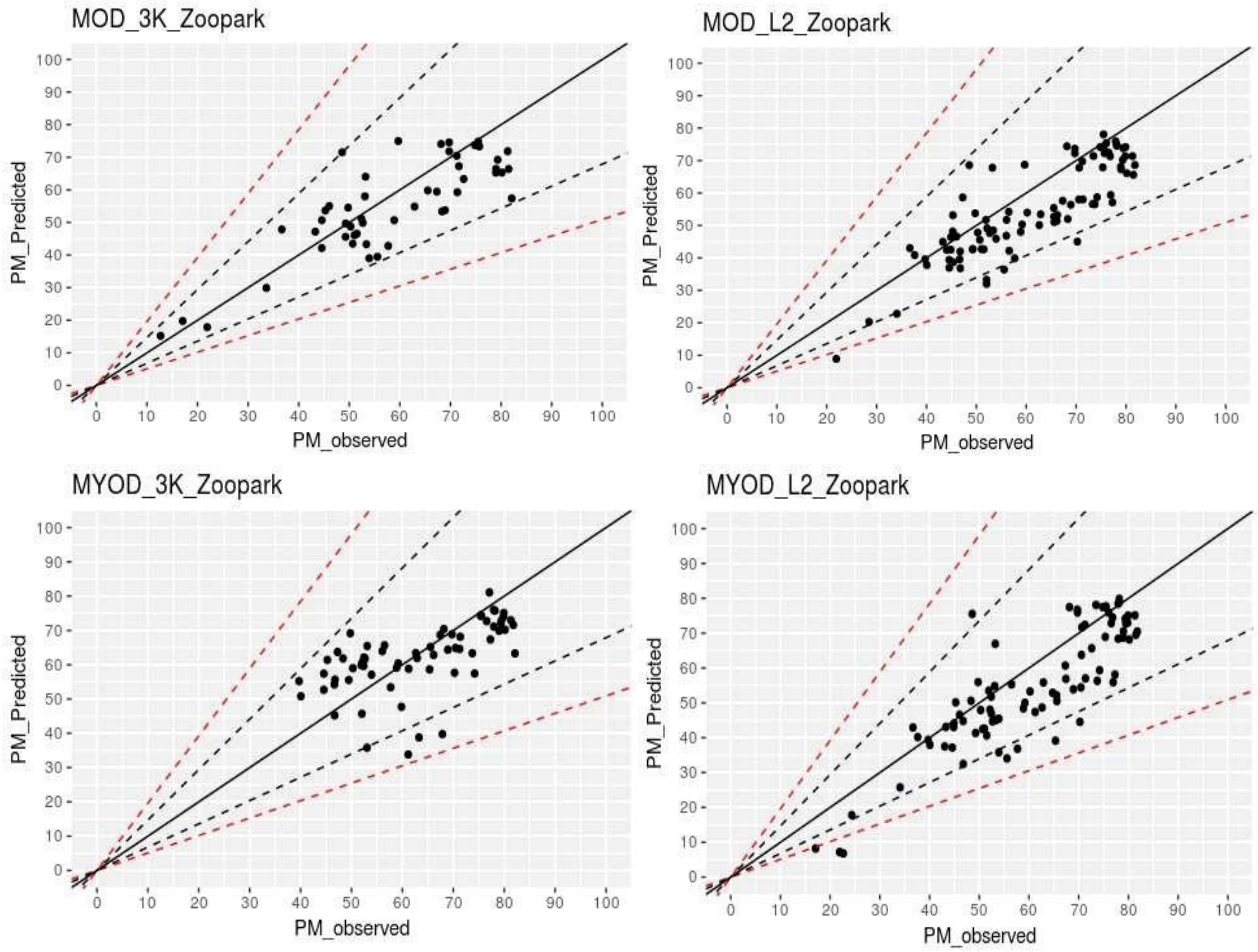

Figure 5.3 Scatter plot for $PM_{2.5}$ Predicted and Observed at Zoopark location for four MODIS AOD product

Shao et al. (2017) in their studies on AOD- $PM_{2.5}$ in Nanjing of the Yangtze River Delta, concluded that there was a high consistency of AOD versus $PM_{2.5}$ and the correlation coefficient was (R) 0.56. In the current study, the correlation coefficients are slightly lower around 0.4 for

various MODIS products. Lower correlation coefficients are reported to be due to desert dust and cloud properties Gopal et al., 2016).

The MOD_3K product has a negative Normalized Mean Bias (NMB) except for the Zoopark location. The correlation coefficients were higher for Zoopark, IDA, and Sanathnagar; lower values for Patancheru, Bollarm, and CU regions. RMSE was higher (54 $\mu g/m^3$) at Patancheru and low for other locations (11-15 $\mu g/m^3$). RMSE values at Patancheru peaked in all MODIS collections when compared with other locations. The MOD_L2 results indicated over-prediction at CU and Zoopark locations, while under-prediction was observed for other locations. The correlation was higher (0.41) at Zoopark while the correlation was low at Patancheru. The RMSE variation range (11-14 $\mu g/m^3$) except for the Patancheru region. The MYOD_3K and MYOD_L2 have nearly similar values in RMSE, d, and NMB indicating good agreement in the correlation coefficient in the MYOD_3K product. Greater resolution data resulted in a higher deviation from the standard line in this study. Kumar et al., (2008) reported that the finer resolution of MODIS_AOD in addition to RH and atmospheric pressure results in a better correlation for the prediction of $PM_{2.5}$ in New Delhi. The Terra AOD product performed better than the Aqua in the present study while the 10km resolution data performed better than the 3km resolution data in the correlation analysis. Similar results were reported by Wang et al., (2019).

MODIS AOD product obtained for 10km and 3 km resolution is used. The quality of the 3 km resolution was generating relatively high noise influencing the accuracy of prediction. Munchak et al., (2013) also reported similar observations. The study considered a linear relationship between $PM_{2.5}$ and meteorological parameters while the $PM_{2.5}$ formation mechanisms are not considered. The model accuracies are influenced by the $PM_{2.5}$ formation mechanism, spatiotemporal heterogeneities, and geographical regions. The best-fit location was identified based on MLR, later the location latitude and longitude were used in the Hybrid Single-Particle Lagrangian Integrated Trajectory model (HYSPLIT) model for back trajectory analysis.

Table 5.2 MODIS AOD and $PM_{2.5}$ summarized statistical parameters for the six locations

	Parameter	Bollaram	Central University	IDA	Patancheru	Sanath nagar	Zoo Park
MOD_3K	RMSE	15	15	11	54	10	12

	d	0.53	0.59	0.81	0.21	0.78	0.76
	NMB	-0.15	-0.02	-0.02	-0.84	-0.04	0.05
	R	0.13	0.13	0.53	-0.18	0.47	0.36
MOD_L2	RMSE	12	14	12	55	11	11
	d	0.52	0.66	0.71	0.22	0.73	0.85
	NMB	-0.009	0.11	-0.03	-0.87	-0.03	0.10
	R	0.34	0.30	0.46	-0.15	0.38	0.64
MYOD_3K	RMSE	15	15	13	47	10	10
	d	0.52	0.73	0.62	0.25	0.81	0.74
	NMB	-0.12	0.14	-0.08	-0.67	-0.02	0.01
	R	0.28	0.38	0.51	-0.11	0.56	0.33
MYOD_L2	RMSE	14	16	11	44	11	11
	d	0.52	0.60	0.82	0.22	0.74	0.80
	NMB	-0.12	0.11	-0.04	-0.67	-0.01	0.09
	R	0.21	0.16	0.59	-0.25	0.42	0.56

5.3 Backward Trajectory analysis for source identification

The backward trajectory simply the air mass trajectory path with suitable end points, based on the end points which will differ from one trajectory to the other one. To club the all these trajectories at one location creates the variations in the grid points to identified the potential grids in study location. For the each of the trajectory required the suitable parameter to convert the grid points. In this study PM2.5 chosen as the identified parameter. As well as the fug data collection was mandatory for the accurate conclusion on the source regions. The daily data was difficult to collect manually so that the Hyderabad study location was chosen for the continues data. From the last chapter the methodology following same for the CWT, PSCF and cluster analysis in this chapter.

5.3.1 Concentration-Weighted Trajectory

The results obtained by CWT analysis for Hyderabad are presented period of May 2017 to May 2019 in Figure 5.4, with Figure 5.4 (a, b, c, d) indicating the CWT analysis for the surface layer represent the trajectory heights with the 100m, 500m, 1000m. Season-wise percentile contributions

of pollutants by trajectories are indicated in Figure 5.4. The colour in the figure reflects the concentrations - the red colour represents high concentrations while the blue represents low $PM_{2.5}$ concentrations. Season-wise weighted trajectory details are presented in Table 5.3. CWT analysis helps in finding the influence of short-range regional transport of air pollution and indicates the direction of trajectories. The surface layer concentrated paths identified for the winter season are dominating. The trajectory paths from East India, North India, and coastal regions are likely the contributing source paths for receptor location considered in the study. However, the weighted trajectory from East India and Coastal regions are more dominating in winter. Two paths are identified in the pre-monsoon, which are from land and sea regions. These are perhaps due to land and sea breeze effects from nearby coastal regions. The two dominating paths are - one from central India and the other from the Bay of Bengal. In the monsoon, trajectories from Western India and the Arabian Sea are observed. However, contributions from local regions are dominating in monsoon. Trajectory from East India, Indo-Gangetic Plain, and coastal regions are in the post-monsoon season. The weighted trajectory paths from the coastal regions and Indo-Gangetic Plain are dominating. For two seasons (winter and pre-monsoon) two paths are identified while for the other two seasons (monsoon and post-monsoon) one transport path at the surface layer is identified. However, the trajectories vary from season to season as meteorological conditions influence the contributions. Gebhart et al., (2011) reported trajectory-based studies and subsequently used the results for source apportionment. Dust outbreaks in Spain were also analysed using trajectory-based models and the results were encouraging (Cabello et al., 2016). The tracking of Hazardous air pollutants from refinery fire was analysed using trajectory studies (Shie and Chan, 2013).

CWT analysis for the elevated layer represent the trajectory heights with the 1500 m, 2000 m. The CWT analysis is presented in Figure 5.4 (a, b, c, d). In CWT analysis, trajectories from all directions were observed in the winter season. However, the dominating paths are from central India and East India. In the pre-monsoon season, the weighted trajectory was from central India, while for monsoon, the dominating trajectories were from West India and the Arabian Sea. For the post-monsoon season, the dominating trajectory was from local regions.

For both the surface and elevated layers, the contributions from central India and East India are predominant in winter and pre-monsoon. In the monsoon season, contributions from local regions

are dominant. As precipitation in monsoon washes the particulates in the air, contributions from other regions are not significant.

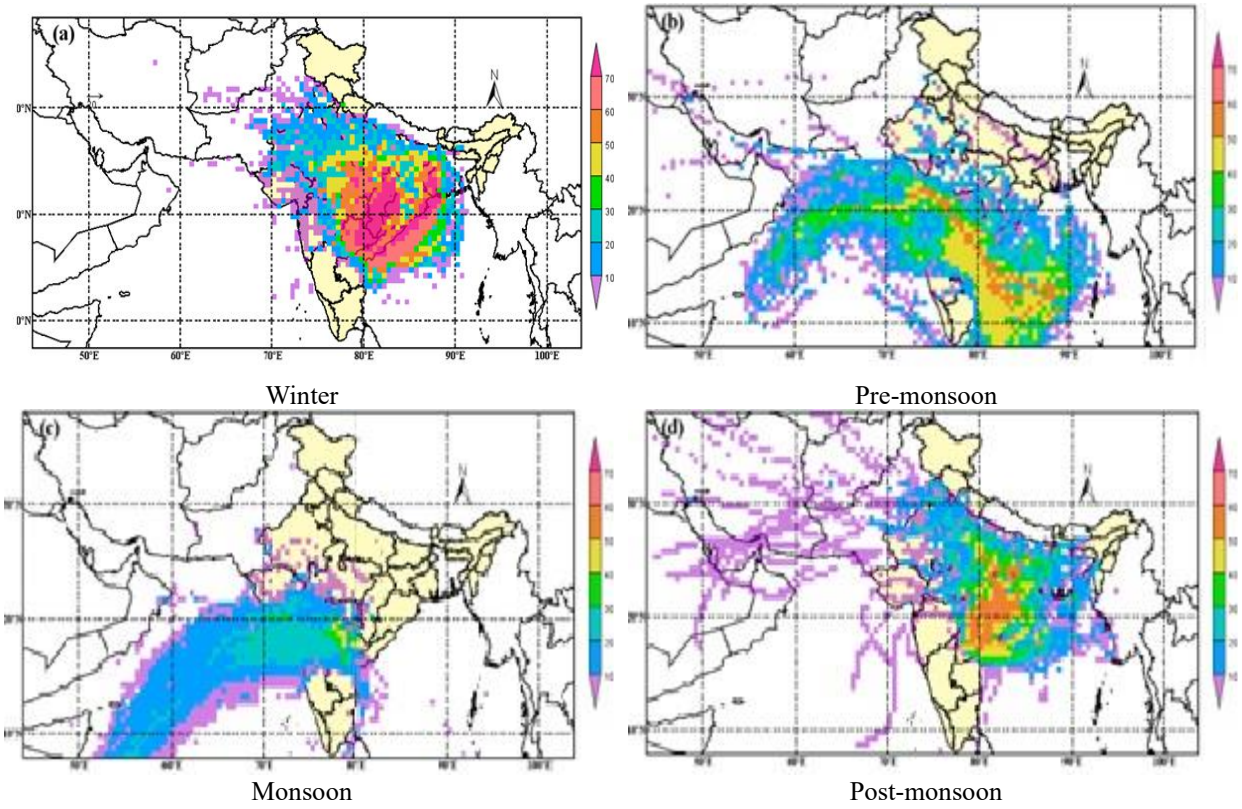

Figure 5.4 CWT analysis for the surface layer.

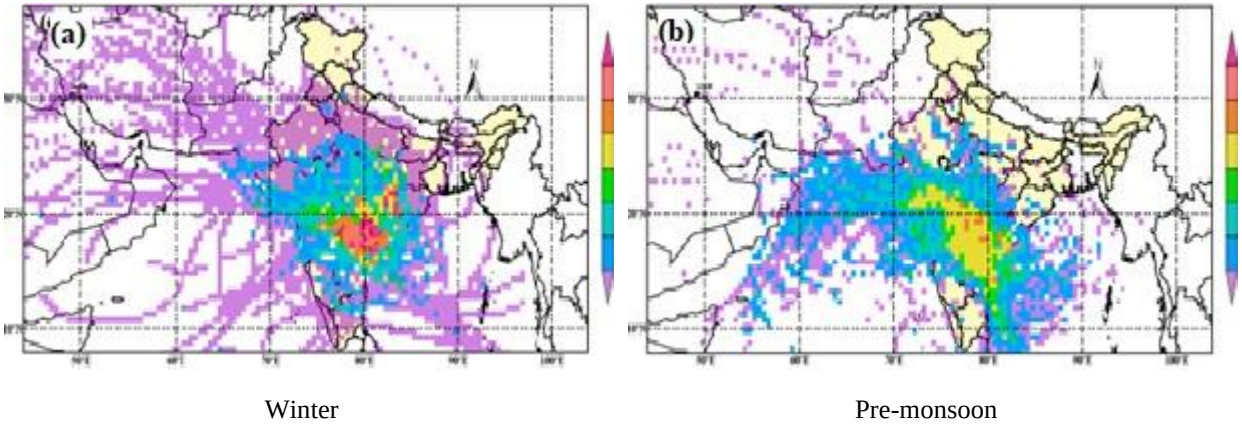

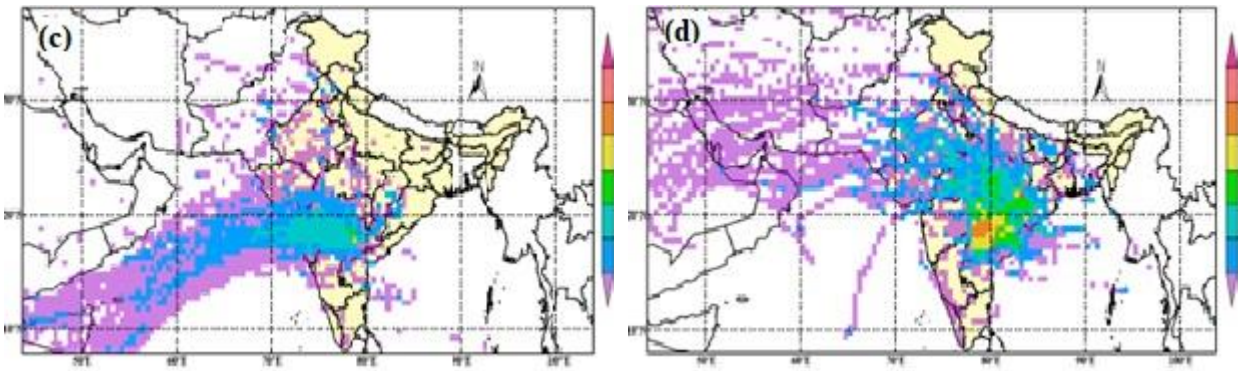

Monsoon Post-monsoon

Figure 5.5 CWT analysis for elevated layer.

5.3.2 Potential Source Contribution Function

The potential source contribution function indicates the source contributions to the receptor locations. PSCF is one of the receptor models that consider meteorological information in determining the source regions contributing to potential pollution. Backward trajectory analysis is used for the PSCF analysis. PSCF is helpful in the identification of determining the relative contributions of potential source regions. Figure 5.6 presents the results of PSCF analysis for the study area at the surface layer. Table 5.3 indicates the predominant source regions contributing $PM_{2.5}$ to the receptor location in the study area. In the winter season, predominant contributions were from Central India, East India, and Coastal Region. Contributions from Central India, the Bay of Bengal, Western India, and the Arabian Sea were predominant in the pre-monsoon season. During monsoon and post-monsoon seasons, contributions from local regions were dominating.

Source contributions for the elevated layer are presented in Figure 5.7 and Table 5.3. In the winter season, dominating source contributions are observed from Central India, Coastal regions, and East India. For the other three seasons, contributions were mostly from local regions. The results of CWT and PSCF analysis indicating dominant trajectories and source regions are mostly similar indicating the credibility and accuracy of the results. Chengming et al., (2020) also reported similar agreement between CWT and PSCF results in their study on assessment of contributions of $PM_{2.5}$ in Weifang, China. PSCF cannot take into account if the $PM_{2.5}$ concentrations of the grids are slightly higher or much higher than the considered standard $PM_{2.5}$ (60 µg/m^3, in the study) concentrations. Because of this limitation, the PSCF method fails to bring clear distinction between strong and moderate sources. However, the CWT model incorporates the relative importance of the potential sources.

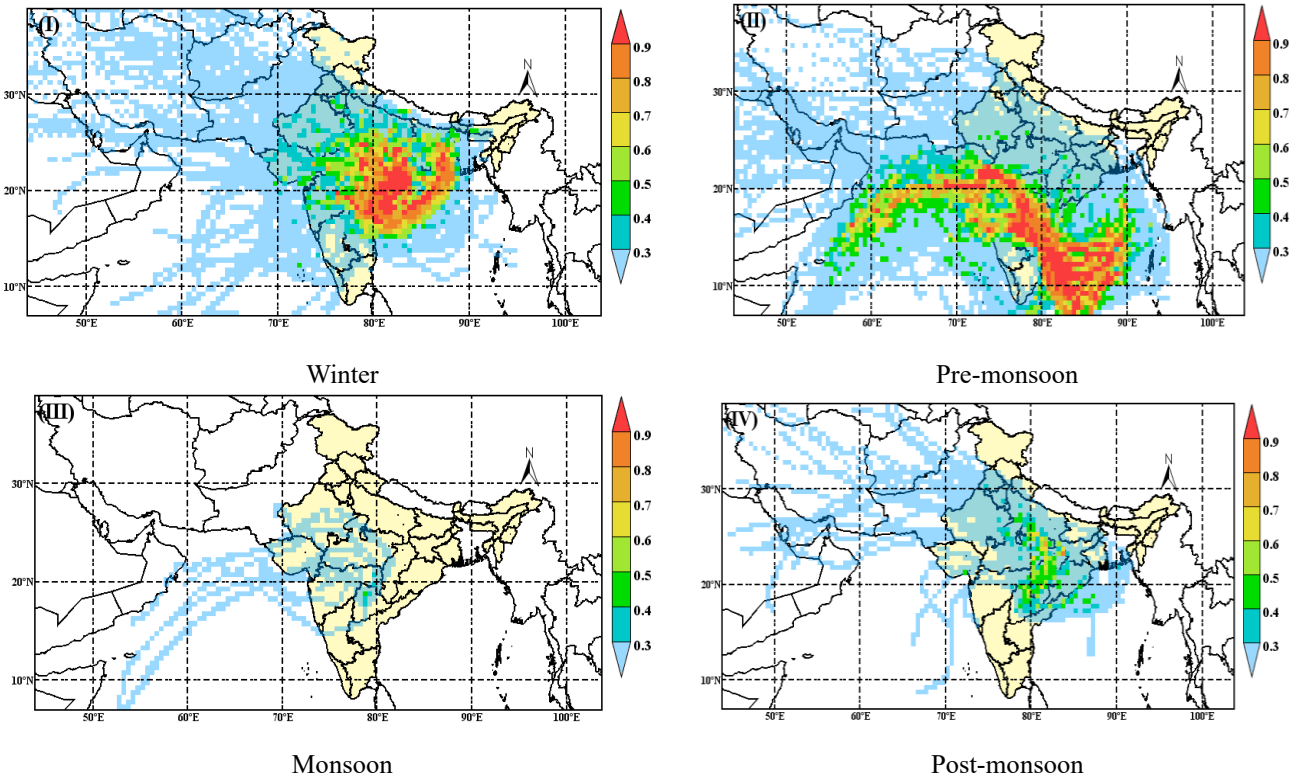

Winter Pre-monsoon

Monsoon Post-monsoon

Figure 5.6 PSCF analysis for the surface layer.

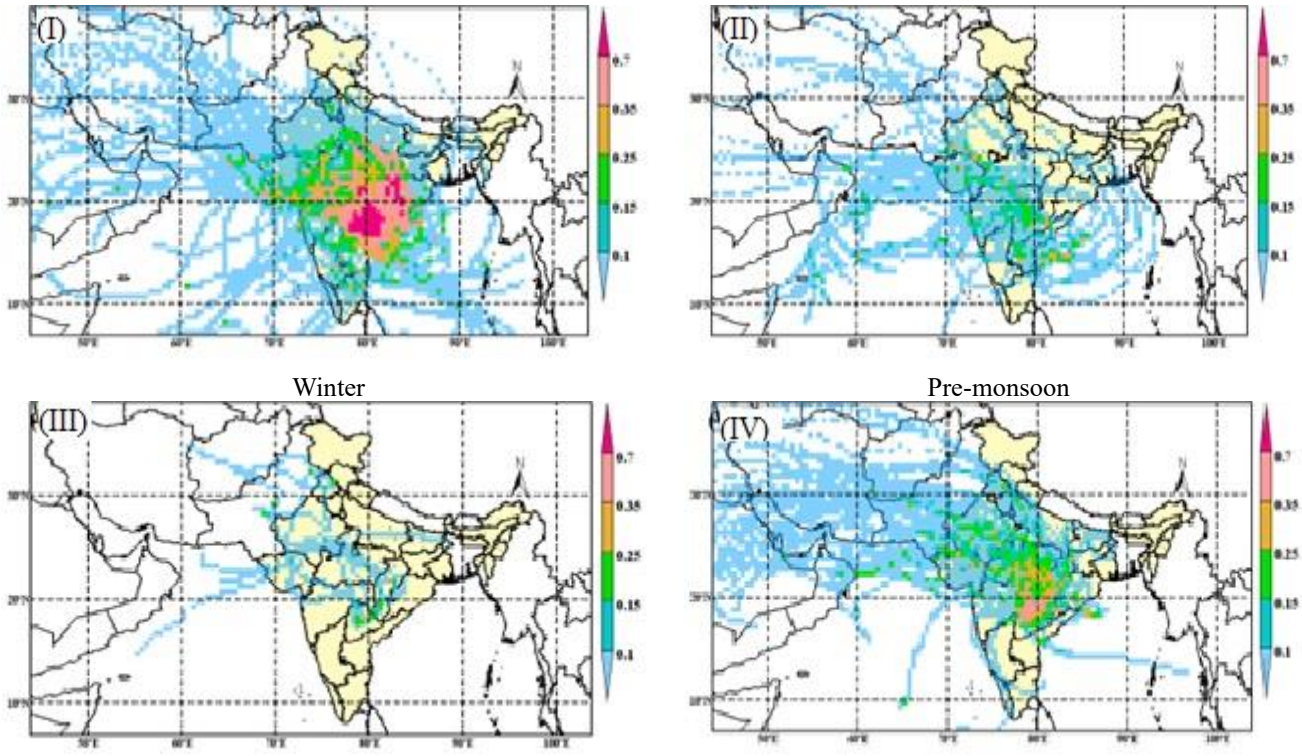

Winter Pre-monsoon

Monsoon Post-monsoon

Figure 5.7 PSCF analysis for elevated layer.

Table 5.3 Results of CWT Analysis and PSCF analysis

Season	Predominant trajectories from CWT Analysis		Predominant source regions from PSCF Analysis	
	Surface Layer	**Elevated Layer**	**Surface Layer**	**Elevated Layer**
Winter	Central India, East India, Coastal Region	Central India, East India	Central India, East India, Coastal Region	Central India, Coastal regions, and East India
Pre-monsoon	Central India, Bay of Bengal, Western India	Central India	Central India, Bay of Bengal, Western India and Arabian Sea	Local regions
Monsoon	Local regions (nearby receptor locations)	Local regions (nearby receptor locations)	Local regions	Local regions
Post-Monsoon	Central India and Indo-Gangetic Plain	Local regions	Central India and Local regions	Central India

5.3.3 Cluster Analysis for Hyderabad

Trajectory cluster analysis was carried out to group trajectories with similar characteristics. The K-means algorithm was used in the study for Cluster analysis. The threshold value was based on the daily base pollution criteria value was set by 60 µg/m^3. The polluted mean and deviation also associated with more than the 60 µg/m^3 of $PM_{2.5}$ concentrations over study region**.** The results of CA for the surface layer are presented in Figure 5.8 (a, b, c, and d). The results obtained using the Trajstat tool are presented in Table 5.4. The trajectories in the study area are grouped into 6 clusters. The color indicates the elevation of the trajectory – red refers to higher elevation while blue refers to lower elevation. In winter, the maximum contribution (38%) was from cluster III which was from East India, Central India, and West India. The polluted mean concentration was 72.65 µg/m^3 and 61 polluted trajectories. Cluster 4, from the Bay of Bengal, is contributing to maximum $PM_{2.5}$ (31.3%) in pre-monsoon. Cluster analysis also indicated long and short-range transport pollution. For instance, in the monsoon season, the pollution is contributed by long-range air mass while in winter it is observed that pollution can be contributed by both long-range (Clusters II and IV) and short-range (Cluster I, III, V, and VI) air masses observed from the Figure 5.8(a).

For Monsoon, the maximum contribution (22%) was from cluster 1 arising from West India and the Arabian Sea; while for post-monsoon, the maximum contribution (29%) was arising from Indo Gangetic Plain and East India. In monsoon, the contributions from lower elevations dominated as there were not many contributions from higher elevations due to rainfall. Also, the lower elevation trajectories were from nearby regions in India. The elevated trajectories were mostly from far away regions indicating long-range transport.

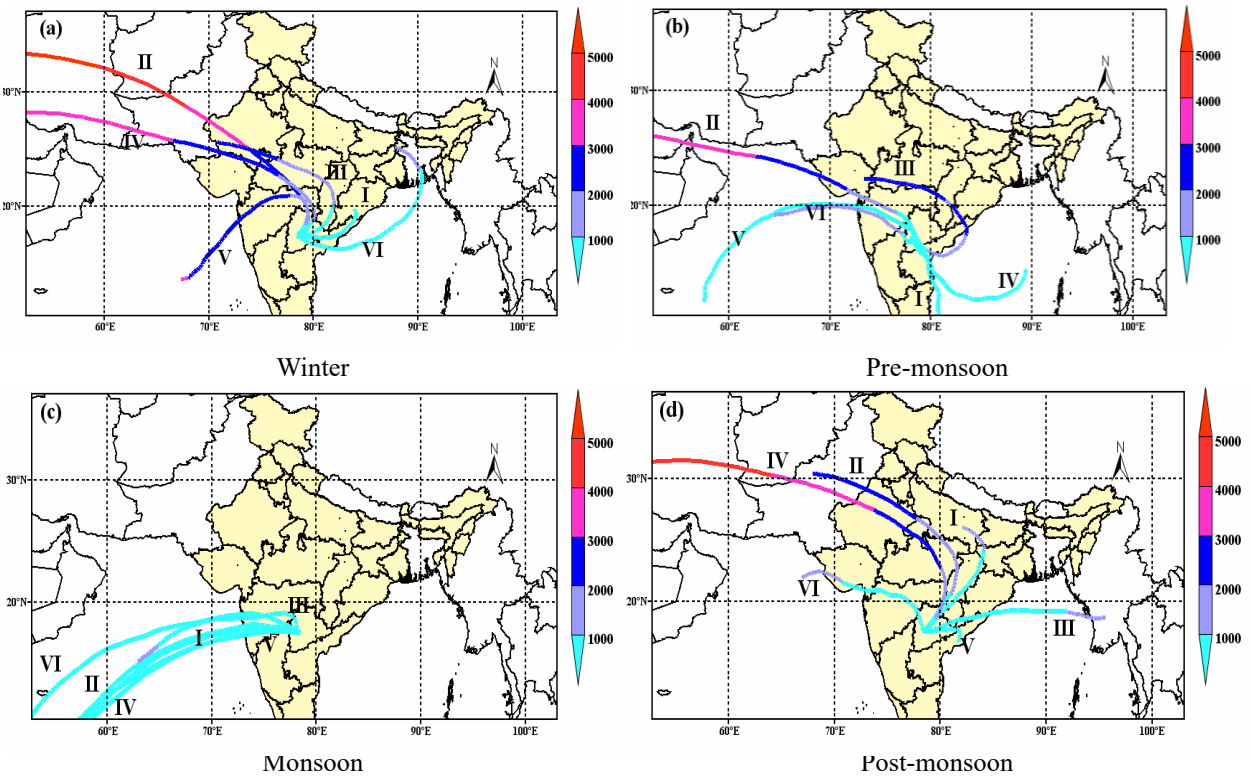

Figure 5.8 Cluster analysis for surface layer.

Table 5.4 Polluted clusters and associated trajectory's numbers at surface layer

Cluster S.No	Number trajectory	Mean value of $PM_{2.5}$ ($\mu g/m^3$)	Standard deviation	Polluted number trajectory	Polluted mean value of $PM_{2.5}$ ($\mu g/m^3$)	Polluted Standard deviation	Ratio (%) of each cluster end points
Winter							
I	202	72.05	8.43	179	74.52	4.83	21.6
II	45	65.21	11.61	29	72.81	5.75	8.33
III	**79**	**68.07**	**10.31**	**61**	**72.65**	**5.78**	**38.1**

IV	163	64.46	12.43	98	73.33	5.55	13.52
V	42	63.71	14.23	26	73.4	5.29	7.22
VI	53	63.54	10.32	35	72.32	5.23	11.23
Pre_monsoon							
I	118	43.85	7.96	0	0	0	18.29
II	49	48.85	10.7	6	69.44	7.18	7.91
III	51	50.71	10.54	9	66.14	4	7.91
IV	199	48.42	11.73	38	66.79	4.4	31.3
V	**115**	**42.25**	**11.75**	**11**	**67.88**	**7.37**	**19.22**
VI	98	47.53	9.57	11	66.37	5.69	15.3
Monsoon							
I	**154**	**21.9**	**5.16**	**0**	**0**	**0**	**22.59**
II	89	25.93	7.04	0	0	0	12.4
III	111	34.64	12.9	10	62.54	2.57	17.15
IV	124	18.9	3.62	0	0	0	18.9
V	133	21.75	4.92	0	0	0	20.9
VI	55	32.85	9.82	2	63.91	4.78	7.95
Post-monsoon							
I	**97**	**55.11**	**19.22**	**42**	**71.21**	**6.44**	**29.23**
II	60	50.37	23.19	24	70.21	5.04	17.76
III	55	40.79	13.32	4	67.08	5.91	15.03
IV	26	54.95	25.27	15	72.26	5.41	8.20
V	67	42.98	22.13	16	69.31	6.21	22.40
VI	16	33.33	27.28	4	72.18	7.53	7.38

Cluster III was more contributing in the Winter season, In the pre-monsoon season cluster IV trajectories are influencing the receptor location pollution levels from the Bay of Bengal region. The monsoon season was dominated by cluster I (ratio of 22.59%) from the Arabian region. Cluster I predominate regions from central India and the IGP region with a ratio of 29.23% in Post

monsoon season. The least number of polluted trajectories in all clusters was observed in the monsoon season.

The results of CA for the elevated layer are presented in Figure 5.9 (a, b, c, and d) and Table 5.5. In the winter season, trajectory IV indicated the highest contribution (57%) and the polluted mean value of 73.17 µg/m^3. The trajectory was from Central India and West India. Cluster II contributed a maximum (23.72%) in pre-monsoon season and it was mostly from the Bay of Bengal and local regions. Most of the clusters in the monsoon season were from the Arabian Sea with a maximum (23.16%) contributed by Cluster V. In post-monsoon, the maximum contribution was by Cluster IV, indicating long-range transport of $PM_{2.5}$. The mean $PM_{2.5}$ concentrations contributed by trajectories are well below the NAAQS standard (60 µg/m^3). Byčenkienė et al., (2014) also employed 6 clusters in their study on the Baltic region and reported relative contributions by clusters from different regions. However, there was no comprehensive study reported for the study area and the region indicating probable source contributions using AOD and MODIS data.

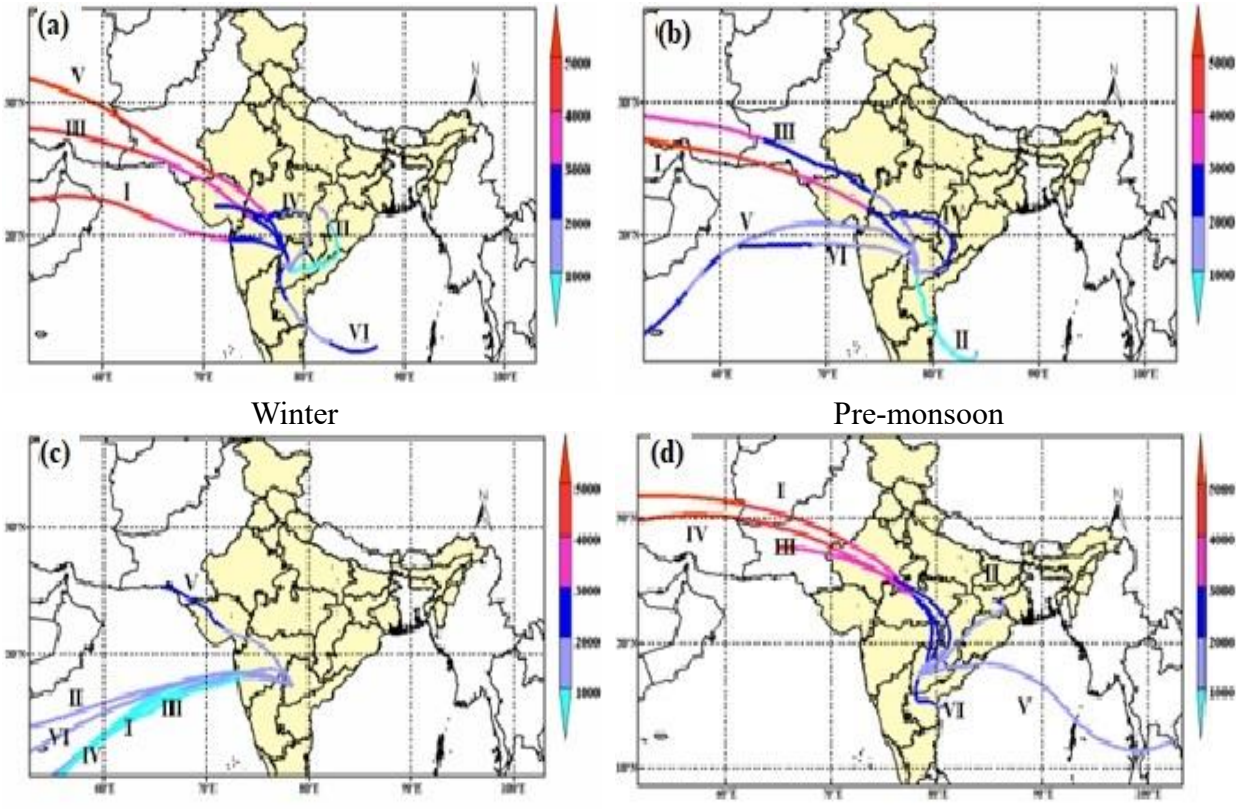

Figure 5.9 Cluster analysis for elevated layer.

Table 5.5 Polluted clusters and associated trajectory's numbers at Elevated layer

Cluster S.No	Number trajectory	Mean value of $PM_{2.5}$ ($\mu g/m^3$)	Standard deviation	Polluted number trajectory	Polluted mean value of $PM_{2.5}$ ($\mu g/m^3$)	Polluted Standard deviation	Ratio (%)of each cluster end points
Winter							
I	35	67.31	9.93	24	72.89	6.13	18.6
II	43	71.09	7.92	39	73.1	4.8	9
III	23	64.09	11.09	16	70.01	7.03	12.6
IV	**57**	**68.8**	**9.5**	**44**	**73.17**	**4.8**	**57**
V	7	66.85	1.89	5	72.67	5.19	3.54
VI	29	68.26	10	19	74.68	4.7	14.65
Pre monsoon							
I	38	50.95	10.7	8	65.81	2.95	9.30
II	101	46.1	10.18	10	67.1	6.05	23.72
III	47	46.78	10.8	6	69.95	6	10.93
IV	72	48.33	10.31	8	67.03	4.56	16.74
V	51	48.51	11.8	7	67.56	8.56	12.09
VI	**111**	**44.94**	**10.99**	**11**	**65.99**	**3.4**	**27.21**
Monsoon							
I	105	19.18	3.84	0	0	0	22.75
II	70	22.77	5.92	0	0	0	17.62
III	50	3.89	10.25	0	0	0	10.25
IV	96	23.99	6.58	0	0	0	19.67
V	**104**	**30.53**	**12.6**	**8**	**62.77**	**2.85**	**23.16**
VI	29	21.03	4.15	0	0	0	6.56
Post monsoon							
I	26	56.38	24.59	16	72.17	5.57	13.1
II	36	38.56	21.38	5	70.59	7.19	17.2
III	45	45.27	20.89	12	68.1	6.56	21.3

IV	**58**	**58.26**	**20.08**	**33**	**71.54**	**5.75**	**25**
V	21	44.42	15.59	1	74.2	0	8.61
VI	28	39.25	17.67	3	69	7.82	14.75

5.4 Wind rose analysis.

In order to determine the maximum frequency of the wind direction and wind speed based on wind rose analysis. The wind roses represent the ground-level winds. The wind rose plots are drawn utilizing Openair package in R program language (Carslaw and Ropkins, 2012). The analysis indicates that the dominating wind direction at Zoopark location was from the E and SE direction at the Zoopark location in the winter season, with nearly 20% of winds from the East direction. The dominating wind direction was from the SE and SW direction at the Zoopark location in autumn season. The mean and standard deviation of wind speed at Zoopark were in the range of 0.78±0.7. The analysis of the wind rose and backward trajectory data revealed consistent patterns in the wind direction within the surface layer. The observations indicated a striking similarity between the wind directions obtained from the backward trajectory analysis and the actual wind directions at the receptor location. This alignment between the two datasets suggests similar agreement in the wind patterns at the location of interest. The findings from both analyses provide robust evidence of a consistent wind flow pattern in the surface layer.

Below are wind rose diagrams for various locations Figure 5.11 illustrates that Sanathnagar experiences high wind speeds during the summer season, while the winter and autumn seasons exhibit the least wind speeds with a consistent dominant direction from the southeast. Additionally, moderate winds are observed in the autumn season. Notably, there is a sudden change in wind direction from summer to autumn in the Sanathnagar region. The observed mean and standard deviation of wind speed fall within the range of 1.25±0.5. Figure 5.12 displays the seasonal wind rose patterns for Patancheru. Dominant winds are observed during the summer season, while the least winds are noted in winter season. Moderate winds are evident during the spring and autumn seasons. In the summer, winds predominantly come from the southwest, while in all other seasons, they are dominated by southeast directions at Patancheru. The mean and standard deviation of wind speed were observed as 1.26±0.7. Figure 5.13 illustrates the wind pattern at IDA. The location exhibits dominant winds from the south in the spring season and west in the summer. In the autumn and winter seasons, winds predominantly come from the southeast. A sudden change

in wind direction is observed from summer to autumn in the wind direction. The mean and standard deviation of wind speed at IDA were observed as 2.1±0.9. Figure 5.14 displays the wind rose for Central University. High wind speeds are evident in the summer season, while moderate winds prevail in the spring season. In both these seasons, winds come from the southwest and southeast directions. In the autumn season, moderate winds from the east direction are observed. During the winter season, winds come from two directions, one from the south and another from the east. The mean and standard deviation of wind speed were observed as 1.6±0.6. Figure 5.15 showcases the wind rose for the Bollaram location. During the summer season, winds dominate from two directions, with high wind speeds from the west and moderate winds from the east. In the autumn and winter seasons, prevailing winds come from the southeast direction. In the spring season, winds predominantly originate from the south direction. The mean and standard deviation of wind speed were observed as 2.6±1.9. In this study, the Bollaram location exhibited the highest wind speeds overall, while the Zoo Park location recorded the lowest. Across all locations, the summer season consistently displayed stronger winds, whereas the winter season consistently had the lowest wind speeds.

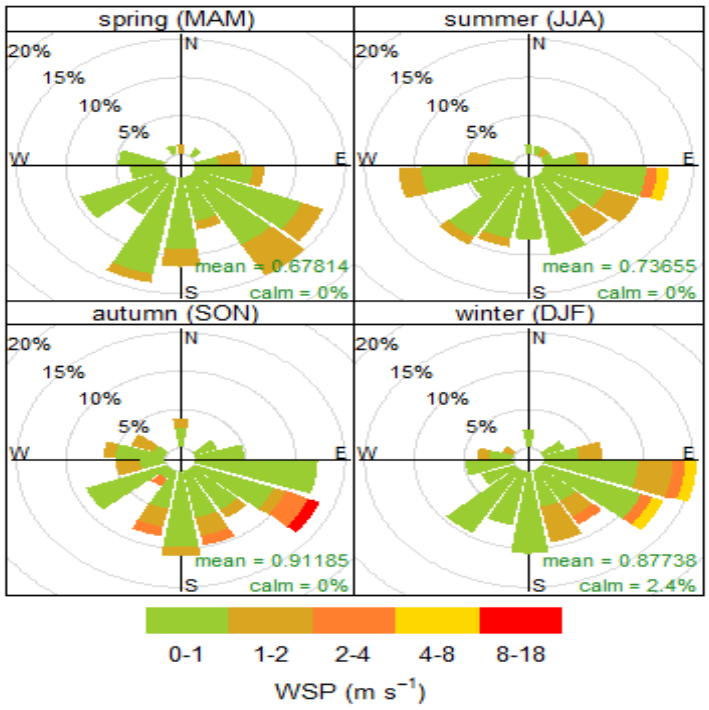

Figure 5.10 Zoopark wind rose diagram for all seasons

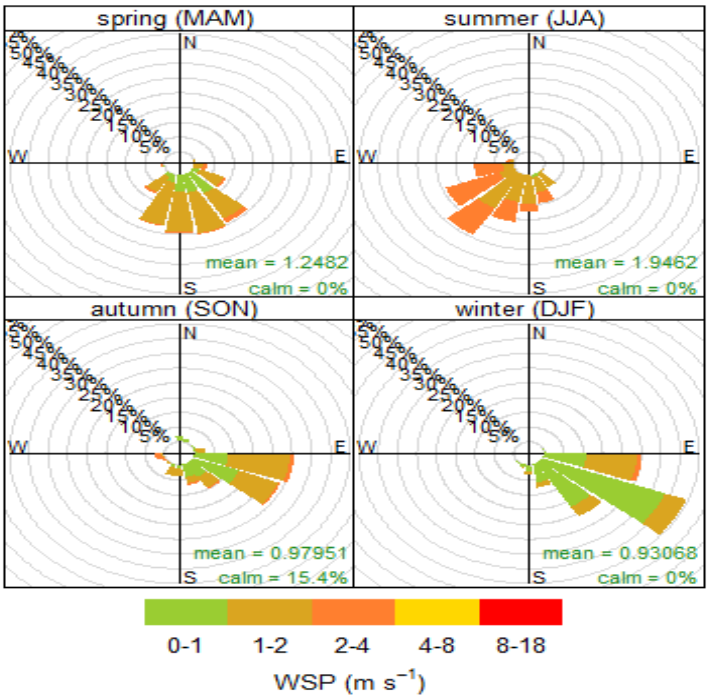

Figure 5.11 Sanathnagar wind rose diagram for all seasons

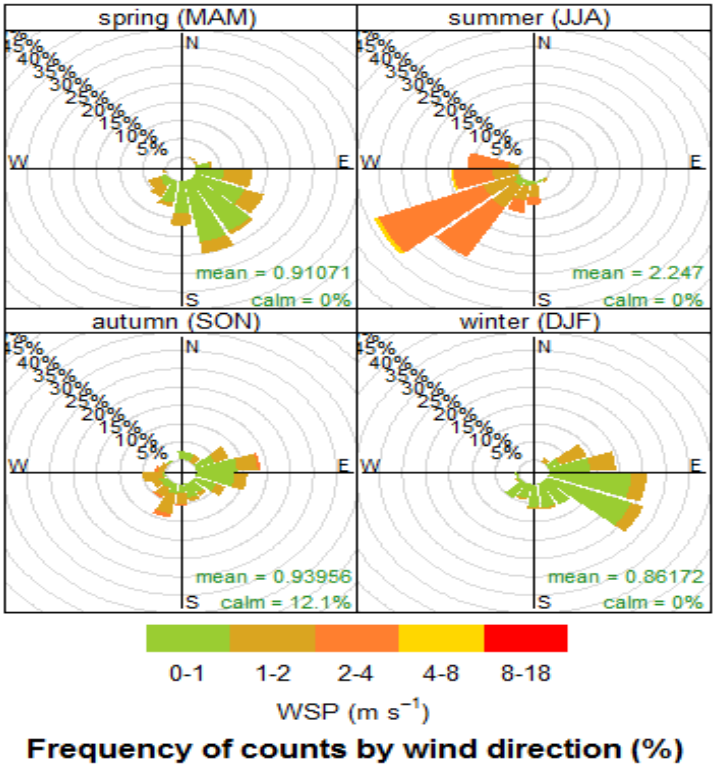

Figure 5.12 Patancheru wind rose diagram for all seasons

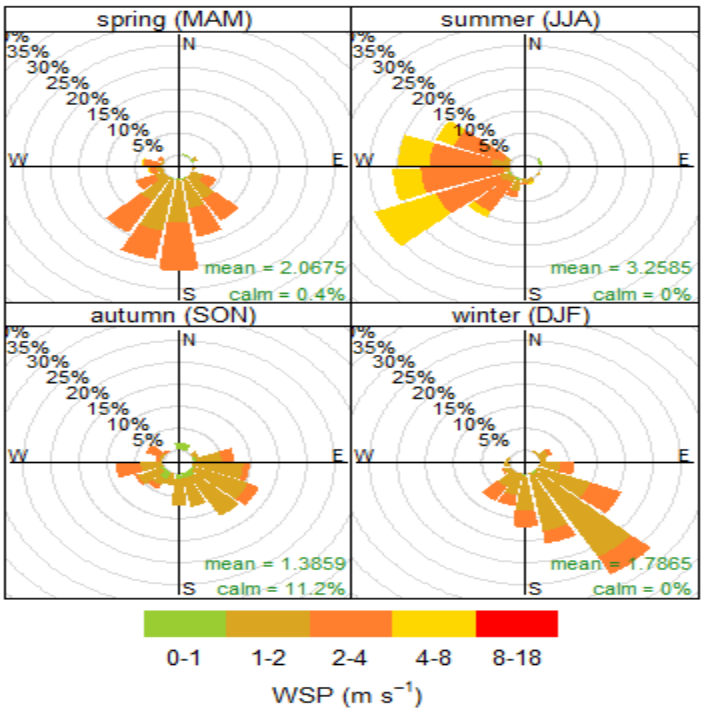

Figure 5.13 IDA wind rose diagram for all seasons

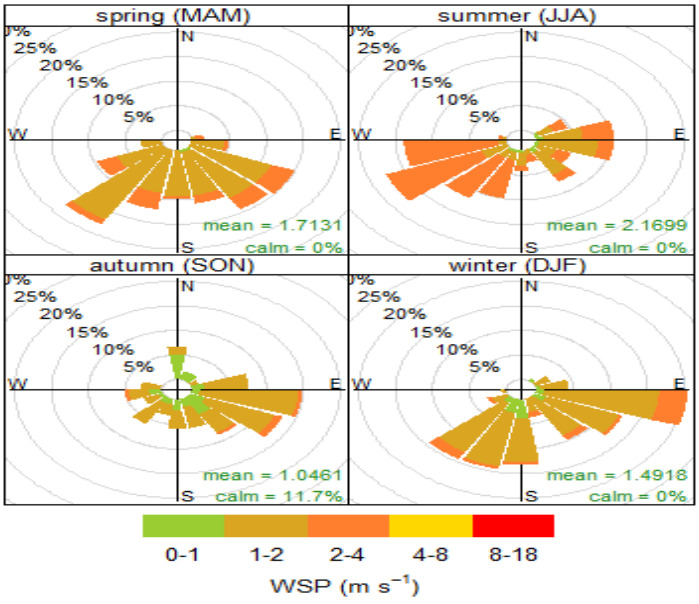

Figure 5.14 CU wind rose diagram for all seasons

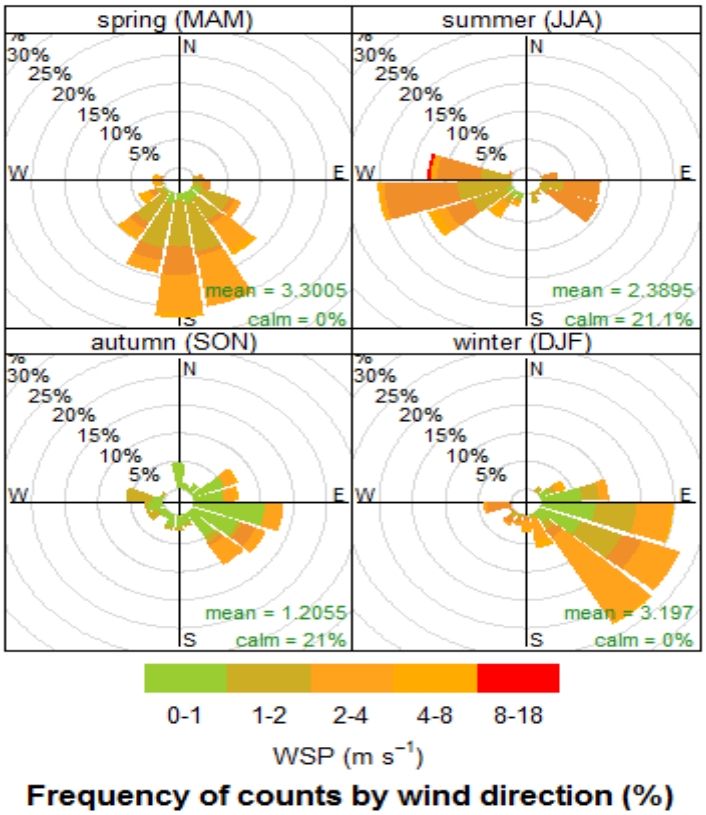

Figure 5.15 Bollaram wind rose diagram for all seasons

5.5 Summary

In this study, ground-level $PM_{2.5}$ retrieval was attempted using meteorological conditions and MODIS Aqua/Terra AOD. Multiple regression analysis using AOD and meteorological conditions suggested that the MODIS Terra aerosol products were in reasonable agreement with predicted $PM_{2.5}$ concentrations. Source identification based on trajectory-based studies by CWT, PSCF, and cluster analysis indicated long-range transport of the $PM_{2.5}$ and potential source regions. East India and Coastal regions were the potential source regions in the winter season. Potential sources perhaps are biomass burning and anthropogenic activities from the source regions. The clusters provided the main mechanism of transporting paths toward the receptor. The high $PM_{2.5}$ aerosol mass concentration at Hyderabad reflects high emissions by local sources such as vehicular transport and other anthropogenic activities. During the winter season, the surface layer experienced the highest levels of pollution, particularly originating from the East coastal regions. These pollution levels were exacerbated by prevailing atmospheric stability conditions. PSCF

analysis indicates dominating source regions from the Central India, East India and Coastal region in the winter season. As compared to other seasons winter season was dominating pollutions in the study region.

The meteorology conditions influence the ground-level particulate concentration and transboundary aerosols. The estimation of PM2.5from MODIS Terra AOD and meteorology conditions the best-fit prediction method at Zoo park location. Research reported indicated a positive correlation between AOD and ground-level $PM_{2.5}$ concentrations. In this study, the elevated layer demonstrated the long transport of pollutants from faraway regions like central India, North West India regions, and East India regions.

Chapter 6 Conclusions

6.1 General

In the present study, an attempt was made to study regional air pollution in two urban locations of Telangana. For Warangal, the study focused on sampling $PM_{2.5}$, and subsequent analysis was carried out to find the heavy metals bound to the particulates. Enrichment factor analysis was performed to identify anthropogenic sources of heavy metals. Heavy metals are significantly found with $PM_{2.5}$, especially in regions dominated by industry, traffic, and other human activities. Both $PM_{2.5}$ and heavy metals are of great concern in view of their persistence and toxicity. The risk associated with inhalable $PM_{2.5}$ along with heavy metals in adults and children was attempted. Source identification studies based on Concentration Weighted Trajectory (CWT), Potential Source Contribution Function (PSCF), and cluster analysis were attempted to arrive at regions contributing to pollution.

Subsequently indirect method of using AOD data from satellites for $PM_{2.5}$ retrievals and use in back trajectory analysis was demonstrated. Hyderabad, which is the capital of Telangana state, is dominated by several anthropogenic activities that result in the degradation of air quality. In this context, an attempt is made in this study, to use CWT, PSCF, and CA for identifying the pollutant source contributions by different regions. The results of the study can be used for the mitigation and regulation of air pollution in the region.

6.2 Conclusions

The concentrations of $PM_{2.5}$ and heavy metals bound to $PM_{2.5}$ in Warangal are high in the post-monsoon season. However, the $PM_{2.5}$ concentrations observed were lower than the standards prescribed by NAAQS (60 $\mu g/m^3$ – 24 hr-average). Ambient heavy metals bound to $PM_{2.5}$ were significant due to emissions from traffic and other anthropogenic activities in urban areas. Zn, Fe and Cu concentrations in $PM_{2.5}$ were significantly higher compared to the concentrations of Ni and Cd. The order of occurrence of heavy metals in descending order was found to be: Zn>Fe>Cu>Ni>Cd. High EF values for Zn, Cu, and Cd indicate higher emissions from combustion and industry. Health risk assessment showed that the ingestion pathway dominates over the dermal and inhalation pathways. Based on HQ and HI index, it may be concluded that there is no significant non-carcinogenic and carcinogenic risk from the metals considered in the study. However, the health risk in children was higher when compared to that for adults. Long-term

sampling can help in better understanding the variations in $PM_{2.5}$ and metal concentrations. Significant concentrations of few heavy metals bound to $PM_{2.5}$ demand for implementation of air pollution control strategies. From the CWT, PSCF, and cluster analysis, it was concluded that the contributions from the West and North-West regions of India dominate at the receptor location.

In this study, an assessment of ground-level $PM_{2.5}$ over Hyderabad region based on multiple regression analysis with the meteorology and retrieved MODIS AOD Terra/Aqua product was attempted. The study suggested that the MODIS Terra AOD product was seen as the best fit for the prediction of $PM_{2.5}$ at the Zoo Park location among the six locations. For other locations, there was a positive correlation with moderate results in terms of applicability. Trajectory based CWT method, PSCF model, and cluster analysis were performed with the seasonal data for winter (December-April), pre-monsoon (April-June), monsoon (June-September), and post-monsoon (October- December) in order to recognize the source paths, regions, and clusters contributing to $PM_{2.5}$ concentrations at the receptor locations. The study identified the long-range transport of $PM_{2.5}$ and potential source regions contributing to $PM_{2.5}$. Central India, East India, and Coastal regions were the potential source regions in the winter season at the surface and elevated layers.

The long-range transport was predominantly from open biomass burning and open coal mine activities. Cluster analysis considered 6 clusters for identifying the probable transporting paths toward the receptor location. The Surface layer Cluster III was the more dominating region in the Winter season with a polluted mean concentration of 72.65 $\mu g/m^3$. Lower boundary layer and low wind speed conditions in winter lead to the entrapment of particulates within the surface level resulting in high ground-level $PM_{2.5}$ concentrations. The lowest number of polluted trajectories in all clusters was observed in the monsoon season at both layers. This is possibly due to the minimum pollution contribution in winter. The high $PM_{2.5}$ aerosol mass concentration in Hyderabad City reflects high emissions from local sources such as vehicular transport and anthropogenic activities in addition to long-range transport as well. With the help of cluster analysis, major clusters contributing to ambient concentrations of $PM_{2.5}$ are identified for all seasons. Furthermore, the contributions were determined and the corresponding number of clusters and their percentage contributions are established. However, choosing a number of clusters for CA is complicated as a lot of information is required to decide the number of clusters for using CA in air pollution analysis. This aspect is perhaps the limitation of cluster analysis.

Long-range potential source regions of $PM_{2.5}$ pollution and their impact on Hyderabad City is assessed during the study. The results of our study offer scientific backing for formulating pollution control measures specific to different regions. Nevertheless, it is important to acknowledge the limitations of the study. For instance, the resolution of the study grid ($0.5^{o}X0.5^{o}$), based on the backward trajectory model, is not a sufficiently high resolution to be applicable to small-scale regions. Additionally, the estimation of $PM_{2.5}$ sources is not flawless, as the calculations solely rely on meteorological data and do not incorporate factors such as dust production and deposition.

6.3 Recommendations

The study yielded valuable insights regarding the policy implications concerning $PM_{2.5}$ pollution in the study region. The findings are beneficial for developing effective pollution control and prevention measures, emphasizing the need for the government to prioritize the regulation of pollutant sources while considering the migration of regional pollution caused by these sources. To illustrate, by analysing the transport patterns of pollutants, it is possible to classify and divide the surrounding pollutant source regions. This discovery suggests the implementation of diverse control and management policies, tailored to each region, to effectively curb pollution. Given that Hyderabad is significantly affected by short-distance pollutant transport from neighboring regions, particular attention should be given to mitigating such transport. For instance, implementing intensive greening measures can help reduce the long-distance transport of $PM_{2.5}$. Additionally, it is crucial to consider the interactions between the city and its surrounding areas, promoting collaborative control and cooperation among different regions.

The PhD work provides valuable insights and recommendations for the development of effective and efficient policies to reduce the air pollution in Warangal and Hyderabad, as well as other similar locations in India and elsewhere. I have also highlighted the main policy implications of the PhD work, such as:

- The need for more comprehensive and representative monitoring and assessment of PM2.5 concentration and sources, using a combination of ground-based, satellite-based, and low-cost sensor data and methods.
- The need for more stringent and specific emission standards and regulations for the major sources of PM2.5, such as vehicles, industries, biomass burning, and dust.

- The need for more integrated and coordinated policy actions and interventions across different sectors and levels of governance, such as transportation, energy, agriculture, urban planning, and public health.
- The need for more control rules and advanced methods in the coal mining activities to decrease the pollution at the source location.
- The need for more strict guidelines following the forest department to control forest fires and improvement in the forest area. the air pollution at the source location
- The need for more public awareness and participation in the policy making and implementation process, as well as the promotion of behavioural changes and alternative practices to reduce the exposure and impact of PM2.5.

6.4 Scope for further study

- In this study, three approaches are used for implementation trajectory-based CWT, PSFC, and CA are used. In the first case, sampling data is used for Warangal, and in the second case, AOD and secondary data of $PM_{2.5}$ is used for attempting CWT, PSFC, and CA. However, the integration of sampling and secondary data will ensure accurate data inputs and hence, better results. This was not attempted for want of finances and time for sampling over the entire region.
- The use of machine learning and deep learning models with satellite data as the input for air pollutant forecasting is a good area for further research. MODIS, TROPOMI, and OMI satellite data could be used for the forecast.
- The inclusion of wind patterns, rainfall patterns, land use changes, and even climate change can be useful for in-depth analysis and modelling.
- Inclusion of source inventory especially traffic data (hourly average vehicle data) and transport emissions and industrial emissions as input can lead to fingerprinting of sources.
- CWT and PSCF analysis as well as additional work that combines emission sources and externally monitored $PM_{2.5}$ concentration data is needed to improve the prediction of $PM_{2.5}$ source regions and validate the analysis results quantitatively. Furthermore, analyses for various years will be further conducted to assess the inter-annual variability. The use of advanced deep learning models could be experimented with larger data sets to achieve better results.

References

Agrawal, G., Mohan, D., Rahman, H., 2021. Ambient air pollution in selected small cities in India: Observed trends and future challenges. IATSS Research 45, 19–30. https://doi.org/10.1016/j.iatssr.2021.03.004

Ambade, B., 2014a. Seasonal variation and sources of heavy metals in hilltop of Dongargarh, Central India. Urban Climate 9, 155–165. https://doi.org/10.1016/j.uclim.2014.08.001

Ambade, B., 2014b. Seasonal variation and sources of heavy metals in hilltop of Dongargarh, Central India. Urban Climate 9, 155–165. https://doi.org/10.1016/j.uclim.2014.08.001

Arku, R.E., Vallarino, J., Dionisio, K.L., Willis, R., Choi, H., Wilson, J.G., Hemphill, C., Agyei-Mensah, S., Spengler, J.D., Ezzati, M., 2008. Characterizing air pollution in two low-income neighborhoods in Accra, Ghana. Science of The Total Environment 402, 217–231. https://doi.org/10.1016/j.scitotenv.2008.04.042

Badarinath, K.V.S., Kharol, S.K., Kaskaoutis, D.G., Sharma, A.R., Ramaswamy, V., Kambezidis, H.D., 2010. Long-range transport of dust aerosols over the Arabian Sea and Indian region — A case study using satellite data and ground-based measurements. Global and Planetary Change 72, 164–181. https://doi.org/10.1016/j.gloplacha.2010.02.003

Balakrishnaiah, G., Raghavendra kumar, K., Suresh Kumar Reddy, B., Rama Gopal, K., Reddy, R.R., Reddy, L.S.S., Swamulu, C., Nazeer Ahammed, Y., Narasimhulu, K., KrishnaMoorthy, K., Suresh Babu, S., 2012. Spatio-temporal variations in aerosol optical and cloud parameters over Southern India retrieved from MODIS satellite data. Atmospheric Environment 47, 435–445. https://doi.org/10.1016/j.atmosenv.2011.10.032

Balakrishnan, K., Ghosh, S., Thangavel, G., Sambandam, S., Mukhopadhyay, K., Puttaswamy, N., Sadasivam, A., Ramaswamy, P., Johnson, P., Kuppuswamy, R., Natesan, D., Maheshwari, U., Natarajan, A., Rajendran, G., Ramasami, R., Madhav, S., Manivannan, S., Nargunanadan, S., Natarajan, S., Saidam, S., Chakraborty, M., Balakrishnan, L., Thanasekaraan, V., 2018. Exposures to fine particulate matter ($PM_{2.5}$) and birthweight in a rural-urban, mother-child cohort in Tamil Nadu, India. Environmental Research 161, 524–531. https://doi.org/10.1016/j.envres.2017.11.050

Banerjee, A.D.K., 2003. Heavy metal levels and solid phase speciation in street dusts of Delhi, India. Environmental Pollution 123, 95–105. https://doi.org/10.1016/S0269-7491(02)00337-8

Banerjee, T., Murari, V., Kumar, M., Raju, M.P., 2015a. Source apportionment of airborne particulates through receptor modeling: Indian scenario. Atmospheric Research 164–165, 167–187. https://doi.org/10.1016/j.atmosres.2015.04.017

Banerjee, T., Murari, V., Kumar, M., Raju, M.P., 2015b. Source apportionment of airborne particulates through receptor modeling: Indian scenario. Atmospheric Research 164–165, 167–187. https://doi.org/10.1016/j.atmosres.2015.04.017

Basha, S., Jhala, J., Thorat, R., Goel, S., Trivedi, R., Shah, K., Menon, G., Gaur, P., Mody, K.H., Jha, B., 2010. Assessment of heavy metal content in suspended particulate matter of coastal industrial town, Mithapur, Gujarat, India. Atmospheric Research 97, 257–265. https://doi.org/10.1016/j.atmosres.2010.04.012

Basith, S., Manavalan, B., Shin, T.H., Park, C.B., Lee, W.-S., Kim, J., Lee, G., 2022. The Impact of Fine Particulate Matter 2.5 on the Cardiovascular System: A Review of the Invisible Killer. Nanomaterials (Basel) 12, 2656. https://doi.org/10.3390/nano12152656

Bell, M.L., Samet, J.M., Dominici, F., 2004. Time-Series Studies of Particulate Matter. Annu. Rev. Public Health 25, 247–280. https://doi.org/10.1146/annurev.publhealth.25.102802.124329

Bernard, A., 2008. Cadmium & its adverse effects on human health. Indian J Med Res 128, 557–564.

Beuck, H., Quass, U., Klemm, O., Kuhlbusch, T.A.J., 2011. Assessment of sea salt and mineral dust contributions to PM_{10} in NW Germany using tracer models and positive matrix factorization. Atmospheric Environment 45, 5813–5821. https://doi.org/10.1016/j.atmosenv.2011.07.010

Bhanuprasad, S.G., Venkataraman, C., Bhushan, M., 2008. Positive matrix factorization and trajectory modelling for source identification: A new look at Indian Ocean Experiment ship observations. Atmospheric Environment 42, 4836–4852. https://doi.org/10.1016/j.atmosenv.2008.02.041

Bhardwaj, P., Pandey, A., Kumar, K., Jain, V.K., 2017. Spatial variation of Aerosol Optical Depth and Solar Irradiance over Delhi -NCR during Summer season. Curr. World Environ 12, 389–395. https://doi.org/10.12944/CWE.12.2.22

Bhat, M.A., Romshoo, S.A., Beig, G., 2017. Aerosol black carbon at an urban site-Srinagar, Northwestern Himalaya, India: Seasonality, sources, meteorology and radiative forcing. Atmospheric Environment 165, 336–348. https://doi.org/10.1016/j.atmosenv.2017.07.004

Bhat, M.S., Afeefa, Q.S., Ashok, K.P., Bashir, A.G., 2014. Brick kiln emissions and its environmental impact: A Review. J. Ecol. Nat. Environ. 6, 1–11. https://doi.org/10.5897/JENE2013.0423

Bhuyan, P., Deka, P., Prakash, A., Balachandran, S., Hoque, R.R., 2018. Chemical characterization and source apportionment of aerosol over mid Brahmaputra Valley, India. Environmental Pollution 234, 997–1010. https://doi.org/10.1016/j.envpol.2017.12.009

Bikkina, P., Sarma, V.V.S.S., Kawamura, K., Bikkina, S., Kunwar, B., Sherin, C.K., 2020. Chemical characterization of wintertime aerosols over the Arabian Sea: Impact of marine sources and long-range transport. Atmospheric Environment 239, 117749. https://doi.org/10.1016/j.atmosenv.2020.117749

Botle, A., Singhal, R.K., Basu, H., V, M., Masih, J., 2020. Health risk assessment of heavy metals associated with Coarse and Quasi-accumulative airborne particulate matter in Mumbai City situated on the Western Coast of India. Environmental Technology & Innovation 19, 100857. https://doi.org/10.1016/j.eti.2020.100857

Bowman, K.P., Lin, J.C., Stohl, A., Draxler, R., Konopka, P., Andrews, A., Brunner, D., 2013. Input Data Requirements for Lagrangian Trajectory Models. Bulletin of the American Meteorological Society 94, 1051–1058. https://doi.org/10.1175/BAMS-D-12-00076.1

Brauer, M., Amann, M., Burnett, R.T., Cohen, A., Dentener, F., Ezzati, M., Henderson, S.B., Krzyzanowski, M., Martin, R.V., Van Dingenen, R., Van Donkelaar, A., Thurston, G.D., 2012. Exposure Assessment for Estimation of the Global Burden of Disease Attributable to Outdoor Air Pollution. Environ. Sci. Technol. 46, 652–660. https://doi.org/10.1021/es2025752

Brauer, M., Casadei, B., Harrington, R.A., Kovacs, R., Sliwa, K., Brauer, M., Davaakhuu, N., Hadley, M., Kass, D., Miller, M., Consuelo Escamilla Nuñez, M., Prabhakaran, D., Su, T.-C., Vaartjes, I.C.H., Vedanthan, R., 2021. Taking a Stand Against Air Pollution—The Impact on Cardiovascular Disease. Journal of the American College of Cardiology 77, 1684–1688. https://doi.org/10.1016/j.jacc.2020.12.003

Broomandi, P., Jahanbakhshi, A., Fathian, A., Darynova, Z., Janatian, N., Nikfal, A., Kim, J.R., Karaca, F., 2022. Impacts of ambient air pollution on UNESCO world cultural heritage sites in Eastern Asia: Dose-response calculations for material corrosions. Urban Climate 46, 101275. https://doi.org/10.1016/j.uclim.2022.101275

Burnett, R., Chen, H., Szyszkowicz, M., Fann, N., Hubbell, B., Pope III, C.A., Apte, J.S., Brauer, M., Cohen, A., Weichenthal, S. and Coggins, J., 2018. Global estimates of mortality associated with long-term exposure to outdoor fine particulate matter. Proceedings of the National Academy of Sciences, 115(38), pp.9592-9597.

Byčenkienė, S., Dudoitis, V., Ulevicius, V., 2014. The Use of Trajectory Cluster Analysis to Evaluate the Long-Range Transport of Black Carbon Aerosol in the South-Eastern Baltic Region. Advances in Meteorology 2014, 1–11. https://doi.org/10.1155/2014/137694

Carvalho, H., 2021. New WHO global air quality guidelines: more pressure on nations to reduce air pollution levels. The Lancet Planetary Health 5, e760–e761. https://doi.org/10.1016/S2542-5196(21)00287-4

Chakraborty, A., Gupta, T., 2010. Chemical Characterization and Source Apportionment of Submicron (PM_1) Aerosol in Kanpur Region, India. Aerosol Air Qual. Res. 10, 433–445. https://doi.org/10.4209/aaqr.2009.11.0071

Chandra, S., Kulshrestha, M.J., Singh, R., Singh, N., 2017. Chemical characteristics of trace metals in PM $_{10}$ and their concentrated weighted trajectory analysis at Central Delhi, India. Journal of Environmental Sciences 55, 184–196. https://doi.org/10.1016/j.jes.2016.06.028

Chang, Y., Huang, K., Xie, M., Deng, C., Zou, Z., Liu, S., Zhang, Y., 2018. First long-term and near real-time measurement of trace elements in China's urban atmosphere: temporal variability, source apportionment and precipitation effect. Atmos. Chem. Phys. 18, 11793–11812. https://doi.org/10.5194/acp-18-11793-2018

Chapple, D.G., Simmonds, S.M., Wong, B.B.M., 2012. Can behavioral and personality traits influence the success of unintentional species introductions? Trends in Ecology & Evolution 27, 57–64. https://doi.org/10.1016/j.tree.2011.09.010

Chaudhari, P.R., Gupta, R., Gajghate, D.G., Wate, S.R., 2012a. Heavy metal pollution of ambient air in Nagpur City. Environ Monit Assess 184, 2487–2496. https://doi.org/10.1007/s10661-011-2133-4

Chaudhari, P.R., Gupta, R., Gajghate, D.G., Wate, S.R., 2012b. Heavy metal pollution of ambient air in Nagpur City. Environ Monit Assess 184, 2487–2496. https://doi.org/10.1007/s10661-011-2133-4

Chelani, A.B., 2018. Estimating $PM_{2.5}$ concentration from satellite derived aerosol optical depth and meteorological variables using a combination model. Atmospheric Pollution Research 10, 847–857. https://doi.org/10.1016/j.apr.2018.12.013

Chen, D., Zhao, N., Lang, J., Zhou, Y., Wang, X., Li, Y., Zhao, Y., Guo, X., 2018. Contribution of ship emissions to the concentration of $PM_{2.5}$: A comprehensive study using AIS data and WRF/Chem model in Bohai Rim Region, China. Science of The Total Environment 610–611, 1476–1486. https://doi.org/10.1016/j.scitotenv.2017.07.255

Cheng, I., Zhang, L., Blanchard, P., Dalziel, J., Tordon, R., 2013. Concentration-weighted trajectory approach to identifying potential sources of speciated atmospheric mercury at an urban coastal site in Nova Scotia, Canada. Atmos. Chem. Phys. 13, 6031–6048. https://doi.org/10.5194/acp-13-6031-2013

Cheng, T., Lu, D., Wang, G., Xu, Y., 2005. Chemical characteristics of Asian dust aerosol from Hunshan Dake Sandland in Northern China. Atmospheric Environment 39, 2903–2911. https://doi.org/10.1016/j.atmosenv.2004.12.045

Carslaw, D. C., and Ropkins, K. 2012. Openair—an R package for air quality data analysis. *Environmental Modelling & Software*, *27*, 52-61.

Cheng, Y., Yu, Q., Liu, J., Du, Z.-Y., Liang, L., Geng, G., Zheng, B., Ma, W., Qi, H., Zhang, Q., He, K., 2021. Strong biomass burning contribution to ambient aerosol during heating season in a megacity in Northeast China: Effectiveness of agricultural fire bans? Science of The Total Environment 754, 142144. https://doi.org/10.1016/j.scitotenv.2020.142144

Chinnam, N., Dey, S., Tripathi, S.N., Sharma, M., 2006. Dust events in Kanpur, northern India: Chemical evidence for source and implications to radiative forcing. Geophys. Res. Lett. 33, L08803. https://doi.org/10.1029/2005GL025278

Chatterjee, D., McDuffie, E.E., Smith, S.J., Bindle, L., van Donkelaar, A., Hammer, M.S., Venkataraman, C., Brauer, M. and Martin, R.V., 2023. Source Contributions to Fine Particulate Matter and Attributable Mortality in India and the Surrounding Region. Environmental Science & Technology, 57(28), pp.10263-10275.

Chowdhury, S., Pozzer, A., Haines, A., Klingmüller, K., Münzel, T., Paasonen, P., Sharma, A., Venkataraman, C., Lelieveld, J., 2022. Global health burden of ambient $PM_{2.5}$ and the contribution of anthropogenic black carbon and organic aerosols. Environment International 159, 107020. https://doi.org/10.1016/j.envint.2021.107020

Colbeck, I., Lazaridis, M., 2010. Aerosols and environmental pollution. Naturwissenschaften 97, 117–131. https://doi.org/10.1007/s00114-009-0594-x

Colbeck, I., Nasir, Z.A., Ali, Z., 2010. Characteristics of indoor/outdoor particulate pollution in urban and rural residential environment of Pakistan. Indoor Air 20, 40–51. https://doi.org/10.1111/j.1600-0668.2009.00624.x

Connan, O., Smith, K., Organo, C., Solier, L., Maro, D., Hébert, D., 2013. Comparison of RIMPUFF, HYSPLIT, ADMS atmospheric dispersion model outputs, using emergency response procedures, with 85Kr measurements made in the vicinity of nuclear reprocessing plant. Journal of Environmental Radioactivity 124, 266–277. https://doi.org/10.1016/j.jenvrad.2013.06.004

Conte, M., Merico, E., Cesari, D., Dinoi, A., Grasso, F.M., Donateo, A., Guascito, M.R., Contini, D., 2020. Long-term characterisation of African dust advection in south-eastern Italy: Influence on fine and coarse particle concentrations, size distributions, and carbon content. Atmospheric Research 233, 104690. https://doi.org/10.1016/j.atmosres.2019.104690

CPCB (2020a) ENVIS centre on control of pollution water, air and noise, ministry of environment, forests, and climate change. Government of India. Central Pollution Control Board. Available at: https://cpcb.nic.in/index.php (accessed 14 July, 2021)

Das, A., Singh, G., Habib, G., Kumar, A., 2020. Non-carcinogenic and Carcinogenic Risk Assessment of Trace Elements of $PM_{2.5}$ During Winter and Pre-monsoon Seasons in Delhi: A Case Study. Expo Health 12, 63–77. https://doi.org/10.1007/s12403-018-0285-y

Das, M., Das, A., Sarkar, R., Mandal, P., Saha, S., Ghosh, S., 2021. Exploring short term spatio-temporal pattern of $PM_{2.5}$ and PM_{10} and their relationship with meteorological parameters during COVID-19 in Delhi. Urban Climate 39, 100944. https://doi.org/10.1016/j.uclim.2021.100944

Das, R., Khezri, B., Srivastava, B., Datta, S., Sikdar, P.K., Webster, R.D., Wang, X., 2015. Trace element composition of $PM_{2.5}$ and PM_{10} from Kolkata – a heavily polluted Indian metropolis. Atmospheric Pollution Research 6, 742–750. https://doi.org/10.5094/APR.2015.083

Datta, A., Suresh, R., Gupta, A., Singh, D., Kulshrestha, P., 2017. Indoor air quality of non-residential urban buildings in Delhi, India. International Journal of Sustainable Built Environment 6, 412–420. https://doi.org/10.1016/j.ijsbe.2017.07.005

Deb, S., Sil, B.S., 2019. Climate change study for the meteorological variables in the Barak River basin in North-East India. Urban Climate 30, 100530. https://doi.org/10.1016/j.uclim.2019.100530

Dholakia, H.H., Bhadra, D., Garg, A., 2014. Short term association between ambient air pollution and mortality and modification by temperature in five Indian cities. Atmospheric Environment 99, 168–174. https://doi.org/10.1016/j.atmosenv.2014.09.071

Diapouli, E., Eleftheriadis, K., Karanasiou, A.A., Vratolis, S., Hermansen, O., Colbeck, I., Lazaridis, M., 2011. Indoor and Outdoor Particle Number and Mass Concentrations in Athens. Sources, Sinks and Variability of Aerosol Parameters. Aerosol Air Qual. Res. 11, 632–642. https://doi.org/10.4209/aaqr.2010.09.0080

Ding, X., Kong, L., Du, C., Zhanzakova, A., Wang, L., Fu, H., Chen, J., Yang, X., Cheng, T., 2017. Long-range and regional transported size-resolved atmospheric aerosols during summertime in urban Shanghai. Science of The Total Environment 583, 334–343. https://doi.org/10.1016/j.scitotenv.2017.01.073

Dos Santos, O.N., Hoinaski, L., 2021. Incorporating gridded concentration data in air pollution back trajectories analysis for source identification. Atmospheric Research 263, 105820. https://doi.org/10.1016/j.atmosres.2021.105820

Draxler, R., Hess, G.D., 1998. An overview of the HYSPLIT_4 modeling system for trajectories, dispersion, and deposition. Aust. Meteor. Mag, 1998 47, 295–308.

Draxler, R.R., Hess, G.D., n.d. NOAA Technical Memorandum ERL ARL-224 31.

Du, X., Guo, H., Zhang, H., Peng, W., Urpelainen, J., 2020. Cross-state air pollution transport calls for more centralization in India's environmental federalism. Atmospheric Pollution Research 11, 1797–1804. https://doi.org/10.1016/j.apr.2020.07.012

Du, Y., Gao, B., Zhou, H., Ju, X., Hao, H., Yin, S., 2013. Health Risk Assessment of Heavy Metals in Road Dusts in Urban Parks of Beijing, China. Procedia Environmental Sciences 18, 299–309. https://doi.org/10.1016/j.proenv.2013.04.039

Du, Z., Hu, M., Peng, J., Zhang, W., Zheng, J., Gu, F., Qin, Y., Yang, Y., Li, M., Wu, Y., Shao, M., Shuai, S., 2018. Comparison of primary aerosol emission and secondary aerosol formation from gasoline direct injection and port fuel injection vehicles. Atmos. Chem. Phys. 18, 9011–9023. https://doi.org/10.5194/acp-18-9011-2018

Dutta, M., Chatterjee, A., 2022. A deep insight into state-level aerosol pollution in India: Long-term (2005–2019) characteristics, source apportionment, and future projection (2023). Atmospheric Environment 289, 119312. https://doi.org/10.1016/j.atmosenv.2022.119312

Falah, S., Mhawish, A., Sorek-Hamer, M., Lyapustin, A.I., Kloog, I., Banerjee, T., Kizel, F., Broday, D.M., 2021. Impact of environmental attributes on the uncertainty in MAIAC/MODIS AOD retrievals: A comparative analysis. Atmospheric Environment 262, 118659. https://doi.org/10.1016/j.atmosenv.2021.118659

Fang, G.-C., Chang, C.-N., Wu, Y.-S., Wang, V., Fu, P.P.-C., Yang, D.-G., Chen, S.-C., Chu, C.-C., 2000. The study of fine and coarse particles, and metallic elements for the daytime and

night-time in a suburban area of central Taiwan, Taichung. Chemosphere 41, 639–644. https://doi.org/10.1016/S0045-6535(99)00507-X

Ferreira-Baptista, L., De Miguel, E., 2005. Geochemistry and risk assessment of street dust in Luanda, Angola: A tropical urban environment. Atmospheric Environment 39, 4501–4512. https://doi.org/10.1016/j.atmosenv.2005.03.026

Fleming, Z.L., Monks, P.S., Manning, A.J., 2012. Review: Untangling the influence of air-mass history in interpreting observed atmospheric composition. Atmospheric Research 104–105, 1–39. https://doi.org/10.1016/j.atmosres.2011.09.009

Freitag, S., Clarke, A.D., Howell, S.G., Kapustin, V.N., Campos, T., Brekhovskikh, V.L., Zhou, J., 2013. Assimilating airborne gas and aerosol measurements into HYSPLIT: a visualization tool for simultaneous assessment of air mass history and back trajectory reliability (preprint). Aerosols/In Situ Measurement/Validation and Intercomparisons. https://doi.org/10.5194/amtd-6-5345-2013

Fu, X.W., Feng, X., Shang, L.H., Wang, S.F., Zhang, H., 2012. Two years of measurements of atmospheric total gaseous mercury (TGM) at a remote site in Mt. Changbai area, Northeastern China. Atmos. Chem. Phys. 12, 4215–4226. https://doi.org/10.5194/acp-12-4215-2012

Gajghate, D.G., Pipalatkar, P., Khaparde, V.V., 2012a. Atmospheric Concentration of Trace Elements, Dry Deposition Fluxes and Source Apportionment Study in Mumbai, in: Lopez, G. (Ed.), Air Quality - New Perspective. InTech. https://doi.org/10.5772/45865

Gajghate, D.G., Pipalatkar, P., Khaparde, V.V., 2012b. Atmospheric Concentration of Trace Elements, Dry Deposition Fluxes and Source Apportionment Study in Mumbai, in: Lopez, G. (Ed.), Air Quality - New Perspective. InTech. https://doi.org/10.5772/45865

Garg, B.D., Cadle, S.H., Mulawa, P.A., Groblicki, P.J., Laroo, C., Parr, G.A., 2000. Brake Wear Particulate Matter Emissions. Environ. Sci. Technol. 34, 4463–4469. https://doi.org/10.1021/es001108h

Githaiga, K.B., Njuguna, S.M., Makokha, V.A., Wang, J., Gituru, R.W., Yan, X., 2020. Assessment of Cu, Zn, Mn, and Fe enrichment in Mt. Kenya soils: evidence for atmospheric deposition and contamination. Environ Monit Assess 192, 167. https://doi.org/10.1007/s10661-020-8123-7

Ghosh, S., Mukherjee, A., & Gaur, A. (2018). Source apportionment of PM2.5 in a megacity in eastern India using principal component analysis and UNMIX receptor models. Environmental monitoring and assessment, 190(1), 1-16.

Gopal, K.R., Obul Reddy, K.R., Balakrishnaiah, G., Arafath, S.Md., Kumar Reddy, N.S., Rao, T.C., Reddy, T.L., Reddy, R.R., 2016. Regional trends of aerosol optical depth and their impact on cloud properties over Southern India using MODIS data. Journal of Atmospheric and Solar-Terrestrial Physics 146, 38–48. https://doi.org/10.1016/j.jastp.2016.05.005

Govardhan, G., Ambulkar, R., Kulkarni, S., Vishnoi, A., Yadav, P., Choudhury, B.A., Khare, M., Ghude, S.D., 2023. Stubble-burning activities in north-western India in 2021: Contribution to air pollution in Delhi. Heliyon 9, e16939. https://doi.org/10.1016/j.heliyon.2023.e16939

Grigoratos, T., Martini, G., 2015. Brake wear particle emissions: a review. Environ Sci Pollut Res 22, 2491–2504. https://doi.org/10.1007/s11356-014-3696-8

Gummeneni, S., Yusup, Y.B., Chavali, M., Samadi, S.Z., 2011. Source apportionment of particulate matter in the ambient air of Hyderabad city, India. Atmospheric Research 101, 752–764. https://doi.org/10.1016/j.atmosres.2011.05.002

Gurugubelli, B., Pervez, S., Tiwari, S., 2013. Characterization and Spatiotemporal Variation of Urban Ambient Dust Fallout in Central India. Aerosol Air Qual. Res. 13, 83–96. https://doi.org/10.4209/aaqr.2012.06.0141

Guttikunda, S.K., Goel, R., Pant, P., 2014. Nature of air pollution, emission sources, and management in the Indian cities. Atmospheric Environment 95, 501–510. https://doi.org/10.1016/j.atmosenv.2014.07.006

Guttikunda, S.K., Gurjar, B.R., 2012. Role of meteorology in seasonality of air pollution in megacity Delhi, India. Environ Monit Assess 184, 3199–3211. https://doi.org/10.1007/s10661-011-2182-8

Han, L., Gao, B., Wei, X., Xu, D., Gao, L., 2016. Spatial distribution, health risk assessment, and isotopic composition of lead contamination of street dusts in different functional areas of Beijing, China. Environ Sci Pollut Res 23, 3247–3255. https://doi.org/10.1007/s11356-015-5535-y

Harrison, R.M., 2020. Airborne particulate matter. Phil. Trans. R. Soc. A. 378, 20190319. https://doi.org/10.1098/rsta.2019.0319

Herman, J.R., Bhartia, P.K., Torres, O., Hsu, C., Seftor, C. and Celarier, E., 1997. Global distribution of UV-absorbing aerosols from Nimbus 7/TOMS data. Journal of Geophysical Research: Atmospheres, 102(D14), pp.16911-16922.

Hoffmann, B., Boogaard, H., De Nazelle, A., Andersen, Z.J., Abramson, M., Brauer, M., Brunekreef, B., Forastiere, F., Huang, W., Kan, H., Kaufman, J.D., Katsouyanni, K., Krzyzanowski, M., Kuenzli, N., Laden, F., Nieuwenhuijsen, M., Mustapha, A., Powell, P., Rice, M., Roca-Barceló, A., Roscoe, C.J., Soares, A., Straif, K., Thurston, G., 2021. WHO Air Quality Guidelines 2021–Aiming for Healthier Air for all: A Joint Statement by Medical, Public Health, Scientific Societies and Patient Representative Organisations. Int J Public Health 66, 1604465. https://doi.org/10.3389/ijph.2021.1604465

Holmes, N.S., Morawska, L., 2006. A review of dispersion modelling and its application to the dispersion of particles: An overview of different dispersion models available. Atmospheric Environment 40, 5902–5928. https://doi.org/10.1016/j.atmosenv.2006.06.003

Hong, Q., Liu, C., Hu, Q., Xing, C., Tan, W., Liu, H., Huang, Y., Zhu, Y., Zhang, J., Geng, T., Liu, J., 2019. Evolution of the vertical structure of air pollutants during winter heavy pollution episodes: The role of regional transport and potential sources. Atmospheric Research 228, 206–222. https://doi.org/10.1016/j.atmosres.2019.05.016

Hu, X., Zhang, Y., Ding, Z., Wang, T., Lian, H., Sun, Y., Wu, J., 2012. Bioaccessibility and health risk of arsenic and heavy metals (Cd, Co, Cr, Cu, Ni, Pb, Zn and Mn) in TSP and $PM_{2.5}$ in Nanjing, China. Atmospheric Environment 57, 146–152. https://doi.org/10.1016/j.atmosenv.2012.04.056

Izhar, S., Goel, A., Chakraborty, A., Gupta, T., 2016. Annual trends in occurrence of submicron particles in ambient air and health risk posed by particle bound metals. Chemosphere 146, 582–590. https://doi.org/10.1016/j.chemosphere.2015.12.039

Jahn, H.J., Kraemer, A., Chen, X.-C., Chan, C.-Y., Engling, G., Ward, T.J., 2013. Ambient and personal PM2.5 exposure assessment in the Chinese megacity of Guangzhou. Atmospheric Environment 74, 402–411. https://doi.org/10.1016/j.atmosenv.2013.04.011

Jeong, J.-H., Shon, Z.-H., Kang, M., Song, S.-K., Kim, Y.-K., Park, J., Kim, H., 2017. Comparison of source apportionment of PM 2.5 using receptor models in the main hub port city of East Asia: Busan. Atmospheric Environment 148, 115–127. https://doi.org/10.1016/j.atmosenv.2016.10.055

Jethva, H., Satheesh, S.K., Srinivasan, J., 2005. Seasonal variability of aerosols over the Indo-Gangetic basin. J. Geophys. Res. 110, D21204. https://doi.org/10.1029/2005JD005938

Jia, C., Holt, J., Nicholson, H., Browder, J.E., Fu, X., Yu, X., Adkins, R., 2021. Identification of origins and influencing factors of environmental odor episodes using trajectory and proximity analyses. Journal of Environmental Management 295, 113084. https://doi.org/10.1016/j.jenvman.2021.113084

Kalaiarasan, G., Balakrishnan, R.M., Sethunath, N.A., Manoharan, S., 2018. Source apportionment studies on particulate matter (PM10 and PM2.5) in ambient air of urban Mangalore, India. Journal of Environmental Management 217, 815–824. https://doi.org/10.1016/j.jenvman.2018.04.040

Kamala C. T., Balaram V., Dharmendra V., Satyanarayanan M., Subramanyam K. S. V., Krishnaiah A., 2014. Application of Microwave Plasma Atomic Emission Spectrometry (MP-AES) for environmental monitoring of industrially contaminated sites in Hyderabad City. Environ Monit Assess 186, 7097–7113. https://doi.org/10.1007/s10661-014-3913-4

Karar, K., Gupta, A.K., 2006. Seasonal variations and chemical characterization of ambient PM10 at residential and industrial sites of an urban region of Kolkata (Calcutta), India. Atmospheric Research 81, 36–53. https://doi.org/10.1016/j.atmosres.2005.11.003

Karar, K., Gupta, A.K., Kumar, A., Biswas, A.K., 2006. Characterization and Identification of the Sources of Chromium, Zinc, Lead, Cadmium, Nickel, Manganese and Iron in Pm10 Particulates at the Two Sites of Kolkata, India. Environ Monit Assess 120, 347–360. https://doi.org/10.1007/s10661-005-9067-7

Kaskaoutis, D.G., Badarinath, K.V.S., Kumar Kharol, S., Rani Sharma, A., Kambezidis, H.D., 2009. Variations in the aerosol optical properties and types over the tropical urban site of Hyderabad, India. J. Geophys. Res. 114, D22204. https://doi.org/10.1029/2009JD012423

Kaskaoutis, D.G., Kharol, S.K., Sifakis, N., Nastos, P.T., Sharma, A.R., Badarinath, K.V.S., Kambezidis, H.D., 2011. Satellite monitoring of the biomass-burning aerosols during the wildfires of August 2007 in Greece: Climate implications. Atmospheric Environment 45, 716–726. https://doi.org/10.1016/j.atmosenv.2010.09.043

Kaufman, Y.J., Remer, L.A., Tanre, D., R-Li, R., Kleidman, R., Mattoo, S., Levy, R.C., Eck, T.F., Holben, B.N., Ichoku, C., Martins, V.J., Koren, I., 2005. A critical examination of the residual cloud contamination and diurnal sampling effects on MODIS estimates of aerosol over ocean. IEEE, Transactions on Geoscience and Remote Sensing 43, 2886e2897

Khan, S.A., Muhammad, S., Nazir, S., Shah, F.A., 2020. Heavy metals bounded to particulate matter in the residential and industrial sites of Islamabad, Pakistan: Implications for non-cancer and cancer risks. Environmental Technology & Innovation 19, 100822. https://doi.org/10.1016/j.eti.2020.100822

Kharol, S.K., Badarinath, K.V.S., Sharma, A.R., Kaskaoutis, D.G., Kambezidis, H.D., 2011. Multiyear analysis of Terra/Aqua MODIS aerosol optical depth and ground observations over tropical urban region of Hyderabad, India. Atmospheric Environment 45, 1532–1542. https://doi.org/10.1016/j.atmosenv.2010.12.047

Khreis, H., Cirach, M., Mueller, N., De Hoogh, K., Hoek, G., Nieuwenhuijsen, M.J., Rojas-Rueda, D., 2019. Outdoor air pollution and the burden of childhood asthma across Europe. Eur Respir J 54, 1802194. https://doi.org/10.1183/13993003.02194-2018

Kinney, P.L., Gichuru, M.G., Volavka-Close, N., Ngo, N., Ndiba, P.K., Law, A., Gachanja, A., Gaita, S.M., Chillrud, S.N., Sclar, E., 2011. Traffic impacts on PM2.5 air quality in

Nairobi, Kenya. Environmental Science & Policy 14, 369–378. https://doi.org/10.1016/j.envsci.2011.02.005

Kong, L., Tan, Q., Feng, M., Qu, Y., An, J., Liu, X., Cheng, N., Deng, Y., Zhai, R., Wang, Z., 2020. Investigating the characteristics and source analyses of PM2.5 seasonal variations in Chengdu, Southwest China. Chemosphere 243, 125267. https://doi.org/10.1016/j.chemosphere.2019.125267

Kong, S., Lu, B., Bai, Z., Zhao, X., Chen, L., Han, B., Li, Z., Ji, Y., Xu, Y., Liu, Y., Jiang, H., 2011. Potential threat of heavy metals in re-suspended dusts on building surfaces in oilfield city. Atmospheric Environment 45, 4192–4204. https://doi.org/10.1016/j.atmosenv.2011.05.011

Kong, S., Lu, B., Ji, Y., Zhao, X., Bai, Z., Xu, Y., Liu, Y., Jiang, H., 2012. Risk assessment of heavy metals in road and soil dusts within PM2.5, PM10 and PM100 fractions in Dongying city, Shandong Province, China. J. Environ. Monit. 14, 791. https://doi.org/10.1039/c1em10555h

Kopas, J., York, E., Jin, X., Harish, S.P., Kennedy, R., Shen, S.V., Urpelainen, J., 2020. Environmental Justice in India: Incidence of Air Pollution from Coal-Fired Power Plants. Ecological Economics 176, 106711. https://doi.org/10.1016/j.ecolecon.2020.106711

Krishna, A.K., Govil, P.K., 2007. Soil Contamination Due to Heavy Metals from an Industrial Area of Surat, Gujarat, Western India. Environ Monit Assess 124, 263–275. https://doi.org/10.1007/s10661-006-9224-7

Kubilay, N., Oguz, T., Koçak, M. and Torres, O., 2005. Ground-based assessment of Total Ozone Mapping Spectrometer (TOMS) data for dust transport over the northeastern Mediterranean. Global Biogeochemical Cycles, 19(1).

Kulshrestha, A., Satsangi, P.G., Masih, J., Taneja, A., 2009. Metal concentration of PM2.5 and PM10 particles and seasonal variations in urban and rural environment of Agra, India. Science of The Total Environment 407, 6196–6204. https://doi.org/10.1016/j.scitotenv.2009.08.050

Kulshrestha, M.J., Singh, R., Engardt, M., 2014. Ambient and Episodic Levels of Metals in PM10 Aerosols and Their Source Apportionment in Central Delhi, India. J. Hazard. Toxic Radioact. Waste 20, A4014002. https://doi.org/10.1061/(ASCE)HZ.2153-5515.0000227

Kumar, A., 2014. Long term (2003–2012) spatio-temporal MODIS (Terra/Aqua level 3) derived climatic variations of aerosol optical depth and cloud properties over a semi arid urban tropical region of Northern India. Atmospheric Environment 83, 291–300. https://doi.org/10.1016/j.atmosenv.2013.10.030

Kumar, A., 2013. Variability of aerosol optical depth and cloud parameters over North Eastern regions of India retrieved from MODIS satellite data. Journal of Atmospheric and Solar-Terrestrial Physics 100–101, 34–49. https://doi.org/10.1016/j.jastp.2013.03.025

Kumar, N., Chu, A., Foster, A., 2008. Remote sensing of ambient particles in Delhi and its environs: estimation and validation. International Journal of Remote Sensing 29, 3383–3405. https://doi.org/10.1080/01431160701474545

Kumar, P., Morawska, L., Biskos, G., Neophytou, M., Di Sabatino, S., Bell, M., … & Vardoulakis, S. (2017). The rise of low-cost sensing for managing air pollution in cities. Environment international, 75, 199-205.

Kumar, P., Pratap, V., Kumar, A., Choudhary, A., Prasad, R., Shukla, A., Singh, R.P., Singh, A.K., 2020. Assessment of atmospheric aerosols over Varanasi: Physical, optical and chemical

properties and meteorological implications. Journal of Atmospheric and Solar-Terrestrial Physics 209, 105424. https://doi.org/10.1016/j.jastp.2020.105424

Kumar, R., Naja, M., Satheesh, S. K., Ojha, N., Joshi, H., Sarangi, T., … & Kotamarthi, V. R. (2016). Influences of the springtime northern Indian biomass burning over the central Himalayas. Journal of Geophysical Research: Atmospheres, 121(22), 13-621.

Kumari, S., Lakhani, A., Kumari, K.M., 2020. Transport of aerosols and trace gases during dust and crop-residue burning events in Indo-Gangetic Plain: Influence on surface ozone levels over downwind region. Atmospheric Environment 241, 117829. https://doi.org/10.1016/j.atmosenv.2020.117829

Lane, T.E., Pinder, R.W., Shrivastava, M., Robinson, A.L., Pandis, S.N., 2007. Source contributions to primary organic aerosol: Comparison of the results of a source-resolved model and the chemical mass balance approach. Atmospheric Environment 41, 3758–3776. https://doi.org/10.1016/j.atmosenv.2007.01.006

Lee, K., Greenstone, M., 2021. Annual Update. Air Quality Life Index.

Levy, R., Hsu, C., et al., 2015. MODIS Atmosphere L2 Aerosol Product. NASA MODIS Adaptive Processing System, Goddard Space Flight Center, USA: http://dx.doi.org/10.5067/MODIS/MOD04_L2.061

Li, D., Yang, T., Zhou, R., Zhu, Z., An, S., 2023. Assessment and sources of heavy metals in the suspended particulate matter, sediments and water of a karst lake in Guizhou Province, China. Marine Pollution Bulletin 189, 114636. https://doi.org/10.1016/j.marpolbul.2023.114636

Li, Hongyan, Zhang, J., Wen, B., Huang, S., Gao, S., Li, Hongyu, Zhao, Z., Zhang, Y., Fu, G., Bai, J., Cui, Y., He, Q., Wang, Z., 2022. Spatial-Temporal Distribution and Variation of NO2 and Its Sources and Chemical Sinks in Shanxi Province, China. Atmosphere 13, 1096. https://doi.org/10.3390/atmos13071096

Liao, T., Wang, S., Ai, J., Gui, K., Duan, B., Zhao, Q., Zhang, X., Jiang, W., Sun, Y., 2017. Heavy pollution episodes, transport pathways and potential sources of PM2.5 during the winter of 2013 in Chengdu (China). Science of The Total Environment 584–585, 1056–1065. https://doi.org/10.1016/j.scitotenv.2017.01.160

Liu, Y., He, K., Li, S., Wang, Z., Christiani, D.C., Koutrakis, P., 2012. A statistical model to evaluate the effectiveness of PM2.5 emissions control during the Beijing 2008 Olympic Games. Environment International 44, 100–105. https://doi.org/10.1016/j.envint.2012.02.003

Loughner, C.P., Fasoli, B., Stein, A.F., Lin, J.C., 2021. Incorporating features from the Stochastic Time-Inverted Lagrangian Transport (STILT) model into the Hybrid Single-Particle Lagrangian Integrated Trajectory (HYSPLIT) model: a unified dispersion model for time-forward and time-reversed applications. Journal of Applied Meteorology and Climatology. https://doi.org/10.1175/JAMC-D-20-0158.1

Luo, J., Zhang, J., Huang, X., Liu, Q., Luo, B., Zhang, W., Rao, Z., Yu, Y., 2020. Characteristics, evolution, and regional differences of biomass burning particles in the Sichuan Basin, China. Journal of Environmental Sciences 89, 35–46. https://doi.org/10.1016/j.jes.2019.09.015

Mahapatra, P.S., Sinha, P.R., Boopathy, R., Das, T., Mohanty, S., Sahu, S.C., Gurjar, B.R., 2018. Seasonal progression of atmospheric particulate matter over an urban coastal region in peninsular India: Role of local meteorology and long-range transport. Atmospheric Research 199, 145–158. https://doi.org/10.1016/j.atmosres.2017.09.001

Mamun, A.A., Cheng, I., Zhang, L., Celo, V., Dabek-Zlotorzynska, E., Charland, J., 2022. Estimation of Atmospheric Dry and Wet Deposition of Particulate Elements at Four Monitoring Sites in the Canadian Athabasca Oil Sands Region. JGR Atmospheres 127. https://doi.org/10.1029/2021JD035787

Mangla, R., J, I., S.S., C., 2020. Inter-comparison of multi-satellites and Aeronet AOD over Indian Region. Atmospheric Research 240, 104950. https://doi.org/10.1016/j.atmosres.2020.104950

Massey, D.D., Kulshrestha, A., Taneja, A., 2013. Particulate matter concentrations and their related metal toxicity in rural residential environment of semi-arid region of India. Atmospheric Environment 67, 278–286. https://doi.org/10.1016/j.atmosenv.2012.11.002

May, A.A., Presto, A.A., Hennigan, C.J., Nguyen, N.T., Gordon, T.D., Robinson, A.L., 2013. Gas-Particle Partitioning of Primary Organic Aerosol Emissions: (2) Diesel Vehicles. Environ. Sci. Technol. 47, 8288–8296. https://doi.org/10.1021/es400782j

Mhawish, A., Banerjee, T., Broday, D.M., Misra, A., Tripathi, S.N., 2017. Evaluation of MODIS Collection 6 aerosol retrieval algorithms over Indo-Gangetic Plain: Implications of aerosols types and mass loading. Remote Sensing of Environment 201, 297–313. https://doi.org/10.1016/j.rse.2017.09.016

Misra, P., Imasu, R., Takeuchi, W., 2019. Impact of Urban Growth on Air Quality in Indian Cities Using Hierarchical Bayesian Approach. Atmosphere 10, 517. https://doi.org/10.3390/atmos10090517

Mitra, S., Das, R., 2020. Health risk assessment of construction workers from trace metals in $PM_{2.5}$ from Kolkata, India. Archives of Environmental & Occupational Health 1–16. https://doi.org/10.1080/19338244.2020.1860877

Mohr, C., Huffman, J.A., Cubison, M.J., Aiken, A.C., Docherty, K.S., Kimmel, J.R., Ulbrich, I.M., Hannigan, M., Jimenez, J.L., 2009. Characterization of Primary Organic Aerosol Emissions from Meat Cooking, Trash Burning, and Motor Vehicles with High-Resolution Aerosol Mass Spectrometry and Comparison with Ambient and Chamber Observations. Environ. Sci. Technol. 43, 2443–2449. https://doi.org/10.1021/es8011518

Mònica, G., Małgorzata J, L., Laura, P.-C., 2022. Air Pollution and Brain Outcomes in Children.

Moorthy, K.K., Babu, S.S., Satheesh, S.K., 2005. Aerosol Characteristics and Radiative Impacts over the Arabian Sea during the Intermonsoon Season: Results from ARMEX Field Campaign. Journal of the Atmospheric Sciences 62, 192–206. https://doi.org/10.1175/JAS-3378.1

Morantes, G., González, J.C., Rincón, G., 2021. Characterisation of particulate matter and identification of emission sources in Greater Caracas, Venezuela. Air Qual Atmos Health 14, 1989–2014. https://doi.org/10.1007/s11869-021-01070-2

Mukherjee, A., Agrawal, M., 2018. Assessment of local and distant sources of urban PM2.5 in middle Indo-Gangetic plain of India using statistical modeling. Atmospheric Research 213, 275–287. https://doi.org/10.1016/j.atmosres.2018.06.014

Munchak, L.A., Levy, R.C., Mattoo, S., Remer, L.A., Holben, B.N., Schafer, J.S., Hostetler, C.A., Ferrare, R.A., 2013. MODIS 3 km aerosol product: applications over land in an urban/suburban region. Atmos. Meas. Tech. 6, 1747–1759. https://doi.org/10.5194/amt-6-1747-2013

Murray, C.J.L., et al., 2020. Global burden of 87 risk factors in 204 countries and territories, 1990–2019: a systematic analysis for the Global Burden of Disease Study 2019. The Lancet 396, 1223–1249. https://doi.org/10.1016/S0140-6736(20)30752-2

Nair, P.R., George, S.K., Sunilkumar, S.V., Parameswaran, K., Jacob, S., Abraham, A., 2006. Chemical composition of aerosols over peninsular India during winter. Atmospheric Environment 40, 6477–6493. https://doi.org/10.1016/j.atmosenv.2006.02.031

Nawrot, T., Plusquin, M., Hogervorst, J., Roels, H.A., Celis, H., Thijs, L., Vangronsveld, J., Van Hecke, E., Staessen, J.A., 2006. Environmental exposure to cadmium and risk of cancer: a prospective population-based study. Lancet Oncol 7, 119–126. https://doi.org/10.1016/S1470-2045(06)70545-9

Negral, L., Suárez-Peña, B., Zapico, E., Fernández-Nava, Y., Megido, L., Moreno, J., Marañón, E., Castrillón, L., 2020. Anthropogenic and meteorological influences on PM10 metal/semi-metal concentrations: Implications for human health. Chemosphere 243, 125347. https://doi.org/10.1016/j.chemosphere.2019.125347

Ni, H., Tian, J., Wang, X., Wang, Q., Han, Y., Cao, J., Long, X., Chen, L.-W.A., Chow, J.C., Watson, J.G., Huang, R.-J., Dusek, U., 2017. PM2.5 emissions and source profiles from open burning of crop residues. Atmospheric Environment 169, 229–237. https://doi.org/10.1016/j.atmosenv.2017.08.063

Nirmalkar, J., Haswani, D., Singh, A., Kumar, S., Sunder Raman, R., 2021. Concentrations, transport characteristics, and health risks of PM2.5-bound trace elements over a national park in central India. Journal of Environmental Management 293, 112904. https://doi.org/10.1016/j.jenvman.2021.112904

Niu, Z., Habre, R., Chavez, T.A., Yang, T., Grubbs, B.H., Eckel, S.P., Berhane, K., Toledo-Corral, C.M., Johnston, J., Dunton, G.F., Lerner, D., Al-Marayati, L., Lurmann, F., Pavlovic, N., Farzan, S.F., Bastain, T.M., Breton, C.V., 2022. Association Between Ambient Air Pollution and Birth Weight by Maternal Individual- and Neighborhood-Level Stressors. JAMA Netw Open 5, e2238174. https://doi.org/10.1001/jamanetworkopen.2022.38174

Ntziachristos, L., Ning, Z., Geller, M.D., Sioutas, C., 2007. Particle Concentration and Characteristics near a Major Freeway with Heavy-Duty Diesel Traffic. Environ. Sci. Technol. 41, 2223–2230. https://doi.org/10.1021/es062590s

Owega, S., Khan, B.-U.-Z., Evans, G.J., Jervis, R.E., Fila, M., 2006. Identification of long-range aerosol transport patterns to Toronto via classification of back trajectories by cluster analysis and neural network techniques. Chemometrics and Intelligent Laboratory Systems 83, 26–33. https://doi.org/10.1016/j.chemolab.2005.12.009

Pakkanen, T.A., Kerminen, V.-M., Loukkola, K., Hillamo, R.E., Aarnio, P., Koskentalo, T., Maenhaut, W., 2003. Size distributions of mass and chemical components in street-level and rooftop PM1 particles in Helsinki. Atmospheric Environment 37, 1673–1690. https://doi.org/10.1016/S1352-2310(03)00011-6

Pal, S.K., Wallis, S.G., Arthur, S., 2018. AN ASSESSMENT OF HEAVY METALS POLLUTION POTENTIAL OF ROAD SEDIMENT DERIVED FROM A SUBURBAN ROAD NETWORK UNDER DIFFERENT WEATHER CONDITIONS. Environ. Eng. Manag. J. 17, 1955–1966. https://doi.org/10.30638/eemj.2018.195

Pang, S., 2014. Application of a second generation microwave plasma atomic emission spectrometer (MP-AES) in the analysis of food samples. PowerPoint-esitys. Agilent technologies. Viitattu, 9, p.2016.

Pandey, A et al., 2021. Health and economic impact of air pollution in the states of India: the Global Burden of Disease Study 2019. The Lancet Planetary Health 5, e25–e38. https://doi.org/10.1016/S2542-5196(20)30298-9

Pandey, B., Agrawal, M., Singh, S., 2014. Assessment of air pollution around coal mining area: Emphasizing on spatial distributions, seasonal variations and heavy metals, using cluster and principal component analysis. Atmospheric Pollution Research 5, 79–86. https://doi.org/10.5094/APR.2014.010

Pandey, M., Pandey, A.K., Mishra, A., Tripathi, B.D., 2017. Speciation of carcinogenic and non-carcinogenic metals in respirable suspended particulate matter (PM10) in Varanasi, India. Urban Climate 19, 141–154. https://doi.org/10.1016/j.uclim.2017.01.004

Pani, S.K., Verma, S., 2014. Variability of winter and summertime aerosols over eastern India urban environment. Atmospheric Research 137, 112–124. https://doi.org/10.1016/j.atmosres.2013.09.014

Pant, P., Guttikunda, S.K., Peltier, R.E., 2016. Exposure to particulate matter in India: A synthesis of findings and future directions. Environmental Research 147, 480–496. https://doi.org/10.1016/j.envres.2016.03.011

Pasha, M.J., Alharbi, B.H., 2015. Characterization of size–fractionated PM 10 and associated heavy metals at two semi–arid holy sites during Hajj in Saudi Arabia. Atmospheric Pollution Research 6, 162–172. https://doi.org/10.5094/APR.2015.019

Pathak, B., Bhuyan, P.K., 2015. Climatology of columnar aerosol properties at a continental location in the upper Brahmaputra basin of north east India: Diurnal asymmetry and association with meteorology. Advances in Space Research 56, 1469–1484. https://doi.org/10.1016/j.asr.2015.07.004

Pathak, B., Biswas, J., Bharali, C., Bhuyan, P.K., 2015. Short term introduction of pollutants into the atmosphere at a location in the Brahmaputra Basin: A case study. Atmospheric Pollution Research 6, 220–229. https://doi.org/10.5094/APR.2015.026

Patil, R.S., Kumar, R., Menon, R., Shah, M.K., Sethi, V., 2013. Development of particulate matter speciation profiles for major sources in six cities in India. Atmospheric Research 132–133, 1–11. https://doi.org/10.1016/j.atmosres.2013.04.012

Piscitello, A., Bianco, C., Casasso, A., Sethi, R., 2021. Non-exhaust traffic emissions: Sources, characterization, and mitigation measures. Science of The Total Environment 766, 144440. https://doi.org/10.1016/j.scitotenv.2020.144440

Platnick, S., et al., 2015. MODIS Atmosphere L3 Monthly Product. NASA MODIS Adaptive Processing System, Goddard Space Flight Center, USA: http://dx.doi.org/10.5067/MODIS/MYD08_M3.061

Police, S., Sahu, S.K., Tiwari, M. and Pandit, G.G., 2018. Chemical composition and source apportionment of PM2. 5 and PM2. 5–10 in Trombay (Mumbai, India), a coastal industrial area. Particuology, 37, pp.143-153.

Pongpiachan, S., Iijima, A., Cao, J., 2018. Hazard Quotients, Hazard Indexes, and Cancer Risks of Toxic Metals in PM10 during Firework Displays. Atmosphere 9, 144. https://doi.org/10.3390/atmos9040144

Prabhu, V., Shridhar, V., 2019. Investigation of potential sources, transport pathway, and health risks associated with respirable suspended particulate matter in Dehradun city, situated in the foothills of the Himalayas. Atmospheric Pollution Research 10, 187–196. https://doi.org/10.1016/j.apr.2018.07.009

Qi, H., Chen, X., Du, Y., Niu, X., Guo, F., Li, W., 2019. Cancer risk assessment of soils contaminated by polycyclic aromatic hydrocarbons in Shanxi, China. Ecotoxicology and Environmental Safety 182, 109381. https://doi.org/10.1016/j.ecoenv.2019.109381

Qi, H., Duan, W., Cheng, S. and Cai, B., 2023. O3 transport characteristics in eastern China in 2017 and 2021 based on complex networks and WRF-CMAQ-ISAM. Chemosphere, p.139258.

Qiao, X., Guo, H., Tang, Y., Wang, P., Deng, W., Zhao, X., Hu, J., Ying, Q., Zhang, H., 2019. Local and regional contributions to fine particulate matter in the 18 cities of Sichuan Basin, southwestern China. Atmos. Chem. Phys. 19, 5791–5803. https://doi.org/10.5194/acp-19-5791-2019

Qu, W., Zhang, X., Wang, Y., Fu, G., 2020. Atmospheric visibility variation over global land surface during 1973–2012: Influence of meteorological factors and effect of aerosol, cloud on ABL evolution. Atmospheric Pollution Research 11, 730–743. https://doi.org/10.1016/j.apr.2020.01.002

Quinn, P.K., 2002. Aerosol optical properties during INDOEX 1999: Means, variability, and controlling factors. J. Geophys. Res. 107, 8020. https://doi.org/10.1029/2000JD000037

Rai, A., Mukherjee, S., Chatterjee, A., Choudhary, N., Kotnala, G., Mandal, T.K., Sharma, S.K., 2020. Seasonal Variation of OC, EC, and WSOC of PM10 and Their CWT Analysis Over the Eastern Himalaya. Aerosol Sci Eng 4, 26–40. https://doi.org/10.1007/s41810-020-00053-7

Ramachandran, S., Rengarajan, R., Jayaraman, A., Sarin, M.M., Das, S.K., 2006. Aerosol radiative forcing during clear, hazy, and foggy conditions over a continental polluted location in north India. J. Geophys. Res. 111, D20214. https://doi.org/10.1029/2006JD007142

Ramachandran, S., Rupakheti, M., 2022. Trends in physical, optical and chemical columnar aerosol characteristics and radiative effects over South and East Asia: Satellite and ground-based observations. Gondwana Research 105, 366–387. https://doi.org/10.1016/j.gr.2021.09.016

Ramachandran, S., Rajesh, T. A., & Meena, R. (2017). Source characterization and apportionment of PM2.5 in Chennai, India. Aerosol and Air Quality Research, 17(1), 216-229.

Ravindra, K., Goyal, A., Mor, S., 2022. Influence of meteorological parameters and air pollutants on the airborne pollen of city Chandigarh, India. Science of The Total Environment 818, 151829. https://doi.org/10.1016/j.scitotenv.2021.151829

Ravishankara, A.R., David, L.M., Pierce, J.R., Venkataraman, C., 2020. Outdoor air pollution in India is not only an urban problem. Proc. Natl. Acad. Sci. U.S.A. 117, 28640–28644. https://doi.org/10.1073/pnas.2007236117

Rohra, H., Taneja, A., 2016. Indoor air quality scenario in India—An outline of household fuel combustion. Atmospheric Environment 129, 243–255. https://doi.org/10.1016/j.atmosenv.2016.01.038

Rolph, G.D., Draxler, R.R., Stein, A.F., Taylor, A., Ruminski, M.G., Kondragunta, S., Zeng, J., Huang, H.-C., Manikin, G., McQueen, J.T., Davidson, P.M., 2009. Description and Verification of the NOAA Smoke Forecasting System: The 2007 Fire Season. Weather and Forecasting 24, 361–378. https://doi.org/10.1175/2008WAF2222165.1

Roy, D., Kim, J., Lee, M., Park, J., 2023. Adverse impacts of Asian dust events on human health and the environment—A probabilistic risk assessment study on particulate matter-bound metals and bacteria in Seoul, South Korea. Science of The Total Environment 875, 162637. https://doi.org/10.1016/j.scitotenv.2023.162637

Rudnick, R.L., Gao, S., 2003. Composition of the Continental Crust, in: Treatise on Geochemistry. Elsevier, pp. 1–64. https://doi.org/10.1016/B0-08-043751-6/03016-4

Sah, D., 2023. Concentration, source apportionment and human health risk assessment of elements in PM2. 5 at Agra, India. Urban Climate, 49, p.101477.

Sah, D., Verma, P.K., Kandikonda, M.K., Lakhani, A., 2019. Pollution characteristics, human health risk through multiple exposure pathways, and source apportionment of heavy metals in PM10 at Indo-Gangetic site. Urban Climate 27, 149–162. https://doi.org/10.1016/j.uclim.2018.11.010

Shao, Y., Liu, H., Chen, J., Fan, Y., Liu, J., Wang, Z., … & Liang, X. (2017). Estimating ground-level PM2. 5 concentrations in Beijing using a satellite-based geographically and temporally weighted regression model. Remote Sensing of Environment, 198, 140-149

Sanduijav, C., Ferreira, S., Filipski, M., Hashida, Y., 2021. Air pollution and happiness: Evidence from the coldest capital in the world. Ecological Economics 187, 107085. https://doi.org/10.1016/j.ecolecon.2021.107085

Sankar, A., Coggins, J.S., Goodkind, A.L., 2020. Effectiveness of air pollution standards in reducing mortality in India. Resource and Energy Economics 62, 101188. https://doi.org/10.1016/j.reseneeco.2020.101188

Saraswat, I., Mishra, R.K., Kumar, A., 2017. Estimation of PM10 concentration from Landsat 8 OLI satellite imagery over Delhi, India. Remote Sensing Applications: Society and Environment 8, 251–257. https://doi.org/10.1016/j.rsase.2017.10.006

Sarkar, S., Chokngamwong, R., Cervone, G., Singh, R.P., Kafatos, M., 2006. Variability of aerosol optical depth and aerosol forcing over India. Advances in Space Research 37, 2153–2159. https://doi.org/Jia

Sathe, Y., Kulkarni, S., Gupta, P., Kaginalkar, A., Islam, S., Gargava, P., 2019. Application of Moderate Resolution Imaging Spectroradiometer (MODIS) Aerosol Optical Depth (AOD) and Weather Research Forecasting (WRF) model meteorological data for assessment of fine particulate matter (PM2.5) over India. Atmospheric Pollution Research 10, 418–434. https://doi.org/10.1016/j.apr.2018.08.016

Satheesh, S.K., Moorthy, K.K., Babu, S.S., Vinoj, V., Dutt, C.B.S., 2008. Climate implications of large warming by elevated aerosol over India. Geophys. Res. Lett. 35, L19809. https://doi.org/10.1029/2008GL034944

Satsangi, P.G., Yadav, S., Pipal, A.S., Kumbhar, N., 2014. Characteristics of trace metals in fine (PM2.5) and inhalable (PM10) particles and its health risk assessment along with in-silico approach in indoor environment of India. Atmospheric Environment 92, 384–393. https://doi.org/10.1016/j.atmosenv.2014.04.047

Seibert, P., Kromp-Kolb, H., Baltensperger, U., Jost, D.T., Schwikowski, M., 1994. Trajectory Analysis of High-Alpine Air Pollution Data, in: Gryning, S.-E., Millán, M.M. (Eds.), Air Pollution Modeling and Its Application X. Springer US, Boston, MA, pp. 595–596. https://doi.org/10.1007/978-1-4615-1817-4_65

Shanavas, A.K., Zhou, C., Menon, R., Hopke, P.K., 2020. PM10 source identification using the trajectory based potential source apportionment (TraPSA) toolkit at Kochi, India. Atmospheric Pollution Research 11, 1535–1542. https://doi.org/10.1016/j.apr.2020.06.019

Shao, P., Xin, J., An, J., Kong, L., Wang, B., Wang, J., Wang, Y., Wu, D., 2017. The empirical relationship between PM2.5 and AOD in Nanjing of the Yangtze River Delta. Atmospheric Pollution Research 8, 233–243. https://doi.org/10.1016/j.apr.2016.09.001

Sharma, D., Kulshrestha, U.C., 2014. Spatial and temporal patterns of air pollutants in rural and urban areas of India. Environmental Pollution 195, 276–281. https://doi.org/10.1016/j.envpol.2014.08.026

Sharma, G., Annadate, S., Sinha, B., 2022. Will open waste burning become India's largest air pollution source? Environmental Pollution 292, 118310. https://doi.org/10.1016/j.envpol.2021.118310

Sharma, M., Maloo, S., 2005. Assessment of ambient air PM10 and PM2.5 and characterization of PM10 in the city of Kanpur, India. Atmospheric Environment 12.

Sharma, R.K., Agrawal, M., Marshall, F.M., 2008. Atmospheric deposition of heavy metals (Cu, Zn, Cd and Pb) in Varanasi City, India. Environ Monit Assess 142, 269–278. https://doi.org/10.1007/s10661-007-9924-7

Sharma, S. K., Mandal, T. K., Jain, S., Saraswati, Parashar, A., & Saxena, M. (2017). Source apportionment of PM2.5 in Delhi using PMF model. Bulletin of environmental contamination and toxicology, 98(1), 64-70.

Shikha, Rajouriya, K., Pipal, A.S., Taneja, A., 2023. Chemical Characterization and Health Risk Assessment of Particulate Matter near National Highway at Urban and Semi- Urban location of Northern India (preprint). In Review. https://doi.org/10.21203/rs.3.rs-2863172/v1

Singh, D.P., Gadi, R., Mandal, T.K., 2011. Characterization of particulate-bound polycyclic aromatic hydrocarbons and trace metals composition of urban air in Delhi, India. Atmospheric Environment 45, 7653–7663. https://doi.org/10.1016/j.atmosenv.2011.02.058

Singh, N., Murari, V., Kumar, M., Barman, S.C., Banerjee, T., 2017. Fine particulates over South Asia: Review and meta-analysis of PM2.5 source apportionment through receptor model. Environmental Pollution 223, 121–136. https://doi.org/10.1016/j.envpol.2016.12.071

Soleimani, M., Amini, N., Sadeghian, B., Wang, D., Fang, L., 2018. Heavy metals and their source identification in particulate matter (PM2.5) in Isfahan City, Iran. Journal of Environmental Sciences 72, 166–175. https://doi.org/10.1016/j.jes.2018.01.002

Soni, A., Kumar, U., Prabhu, V., Shridhar, V., 2020. Characterization, Source Apportionment and Carcinogenic Risk Assessment of Atmospheric Particulate Matter at Dehradun, situated in the Foothills of Himalayas. Journal of Atmospheric and Solar-Terrestrial Physics 199, 105205. https://doi.org/10.1016/j.jastp.2020.105205

Soni, M., Payra, S., Verma, S., 2018. Particulate matter estimation over a semi arid region Jaipur, India using satellite AOD and meteorological parameters. Atmospheric Pollution Research 9, 949–958. https://doi.org/10.1016/j.apr.2018.03.001

Sreekanth, V., 2013. Satellite derived aerosol optical depth climatology over Bangalore, India. Advances in Space Research 51, 2297–2308. https://doi.org/10.1016/j.asr.2013.01.022

Sreekanth, V., Mahesh, B., Niranjan, K., 2017. Satellite remote sensing of fine particulate air pollutants over Indian mega cities. Advances in Space Research 60, 2268–2276. https://doi.org/10.1016/j.asr.2017.08.008

Stein, A.F., Draxler, R.R., Rolph, G.D., Stunder, B.J.B., Cohen, M.D., Ngan, F., 2015. NOAA's HYSPLIT Atmospheric Transport and Dispersion Modeling System. Bulletin of the American Meteorological Society 96, 2059–2077. https://doi.org/10.1175/BAMS-D-14-00110.1

Sudheer, A.K., Rengarajan, R., 2012. Atmospheric Mineral Dust and Trace Metals over Urban Environment in Western India during Winter. Aerosol Air Qual. Res. 12, 923–933. https://doi.org/10.4209/aaqr.2011.12.0237

Sunder Raman, R., Kumar, S., 2016. First measurements of ambient aerosol over an ecologically sensitive zone in Central India: Relationships between PM2.5 mass, its optical properties,

and meteorology. Science of The Total Environment 550, 706–716. https://doi.org/10.1016/j.scitotenv.2016.01.092

Suryawanshi, P.V., Rajaram, B.S., Bhanarkar, A.D., Chalapati Rao, C.V., 2016a. Determining heavy metal contamination of road dust in Delhi, India. ATM. https://doi.org/10.20937/ATM.2016.29.03.04

Suryawanshi, P.V., Rajaram, B.S., Bhanarkar, A.D., Chalapati Rao, C.V., 2016b. Determining heavy metal contamination of road dust in Delhi, India. ATM. https://doi.org/10.20937/ATM.2016.29.03.04

Tarín-Carrasco, P., Im, U., Geels, C., Palacios-Peña, L., Jiménez-Guerrero, P., 2021. Contribution of fine particulate matter to present and future premature mortality over Europe: A non-linear response. Environment International 153, 106517. https://doi.org/10.1016/j.envint.2021.106517

Tariq, S., Nawaz, H., Ul-Haq, Z., Mehmood, U., 2021. Investigating the relationship of aerosols with enhanced vegetation index and meteorological parameters over Pakistan. Atmospheric Pollution Research 12, 101080. https://doi.org/10.1016/j.apr.2021.101080

Tasic, M., Mijic, Z., Rajsic, S., Zekic, A., Perisic, M., Stojic, A., Tasic, M., 2010. Characteristics and Application of Receptor Models to the Atmospheric Aerosols Research, in: Kumar, A. (Ed.), Air Quality. Sciyo. https://doi.org/10.5772/9756

Tegen, I., Schepanski, K., 2018. Climate Feedback on Aerosol Emission and Atmospheric Concentrations. Curr Clim Change Rep 4, 1–10. https://doi.org/10.1007/s40641-018-0086-1

Tian, H.Z., Zhu, C.Y., Gao, J.J., Cheng, K., Hao, J.M., Wang, K., Hua, S.B., Wang, Y., Zhou, J.R., 2015. Quantitative assessment of atmospheric emissions of toxic heavy metals from anthropogenic sources in China: historical trend, spatial distribution, uncertainties, and control policies. Atmos. Chem. Phys. 15, 10127–10147. https://doi.org/10.5194/acp-15-10127-2015

Tian, J., Wang, Q., Zhang, Y., Yan, M., Liu, H., Zhang, N., Ran, W., Cao, J., 2021. Impacts of primary emissions and secondary aerosol formation on air pollution in an urban area of China during the COVID-19 lockdown. Environment International 150, 106426. https://doi.org/10.1016/j.envint.2021.106426

Tiwari, S., Pandithurai, G., Attri, S.D., Srivastava, A.K., Soni, V.K., Bisht, D.S., Anil Kumar, V., Srivastava, M.K., 2015. Aerosol optical properties and their relationship with meteorological parameters during wintertime in Delhi, India. Atmospheric Research 153, 465–479. https://doi.org/10.1016/j.atmosres.2014.10.003

Trancoso, R., Behr, Y., Hurst, T., Deligne, N.I., 2022. Towards real-time probabilistic ash deposition forecasting for New Zealand. J Appl. Volcanol. 11, 13. https://doi.org/10.1186/s13617-022-00123-0

Tripathi, S.N., 2005. Aerosol black carbon radiative forcing at an industrial city in northern India. Geophys. Res. Lett. 32, L08802. https://doi.org/10.1029/2005GL022515

Tursumbayeva, M., Muratuly, A., Baimatova, N., Karaca, F., Kerimray, A., 2023. Cities of Central Asia: New hotspots of air pollution in the world. Atmospheric Environment 309, 119901. https://doi.org/10.1016/j.atmosenv.2023.119901

Tyagi, B., Choudhury, G., Vissa, N.K., Singh, J., Tesche, M., 2021. Changing air pollution scenario during COVID-19: Redefining the hotspot regions over India. Environmental Pollution 271, 116354. https://doi.org/10.1016/j.envpol.2020.116354

U.S EPA, n.d. U.S. EPA (U.S. Environmental Protection Agency), 1998. Integrated Risk Information System, IRIS Substance List.
US EPA 2004b, n.d. U.S. EPA (U.S. Environmental Protection Agency) (2004b) Region 9, preliminary remediation goals, air–water calculations.
US EPA 2004c, n.d. U.S. EPA (U.S. Environmental Protection Agency) (2004c) Risk Assessment Guidance for Superfund volume 1: human health evaluation manual (Part E, Supplemental Guidance for Dermal Risk Assessment). Office of Superfund Remediation and Technology Innovation, Washington DC.
US EPA 2007, n.d. U.S. EPA (U.S. Environmental Protection Agency) (2007).Guidance for evaluating the Oral bioavailability of Metals in Soils for Use in Human Health Risk Assessment.
US EPA 2009a, n.d. U.S. EPA (U.S. Environmental Protection Agency) (2009a) Risk Assessment Guidance for Superfund vol I: human health evaluation manual (Part F, Supplemental Guidance for Inhalation Risk Assessment). Office of Superfund Remediation and Technology Innovation, Washington DC.
US EPA 2009b, n.d. U.S. EPA (U.S. Environmental Protection Agency) (2009b) Risk Assessment Guidance for Superfund volume 1: human health evaluation manual (Part F, Supplemental Guidance for Dermal Risk Assessment). Office of Superfund Remediation and Technology Innovation, Washington DC.
Vadrevu, K.P., Ellicott, E., Badarinath, K.V.S., Vermote, E., 2011. MODIS derived fire characteristics and aerosol optical depth variations during the agricultural residue burning season, north India. Environmental Pollution 159, 1560–1569. https://doi.org/10.1016/j.envpol.2011.03.001
Valiulis, D., 2008. Heavy metal penetration into the human respiratory tract in Vilnius. Lithuanian J. Phys. 48, 349–355. https://doi.org/10.3952/lithjphys.48407
Vellingiri, K., Kim, K.-H., Lim, J.-M., Lee, J.-H., Ma, C.-J., Jeon, B.-H., Sohn, J.-R., Kumar, P., Kang, C.-H., 2016. Identification of nitrogen dioxide and ozone source regions for an urban area in Korea using back trajectory analysis. Atmospheric Research 176–177, 212–221. https://doi.org/10.1016/j.atmosres.2016.02.022
Vijayanand, C., Rajaguru, P., Kalaiselvi, K., Selvam, K.P., Palanivel, M., 2008. Assessment of heavy metal contents in the ambient air of the Coimbatore city, Tamilnadu, India. Journal of Hazardous Materials 160, 548–553. https://doi.org/10.1016/j.jhazmat.2008.03.071
Wang, M., Zhang, H., 2018. Accumulation of Heavy Metals in Roadside Soil in Urban Area and the Related Impacting Factors. IJERPH 15, 1064. https://doi.org/10.3390/ijerph15061064
Wang, Q., Zeng, Q., Tao, J., Sun, L., Zhang, L., Gu, T., Wang, Z., Chen, L., 2019. Estimating PM2.5 Concentrations Based on MODIS AOD and NAQPMS Data over Beijing–Tianjin–Hebei. Sensors 19, 1207. https://doi.org/10.3390/s19051207
Wang, X., Wu, Z., Liang, G., 2009. WRF/CHEM modeling of impacts of weather conditions modified by urban expansion on secondary organic aerosol formation over Pearl River Delta. Particuology 7, 384–391. https://doi.org/10.1016/j.partic.2009.04.007
Wang, Y., Jia, C., Tao, J., Zhang, L., Liang, X., Ma, J., Gao, H., Huang, T., Zhang, K., 2016. Chemical characterization and source apportionment of PM2.5 in a semi-arid and petrochemical-industrialized city, Northwest China. Science of The Total Environment 573, 1031–1040. https://doi.org/10.1016/j.scitotenv.2016.08.179
Wang, Y.Q., 2019. An Open Source Software Suite for Multi-Dimensional Meteorological Data Computation and Visualisation. JORS 7, 21. https://doi.org/10.5334/jors.267

Wang, Y.Q., 2014. MeteoInfo: GIS software for meteorological data visualization and analysis: Meteorological GIS software. Met. Apps 21, 360–368. https://doi.org/10.1002/met.1345

Wang, Y.Q., Zhang, X.Y., Draxler, R.R., 2009. TrajStat: GIS-based software that uses various trajectory statistical analysis methods to identify potential sources from long-term air pollution measurement data. Environmental Modelling & Software 24, 938–939. https://doi.org/10.1016/j.envsoft.2009.01.004

Wei, X., Gao, B., Wang, P., Zhou, H., Lu, J., 2015. Pollution characteristics and health risk assessment of heavy metals in street dusts from different functional areas in Beijing, China. Ecotoxicology and Environmental Safety 112, 186–192. https://doi.org/10.1016/j.ecoenv.2014.11.005

Westbrook, J.K., Eyster, R.S., Allen, C.T., 2011. A model for long-distance dispersal of boll weevils (Coleoptera: Curculionidae). Int J Biometeorol 55, 585–593. https://doi.org/10.1007/s00484-010-0359-4

World Health Organization, 2021. WHO global air quality guidelines: particulate matter (PM2. 5 and PM10), ozone, nitrogen dioxide, sulfur dioxide and carbon monoxide. World Health Organization.

Wong, M.S., Nichol, J.E., Lee, K.H., 2013. Estimation of aerosol sources and aerosol transport pathways using AERONET clustering and backward trajectories: a case study of Hong Kong. International Journal of Remote Sensing 34, 938–955. https://doi.org/10.1080/01431161.2012.714500

Woodruff, T.J., Darrow, L.A., Parker, J.D., 2008. Air pollution and postneonatal infant mortality in the United States, 1999-2002. Environ Health Perspect 116, 110–115. https://doi.org/10.1289/ehp.10370

World Health Organization, 2009. World health statistics 2009. Estadísticas sanitarias mundiales 2009 149.

Xia, L., Gao, Y., 2011. Characterization of trace elements in PM2.5 aerosols in the vicinity of highways in northeast New Jersey in the U.S. east coast. Atmospheric Pollution Research 2, 34–44. https://doi.org/10.5094/APR.2011.005

Xie, J., Jin, L., Cui, J., Luo, X., Li, J., Zhang, G., Li, X., 2020. Health risk-oriented source apportionment of PM2.5-associated trace metals. Environmental Pollution 262, 114655. https://doi.org/10.1016/j.envpol.2020.114655

Xing, Y.-F., Xu, Y.-H., Shi, M.-H., Lian, Y.-X., 2016. The impact of PM2.5 on the human respiratory system. J Thorac Dis 8, E69-74. https://doi.org/10.3978/j.issn.2072-1439.2016.01.19

Xu, J., Tai, X., Betha, R., He, J., Balasubramanian, R., 2015. Comparison of physical and chemical properties of ambient aerosols during the 2009 haze and non-haze periods in Southeast Asia. Environ Geochem Health 37, 831–841. https://doi.org/10.1007/s10653-014-9667-7

Yadav, R., Sahu, L.K., Beig, G., Jaaffrey, S.N.A., 2016. Role of long-range transport and local meteorology in seasonal variation of surface ozone and its precursors at an urban site in India. Atmospheric Research 176–177, 96–107. https://doi.org/10.1016/j.atmosres.2016.02.018

Yadav, R., Sahu, L.K., Beig, G., Tripathi, N., Maji, S., Jaaffrey, S.N.A., 2019. The role of local meteorology on ambient particulate and gaseous species at an urban site of western India. Urban Climate 28, 100449. https://doi.org/10.1016/j.uclim.2019.01.003

Yadav, S., Tripathi, S.N., Rupakheti, M., 2022. Current status of source apportionment of ambient aerosols in India. Atmospheric Environment 274, 118987. https://doi.org/10.1016/j.atmosenv.2022.118987

Yan, H., Li, Q., Feng, K., Zhang, L., 2023. The characteristics of PM emissions from construction sites during the earthwork and foundation stages: an empirical study evidence. Environ Sci Pollut Res 30, 62716–62732. https://doi.org/10.1007/s11356-023-26494-4

Yan, X., Zang, Z., Liang, C., Luo, N., Ren, R., Cribb, M., Li, Z., 2021. New global aerosol fine-mode fraction data over land derived from MODIS satellite retrievals. Environmental Pollution 276, 116707. https://doi.org/10.1016/j.envpol.2021.116707

Yang, Q., Yuan, Q., Yue, L., Li, T., Shen, H., Zhang, L., 2019. The relationships between PM2.5 and aerosol optical depth (AOD) in mainland China: About and behind the spatio-temporal variations. Environmental Pollution 248, 526–535. https://doi.org/10.1016/j.envpol.2019.02.071

Yassin, M.F., Almutairi, S.K., Al-Hemoud, A., 2018. Dust storms backward Trajectories' and source identification over Kuwait. Atmospheric Research 212, 158–171. https://doi.org/10.1016/j.atmosres.2018.05.020

Yusup, Y., Alqaraghuli, W.A.A., Alkarkhi, A.F.M., 2016. Factor analysis and back trajectory of PM and its metal constituents. Environmental Forensics 17, 319–337. https://doi.org/10.1080/15275922.2016.1177757

Zeeshan, M., Kim Oanh, N.T., 2014. Assessment of the relationship between satellite AOD and ground PM10 measurement data considering synoptic meteorological patterns and Lidar data. Science of The Total Environment 473–474, 609–618. https://doi.org/10.1016/j.scitotenv.2013.12.058

Zeng, Y., Hopke, P.K., 1989. A study of the sources of acid precipitation in Ontario, Canada. Atmospheric Environment (1967) 23, 1499–1509. https://doi.org/10.1016/0004-6981(89)90409-5

Zhang, B., Rong, Y., Yong, R., Qin, D., Li, M., Zou, G. and Pan, J., 2022. Deep learning for air pollutant concentration prediction: A review. Atmospheric Environment, p.119347.

Zhang, X., Feng, X., Tian, J., Zhang, Y., Li, Z., Wang, Q., Cao, J., Wang, J., 2023. Dynamic harmonization of source-oriented and receptor models for source apportionment. Science of The Total Environment 859, 160312. https://doi.org/10.1016/j.scitotenv.2022.160312

Zhang, X.-Y., Tang, L.-S., Zhang, G., Wu, H.-D., 2009. Heavy Metal Contamination in a Typical Mining Town of a Minority and Mountain Area, South China. Bull Environ Contam Toxicol 82, 31–38. https://doi.org/10.1007/s00128-008-9569-4

Zhang, Y., Cai, J., Wang, S., He, K., Zheng, M., 2017. Review of receptor-based source apportionment research of fine particulate matter and its challenges in China. Science of The Total Environment 586, 917–929. https://doi.org/10.1016/j.scitotenv.2017.02.071

Zhao, S., Tian, H., Luo, L., Liu, H., Wu, B., Liu, S., Bai, X., Liu, W., Liu, X., Wu, Y., Lin, S., Guo, Z., Lv, Y., Xue, Y., 2021. Temporal variation characteristics and source apportionment of metal elements in PM2.5 in urban Beijing during 2018–2019. Environmental Pollution 268, 115856. https://doi.org/10.1016/j.envpol.2020.115856

Zheng, N., Liu, J., Wang, Q., Liang, Z., 2010. Health risk assessment of heavy metal exposure to street dust in the zinc smelting district, Northeast of China. Science of The Total Environment 408, 726–733. https://doi.org/10.1016/j.scitotenv.2009.10.075

Publications based on present work:

Ashok, S. and Sekhar, M.C., 2023. Assessment of PM2. 5 bound Heavy Metals and Associated Health impact-A case study in Warangal City, India. *Research Journal of Chemistry and Environment*, 27, 5. DOI: https://doi.org/10.25303/2705rjce027041.

Ashok, S., Sekhar, M. C., & Reddy, D. R. B. 2022. Estimation of surface PM2.5 with MODIS Aerosol optical depth and source identification using trajectory analysis: A case of Hyderabad City, India. *International Journal of Environment*, 11(2), 23–52. DOI: https://doi.org/10.3126/ije.v11i2.44538

Ashok, S., Sekhar, M.C. and Reddy, D., 2022. Retrieving MODIS AOD and Evaluation of Ground-level $PM_{2.5}$ in Addition to the Identification of Potential Source Regions Over South India. *Indian Journal of Ecology*, 49(6), 2395-2403. DOI: 10.55362/IJE/2022/3839

Conference proceedings based on present work:

Ashok, S and Sekhar, M. C. (2019). State of art Review on future effects in climate change with respective soil properties [Paper presentation], ICGGE-2019, MNNIT Allahabad, India